( )	
Title(English)	A New Mechanism on the Generation of Electron Spin Polarization through Interactions between Radical and Excited Molecule
( )	
Author(English)	Akio Kawai
( )	: , : , : 2396 , :1992 3 26 , : , :
Citation(English)	Degree:Doctor of Science, Conferring organization: , Report number: 2396 , Conferred date:1992/3/26, Degree Type:Course doctor, Examiner:
( )	
Type(English)	Doctoral Thesis

A New Mechanism of the Generation of Electron Spin Polarization through Interactions between Radical and Excited Molecule

Akio Kawai

Department of Chemistry
Tokyo Institute of Technology
1992.

CONTENTS

<FIGURE CAPTIONS>

Fig.1-2-1　Schematic representation of triplet mechanism.　One phase polarization
is generated on radicals by spin polarized triplet molecule.

Fig.1-2-2　Singlet and triplet energy levels of radical pair
in an external magnetic field.

Fig.1-2-3　CIDEP patterns of radicals generated by radical pair mechanism.　A and E
represent microwave absorption and emission, respectively.　In this figure,
TR-ESR spectra are shown for the radical with quartet hyperfine structure.

Fig.1-2-4　Observed (a) and simulated (b) spectra of naphthylmethyl radical generated
by 308 nm excitation of 1-chloromethylnaphthalene in benzene.

Fig.1-2-5　Simulated spectra of naphthylmethyl radical assuming RPM of the triplet
G-pair of naphthylmethyl radical and chlorine atom (a) and assuming
F-pair RPM of naphthylmethyl radicals (b).

Fig.1-3-1　Simulated spectra of the radical pair with J value of
a) 0.1 G, b) 1.0 G and c) 10 G.　Upper row shows equilibrium spectra
and lower row shows spin-polarized spectra.

Fig.1-3-2　Schematic representation of the magnetic field effects on the
radical reaction.　a) Δg mechanism and
b) strongly spin-orbit coupling mechanism.

Fig.1-4-1　Energy diagram of the radical triplet pair assuming J>0.

Fig.2-1-1　Schematic representation of the experimental apparatus.

Fig.2-2-1　TR-ESR spectrum obtained in benzophenone-triethylamine (0.36 M)
in benzene by 308 nm laser excitation.　The gate is opened
from 1.0 to 1.5 μs after excitation pulse.

CHAPTER I

Overview of "SPIN CHEMISTRY"

1-1 Contribution of Magnetic Resonance Technique to Photochemistry.

Since the inventions of the magnetic resonance technique about 40 years ago, a large amount of information about the chemical species have provided the new sight from the view point of electron and nuclear spin angular momentum. Almost all of the magnetic resonance studies have been carried out with ESR and NMR. NMR spectroscopy has been widely utilized for the analysis of the complicated structures of organic compounds, which, in a way, induced the modern total synthetic works of the natural organic compounds. This point is the most excellent results of the NMR spectroscopy, but they are only restricted to the static information of the compounds. In the dynamic studies, CIDNP (Chemically Induced Dynamic Nuclear Polarization),[1] which is observed by NMR spectroscopy, has been used to investigate the photochemical reaction mechanisms. However, this technique is indirect because only the products of the reactions are monitored.

The other magnetic resonance technique, ESR spectroscopy, has been utilized for the analysis of the structures of free radicals and metal compounds with paramagnetism. ESR has an advantage which can selectively measure some kinds of compounds. NMR observes all compounds included in the target media whereas ESR detects only species with unpaired electrons. Therefore, ESR is suitable for the studies of paramagnetic intermediate species in photochemistry. However, conventional ESR method does not have high sensitivity and time resolution enough to measure the short lived paramagnetic species.

Great efforts are made to improve the time resolution and sensitivity of ESR measurements, and, as a results, a lot of ESR techniques have been invented, that are, the

electron spin echo envelope modulation analysis,[2] FT–ESR technique,[3] optically detected ESR methods,[4] reaction yield detected magnetic resonance method[5] and so on.[6] In these methods, time resolution is improved to about 10 ns at the maximum. Recently, these methods are mainly applied for the studies of radical pairs in the initial photochemical stages.[7] On the other hand, another approach has been carried out to make better the time resolution and sensitivity by probing electron spin polarization called CIDEP (Chemically Induced Dynamic Electron Polarization).[8] CIDEP is the non–Boltzmann distribution of the electron spin states, which causes emission or enhanced absorption in ESR. By this phenomenon, ESR intensity is enhanced and thus, the sensitivity rises. CIDEP enables us to make ESR measurements in microsecond time region and this type of ESR measurements is called time resolved (TR) ESR in which the conventional CW–ESR signal is detected only within the time window appropriate for the target intermediate species. TR–ESR measurements have been widely employed in the investigation of dynamics of intermediate paramagnetic species because of its easiness.

As all the static and dynamic studies of magnetic resonance are based on the spin angular momentum, they are included in the field so called "Spin Chemistry".[9] Spin chemistry also includes the magnetic field effects on the reactions[10] and quenching processes[11] as well as ESR and NMR studies The recent subjects of spin chemistry are mainly on the dynamics of excited states and reactions owing to the development of detection systems. CIDEP studies are one of such fields.

1–2 Conventional Sources of Electron Spin Polarization.

CIDEP is an indispensable phenomenon for TR–ESR measurements and its generation mechanism have been investigated since the first observation of CIDEP in 1963 by Fessenden and Schuler.[12] According to these studies, there are two main mechanisms for CIDEP generation: One is the triplet mechanism (TM)[13] and the other is the radical pair mechanism (RPM).[1,8,14] In what follows, these mechanisms will be described.

Triplet Mechanism

In many aromatic and calbonyl compounds, the triplet states are generated by the anisotropic intersystem crossing (ISC)[15] following photoexcitation, in which three degenerated sublevels are initially populated with non–Boltzmann distribution. The ISC rate from S_1 to each triplet sublevel is determined by the electronic and spin characters of the S_1 state and T_1 sublevels. If such spin polarized triplet state reacts to produce free radicals within the spin relaxation time of the triplet state, it is expected for the generated radicals to show the same spin polarization as that of their precursor triplet state. Figure 1–2–1 shows the model of TM. In this example, the T_z sublevel of reaction precursor is populated in the absence of external magnetic field. In the TR–ESR measurements, as external magnetic field is applied, triplet sublevels mix with each other by Zeemann effect of external magnetic field and, hence, the ratio of the populations are modified. The triplet state has the same spin alignment along the magnetic field except the magnitude of spin polarization and the photoproduced radicals succeed to the spin polarization of its precursor. Therefore, these spin polarized radicals show total absorptive or emissive ESR signals depend on the spin polarization of the triplet state.

The first observation of TM was reported by Wong et al.[13] They observed the total emissive ESR signal of 1,4–naphthoquinone radical generated by hydrogen abstraction

3

reaction. This means that the precursor triplet state of 1,4-naphthoquinone is effectively populated on $T_z(\alpha\alpha)$ sublevel and produce the semiquinone radical with α spin enhanced population that induces the emission of resonanced microwave. As the reaction precursor has two α spins and abstracted hydrogen should have β spin to form the chemical bond, generated dehydrogenized radical also shows α spin enhanced population. Consequently, both radicals are generated with α spin enhanced population. Atkins et al.[16] and Pedersen et al.[17] expanded TM theory for the random oriented system and formulated it including molecular rotations.

Radical Pair Mechanism

In the case of TM, CIDEP of radicals depends on spin polarization of their precursor but the RPM originates through magnetic and exchange interactions within pairs of radicals, which are created by the dissociation of parent molecules (germinate radical pair, G–RP) or by diffusion of radicals (free radical pair, F–RP). Though TM makes single phase spin polarization on radical, RPM causes the two phase electron spin polarization on radicals.

The potential of the radical pair is shown in Fig.1-2-2. The S and T_0 states of radical pair mix with each other through the hyperfine interaction of radicals. This mixing rate depends on the magnitude of hyperfine interaction which is determined by the quantum number of nuclear spin state. Hence the mixing rates are different for each hyperfine line. Spin polarization is generated by the $S-T_0$ mixing and the hyperfine dependent polarization happens to radical.

RPM signal pattern depends on the spin multiplicity of reaction precursor and species of partner of radical pair and it is useful to study the reaction processes from the pattern of CIDEP. McLauchlan et al.[18] observed the spin polarized ESR spectrum of ketyl radicals produced in the photolysis of aza-aromatic and aliphatic compounds. They

discussed the reaction mechanisms and the properties of precursor triplet states from the CIDEP signals. Many other investigations have been reported by the analysis of CIDEP pattern. The relations of CIDEP pattern of radicals and their reaction precursor states are described in Fig.1-2-3. Single phase polarization is called net polarization whereas the hyperfine dependent two phase polarization is called multiplet polarization. For example, singlet precursor reactions yield the radicals with A/E (Absorption in low magnetic field and Emission in high magnetic field) type CIDEP pattern.

Figure 1-2-4 shows the CIDEP spectrum of 1-naphthylmethyl radical (1NMR) produced in the photolysis of 1-chloromethylnaphthalene in benzne.[19] Computer simulation for this CIDEP spectrum was carried out according to the diffusion controlled CIDEP theory. Figure 1-2-5a and 1-2-5b show theoretical CIDEP spectra of 1NMR assuming G-RPM of chlorine atom and 1NMR and F-RPM of 1NMR pair, respectively. The simulated spectrum in Fig. 1-2-4b is obtained by the sum of both signals with ratio of 5 : 2. It is clear that the simulated spectrum successfully reproduce the observed spectrum. This demonstrates the capability to analyze the CIDEP mechanism using the simulation based on CIDEP theory.

At present, these two main mechanisms successfully explain the TR-ESR spectra. Therefore, it is believed that the CIDEP theories are completely put in a good condition.
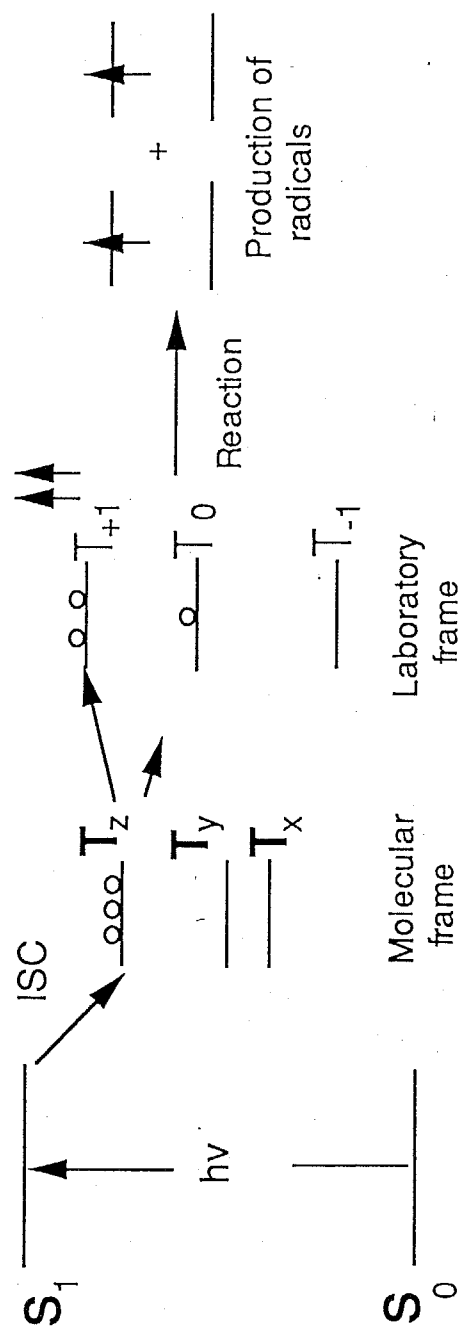
Fig.1–2–1 Schematic representation of triplet mechanism. One phase polarization is generated on radicals by spin polarized triplet molecule.
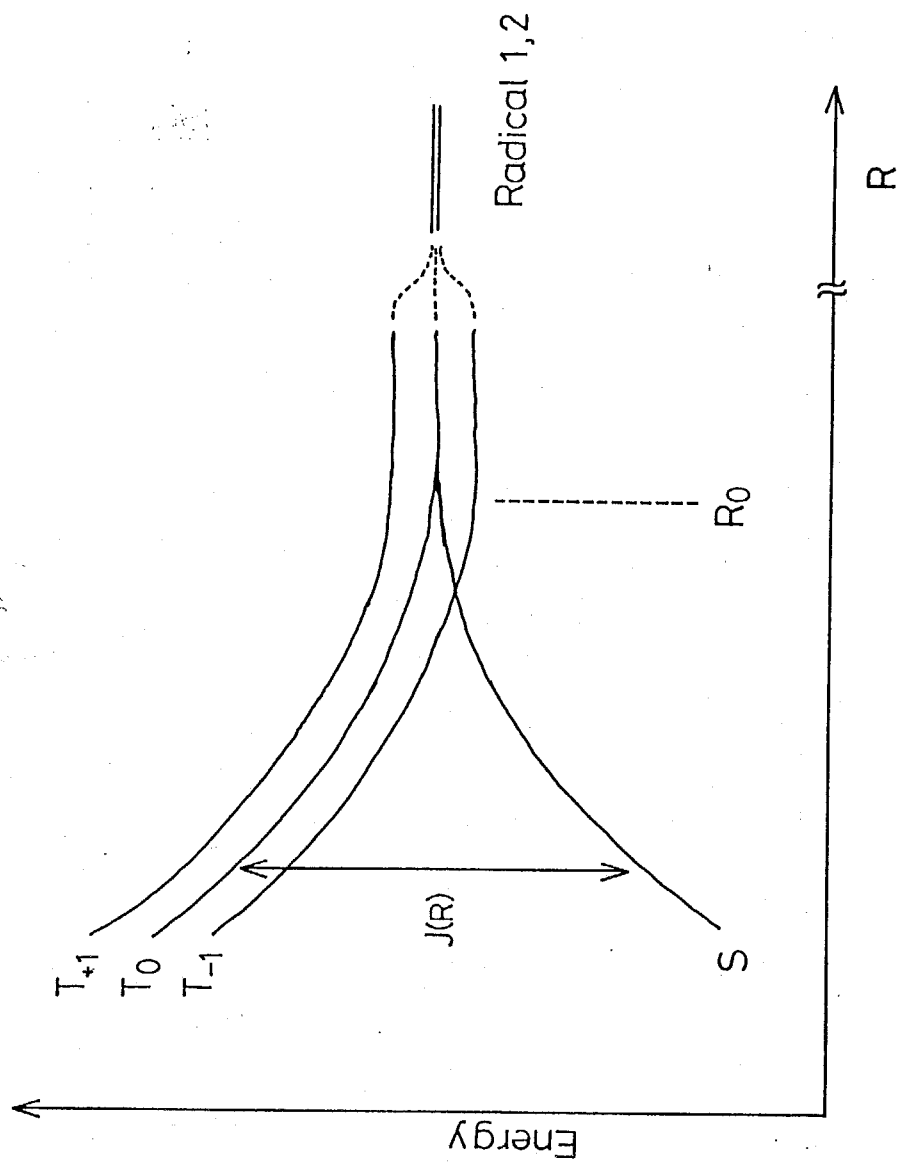
Fig.1-2-2 Singlet and triplet energy levels of radical pair in an external magnetic field.

Radical Pair

Boltzmann distribution ⇒ CIDEP
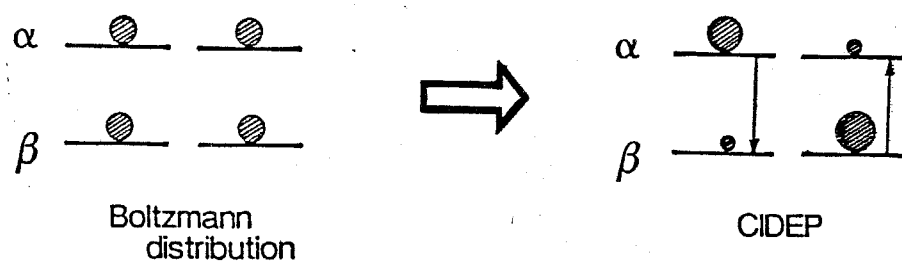
a) Multiplet

Singlet Precursor

A / E

Triplet Precursor

E / A
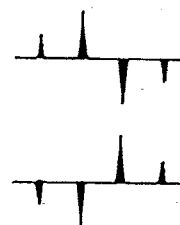
b) Δ g

g value (large)   g value (small)

Singlet Precursor
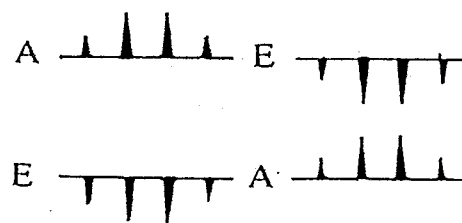
A   E

Triplet Precursor

E   A

Fig.1–2–3 CIDEP patterns of radicals generated by radical pair mechanism. A and E represent microwave absorption and emission, respectively. In this figure, TR–ESR spectra are shown for the radical with quartet hyperfine structure.

8

a)

b)

Abs.

Em.

20 G

Fig.1-2-4 Observed (a) and simulated (b) spectra of naphthylmethyl radical generated
by 308 nm excitation of 1-chloromethylnaphthalene in benzene.

9
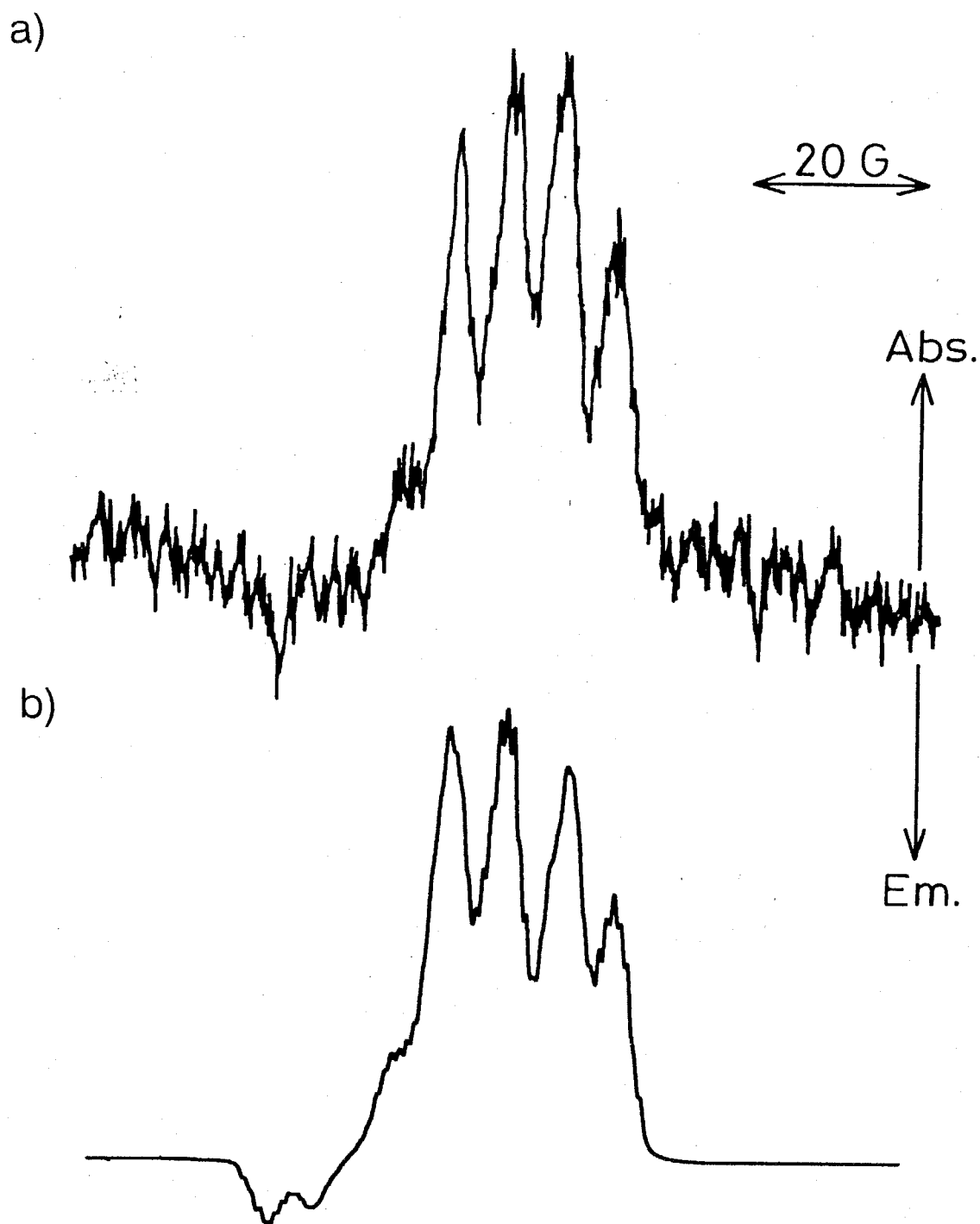
Fig.1-2-5 Simulated spectra of naphthylmethyl radical assuming RPM of the triplet

G-pair of naphthylmethyl radical and chlorine atom (a) and assuming

F-pair RPM of naphthylmethyl radicals (b).

1–3 Recent Trends in Spin Chemistry.

Recent targets of spin chemistry mainly lie in the dynamics of short lived paramagnetic spices. The CIDEP studies on radical pair and magnetic field effects on chemical kinetics have been well studied in this decade.

Recent CIDEP studies on the photochemical processes seem to concentrate on photogenerated spin correlated radical pairs. McLauchlan et al.[20] first interpreted the TR–ESR spectra of radical pair in which the four spin states of the correlated pair is involved in the ESR transitions and each hyperfine lines of the radical exhibits the E/A (Emission/Absorption) nature. The simulated spectra of spin correlated pairs reported by McLauchlan et al.[20] are shown in Fig.1–3–1 under various conditions. By the fitting of the spectrum observed, the magnitude of exchange interactions is estimated for the pair. Radical pairs are really observed in many systems such as photogenerated radical pair in micells,[21] ion radical pairs in normal solvents[22] and so on.[23] Especially, the ion radical pair of photosynthetic center has been extensively investigated concerning the spin polarization and the primary events of photosynthetic center.[24] Hore and his coworkers[25] reported the anisotropy of singlet–triplet interconversion of radical pairs involved in photosynthetic charge separation. Hoff and his coworkers[26] studied the structure of charge separated pairs by TR–ESR combined with the results of other ESR technique.

Magnetic field effects on chemical kinetics have been studied by Nagakura and his coworkers[10] and the Δg effects were reported on the reaction rate of free radicals in micellar solution, in which the only T_0 state of the radical pair coupled with the S state due to the Δg effect. Recently, Steiner and his coworkers[27] reported the spin orbit coupling dependent magnetic field effects on chemical kinetics, in which T_{+1} and T_{-1} states as well as S state caused the reaction because of the spin orbit coupling. The concept of these mechanisms are visualized in Fig.1–3–2. Such new mechanisms reveal the complicated nature of the reactions of free radicals.
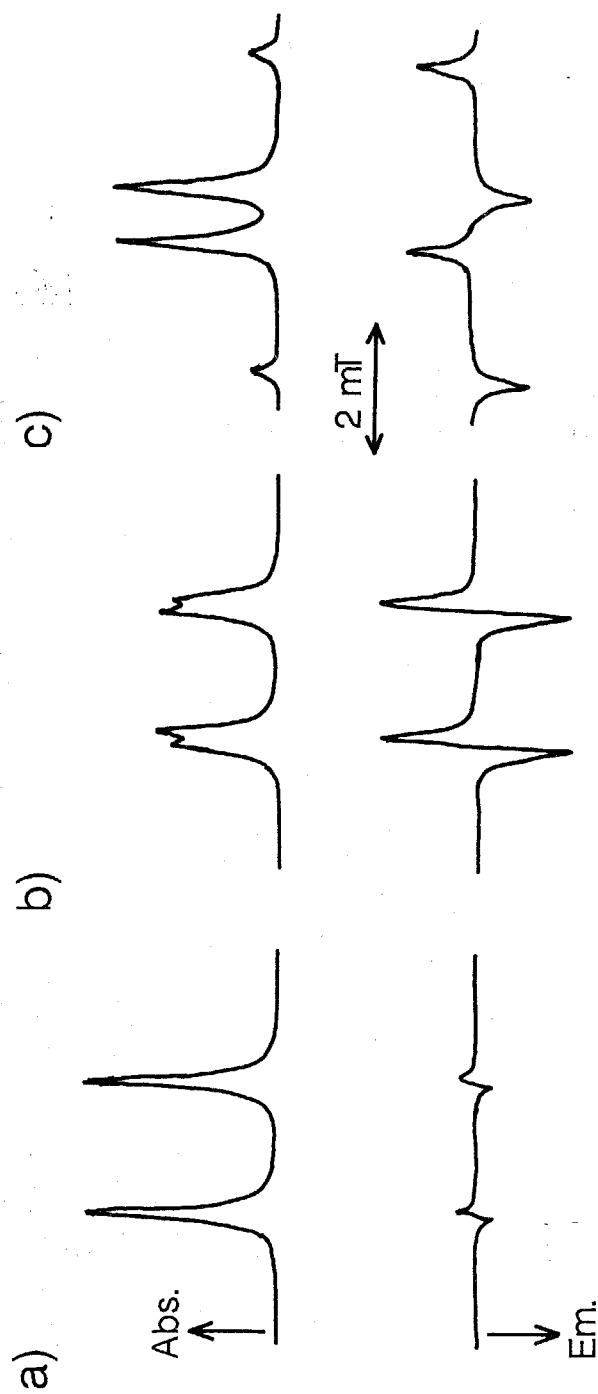
Fig.1-3-1 Simulated spectra of the radical pair with J value of
a) 0.1 G, b) 1.0 G and c) 10 G. Upper row shows equilibrium spectra
and lower row shows spin-polarized spectra.
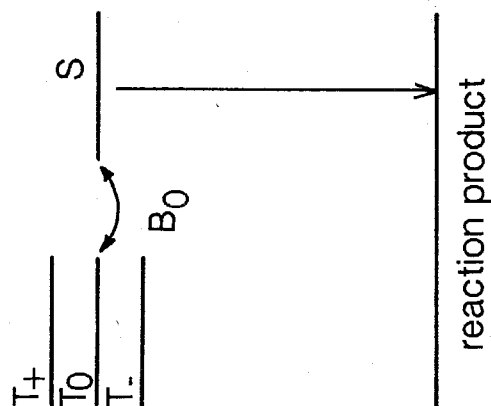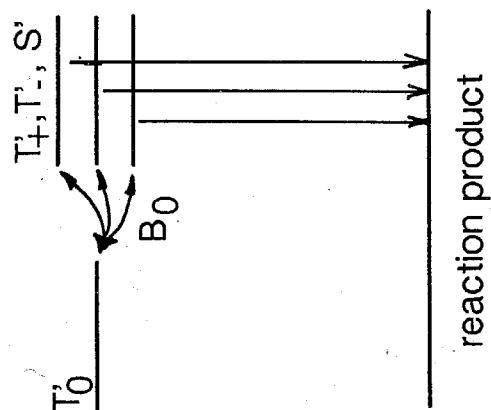
Fig.1-3-2 Schematic representation of the magnetic field effects on the

radical reaction. a) Δg mechanism and

b) strongly spin-orbit coupling mechanism.

1-4 New Mechanism of the CIDEP Generation.

The recent interests in the spin chemistry converges on the nature of the radical–radical interactions such as radical pair and magnetic field effects on the radical reactions. However, photochemically produced radicals are not the only species playing a role in the events at the initial photochemical stages and, excited molecules must be included in these events. Quenching of the excited molecules by the free radicals is one of such phenomena.[28] Recently, Blattler et al.[29] reported the CIDEP generation in the interactions between triplet molecule and free radicals, which is called radical–triplet pair mechanism (RTPM). They observed the net emissive CIDEP on free radicals in triplet–doublet systems. According to their RTPM, radicals always show net emissive polarization regardless of the triplet polarization. In RTPM, doublet and quartet states are considered for the radical–triplet encounter pair. The energy of these states are indicated in Fig.1–4–1 assuming that the electron exchange interaction, J, is a positive value. They calculated the quartet–doublet mixing by the zero field interaction (zfs) of the triplet molecule under the initial condition that the doublet states were empty due to triplet quenching with the radical. Using the second order perturbation theory, they obtained the following equation of radical spin polarization.

$$P = -D^2J/24\omega$$

$$x \; \{(2\omega + 3J)^{-2}[1-\cos(2w + 3J)t]$$

$$+ (2\omega - 3J)^{-2}[1-\cos(2\omega - 3J)t]$$

$$+ 2(3J)^{-2}[1-\cos(3Jt)]\}$$

$$= 1/72 \; x \; \omega JD^2t^4$$

where D is the D value of the triplet state and ω is the Zeeman energy. This equation gives the positive value of P which corresponds to the net emissive electron spin polarization on free radicals. They attributed the results of this mechanism to their

experimental results of net emissive polarization.

RTPM is the new sight in the CIDEP studies and the details of the mechanism should be examined. Furthermore, RTPM itself should be examined with a lot of experimental results of radical–triplet interactions.

One of the purpose of this thesis is to construct the exact RTPM which is described in Chapter III where the greatly modified RTPM is proposed.[30] Moreover, according to the concept of RTPM, interesting CIDEP generation in the radical–excited singlet molecule system is discovered[31] which is described in Chapter IV.

As mentioned above, recent trends in spin chemistry are mainly on the radical–radical interactions. These works are owing to the concept of RPM supported by the old CIDEP studies. Hence, if the RTPM is constructed in good order, it would be possible to open a new field in the radical–excited molecule interactions by probing CIDEP signals due to RTPM. Thus, the trial applications of RTPM are introduced in the final chapter with a future of spin chemistry in my mind.
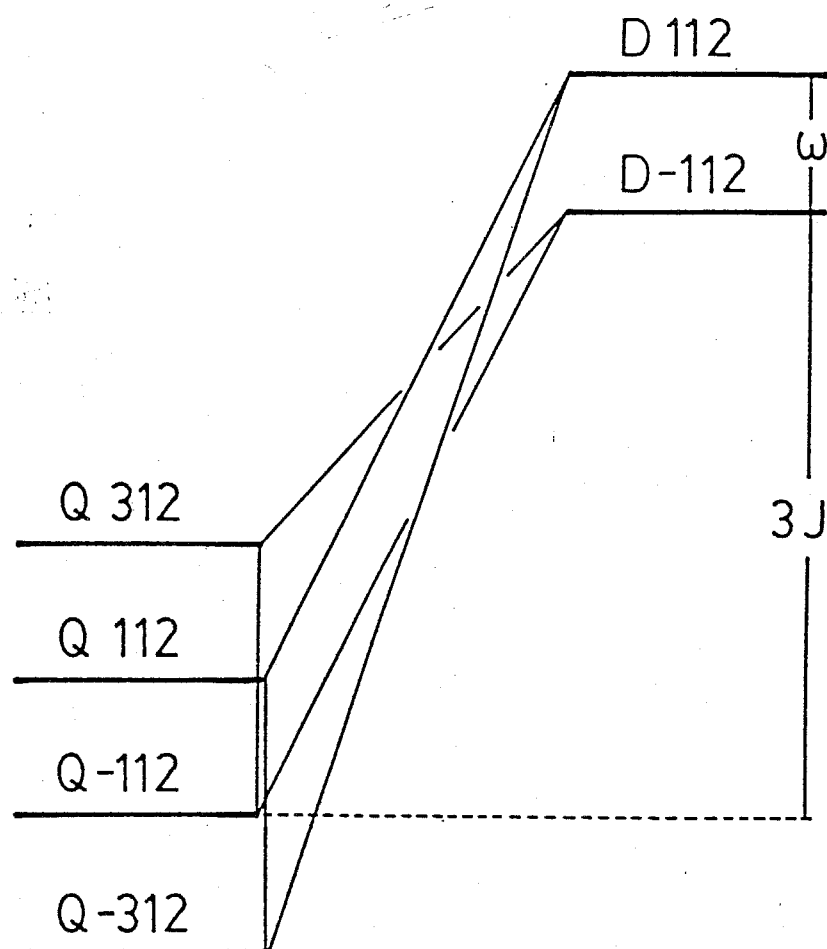
Fig.1-4-1 Energy diagram of the radical triplet pair assuming J>0.

References

[1] K. M. Salikhov, Yu. N. Molin, R. Z. Sagdeev and A. L. Buchachenko,

    Spin Polarization and Magnetic Field Effects in Radical Reactions,

    Elsevier, New York, (1984).

[2] W. J. Buma, E. J. J. Groenen, J. Schmidt and R. de Beer,

    J. Chem. Phys., **91**, 6549, (1989).

[3] G. Kroll, M. Pluschau, K. P. Dinse and H. van Willigen,

    J. Chem. Phys., **93**, 8709, (1990).

[4] D. W. Werst and A. D. Trifunac, *J. Phys. Chem.*, **95** 3466, (1991).

[5] Yu. N. Molin, O. A. Anisimov, V. I. Melekhov and S. N. Smirnov,

    J. Chem. Soc., Faraday Discuss., **78**, 289, (1984).

[6] L. Kevan and M. K. Bowman (Eds.), *Modern Pulsed and Continuous–Wave*

    Electron Spin Resonance, John Wiley & Sons, Inc. (1990).

[7] For example, J. R. Norris, A. L. Morris, M. C. Thurnauer and J. Tang,

    J. Chem. Phys., **92**, 4239, (1990).

[8] R. Kaptein in L. T. Muss, P. W. Atkins, K. A. McLauchlan and J. B. Pedersen

    (Eds.), *Chemically Induced Magnetic Polarization*, Reidel, Dordrecht, (1977).

[9] Such dynamical study is the young area of chemistry and internatinal conference

    was held first time in 1991 for this field and called "Spin Chemistry".

[10] Y. Sakaguchi, S. Nagakura and H. Hayashi, *Chem. Phys. Lett.*,

    72, 420, (1980) and references therein.

[11] P. W. Atkins and G. T. Evans, *Mol. Phys.*, **29**, 921, (1975)

[12] R. W. Fessenden and R. H. Schuler, *J. Chem. Phys.*, **39**, 2147, (1963).

[13] S. K. Wong and J. K. S. Wan, *J. Am. Chem. Soc.*, **94**, 7197, (1972).

[14] F. J. Adrian, *Rev. Chem. Intermediate*, **3**, 3, (1979).

[15] S. P. McGlynn, T. Azumi, M. Kinoshita,

   Molecular Spectroscopy of the Triplet State, Prentice–Hall, Inc. (1969).

[16] P. W. Atkins and G. T. Evans, *Mol. Phys.*, **27**, 1633, (1974).

[17] J. B. Pedersen and J. H. Freed, *J. Chem. Phys.*, **62**, 1790, (1975).

[18] S. Basu, K. A. McLauchlan and A, J, D. Ritchie, *Chem. Phys. Lett.*, **79**, 95, (1983).

   ; A. I. Grant and K. A. McLauchlan, *Chem. Phys. Lett.*, **101**, 120, (1983).

   ; C. D. Buckley and K. A. McLauchlan, *Chem. Phys.*, **86**, 323, (1984).

[19] A. Kawai, T. Okutsu and K. Obi, *Chem. Phys. Lett.*, **174**, 213, (1990).

[20] C. D. Buckely, D. A. Hunter, P. J. Hore and K. A. McLauchlan,

   Chem. Phys. Lett., **135**, 307, (1987).

[21] G. L. Closs, M. D. E. Forbes and J. R. Norris, Jr *J. Phys. Chem.* **91**, 3592, (1987).

[22] H. Murai and K. Kuwata, *Chem. Phys. Lett.*, **164**, 567, (1989).

[23] K. Tominaga, S. Yamauchi and N. Hirota, *J. Chem. Phys.*, **92**, 5175, (1990).

[24] For example, K. Hasharoni, H. Levanon, J. Tang, M. K. Bowman, J. R. Norris,

   D. Gust, T. A. Moore and A. L. Moore, *J. Am. Chem. Soc.*, **112**, 6477, (1990).

[25] P. J. Hore, D. A. Hunter, D. J. Riley, J. J. Semlyen, F. G. H. van Wijk,

   T. J. Schaafsma, P. Gast, and A. J. Hoff, *Res. Chem. Intermediates*, **16** 127, (1991).

[26] A. J. Hoff, *Quart. Rev. Biophys.*, **17**, 153, (1984).

[27] U. E. Steiner, H. J. Wolff, T. Ulrich and T. Ohno, *J. Phys. Chem.*, **93**, 5147, (1989).

[28] J. B. Birks, *Photophysics of Aromatic Molecules*, New York. Wiley, (1970).

[29] C. Blättler, F. Jent and H. Paul, *Chem. Phys. Lett.*, **166**, 375, (1990).

[30] A. Kawai, T. Okutsu and K. Obi, *J. Phys. Chem.*, **95**, 9130, (1991).

[31] A. Kawai and K. Obi, *J. Phys. Chem.*, (1992) in press.

CHAPTER II

EXPERIMENTAL

2-1 Apparatus.

a) TR-ESR Measurements

To measure the short-lived (<1ms) paramagnetic spices generated in the initial photochemical stages, an ESR spectrometer should have its time resolution of microsecond order. A conventional continuous-wave ESR spectrometer has the time resolution of millisecond order with using the magnetic field modulation (100 kHz field modulation). The technique of the TR-ESR measurements used in this study is similar to one reported by Kim and Weissman.[1] The TR-ESR measurements are carried out without field modulation to improve the time resolution. Transient ESR signals generated by the pulsed laser irradiation were detected by a diode of a conventional X-band ESR spectrometer (Varian E-112) and transferred to a boxcar integrator (Stanford SR-250) for time resolved ESR spectra or a transient digitizer (Iwatsu DM901) combined with a personal computer for time profiles of ESR signals. A wide band amplifier (LH0032 10 MHz) was inserted between the detection system and signal analyzer for the transient ESR signals of microsecond order. Excitation light sources were a pulsed nitrogen laser (Molectron UV-24) or a XeCl excimer laser (Lambda Physik LPX 100). Pulse width is 7 ns and energy is 4 mJ/pulse for the nitrogen laser and 20 ns and 100 mJ/pulse, respectively, for the XeCl excimer laser. The frequency of microwave and the strength of magnetic field were measured by a microwave counter (Advantest TR5212) and an NMR field meter (ECHO ELECTRONICS EFM-2013), respectively. Schematic diagram of an experimental apparatus used for TR-ESR spectroscopy is shown in Fig.2-1-1. In the observation of TR-ESR spectrum, the sweep rate of magnetic field was adjusted to obtain the entire spectrum in 16-30 min.

b) Optical Spectra Measurements

Absorption and emission spectra were obtained by a SHIMADZU UV2200 spectrometer and JASCO FP–550A spectrofluormeter, respectively.

2–2 *Analysis of Time Resolved ESR signals*

a) TR–ESR Spectra

TR–ESR spectrum of the radical shows the same hyperfine structure as that of CW–ESR and it is possible to assign the radical structure by conventional method. The one point to pay attention is the phase of its spectrum. As the TR–ESR measurements are owing to the CIDEP of radicals, intensities of each hyperfine line are different from that expected for CW–ESR. Hence, the simulation must be carried out for each spectrum by the CIDEP theories described in Chap.I, as well as assignment of radical itself.

b) Time Profile of CIDEP Signal

An appropriate microwave power must be used for each chemical system with taking care of the influence of Torrey oscillation,[2] which results from the microwave power and magnetic relaxation time, T_1 and T_2. Bloch equations written in a reference frame rotating at the Larmor frequency[3] may be given as several forms depending on the photochemistry of each system. Here, one example of Bloch equation is shown as follows for the system in which concentration and spin polarizations of radical are changing with time,[4]

$$\dot{M}(t) = L\,M(t) + T_1^{-1}\,M_{sp}(t) - T_c^{-1}(t)\,M(t)$$

where $M(t)$ and $M_{sp}(t)$ are the magnetization vectors and L is the usual matrix of bloch equation and T_c^{-1} is the instantaneous lifetime of the radical. Magnetization vectors and the matrix are given by

$$M(t) = \begin{pmatrix} M_x(t) \\ M_y(t) \\ M_z(t) \end{pmatrix} \qquad M_{sp}(t) = n(t)\{P_{eq} + P(t)\} \begin{pmatrix} 0 \\ 0 \\ 1 \end{pmatrix} \qquad L = \begin{pmatrix} -T_2^{-1} & \Delta\omega & 0 \\ -\Delta\omega & -T_2^{-1} & \omega_1 \\ 0 & -\Delta\omega & -T_1^{-1} \end{pmatrix}$$

where $n(t)$ is the radical concentration, P_{eq} is the spin polarization at thermal equilibrium, $P(t)$ is the spin polarization generated at time t, $\Delta\omega$ is the offset from the resonance magnetic field of an observed hyperfine line and ω_1 is the magnetic field strength of microwave. T_c^{-1} is given by the equation,

$$T_c^{-1} = -\dot{n}(t)/n(t)$$

One of the famous solution of this equation was given by Hore and McLauchlan.[5] In their treatment, radicals and $P(t)$ were produced instantaneously at $t=0$ and radicals kinetics obeyed the following equation.

$$\dot{n}(t) = -k_1 \, n(t) - k_2 \, \{n(t)\}^2$$

As M_y is measured in TR–ESR, results of M_y are important. The solution of the equation under these conditions are given by

$$M_y = n(t)\{P(0) * g_y(t) + P_{eq} * G_y(t)\}$$

$$G_y = 1/T_1 \int_0^\infty g_y(t')\, dt'$$

$$g_y(t) = (\omega_1/b)\, e^{at} \sin(bt)$$

where

$$a = 1/T_1 + 1/T_2 \;, \quad \delta = 1/T_2 - 1/T_1 \;, \quad b = \{\omega_1^2 - (\delta/2)^2\}^{1/2}$$

According to the solution, a time profile of ESR signal oscillates with a frequency of ω_1

when $\omega_1 > \delta/2$, which is called Torrey oscillation. From this result, one can understand that the Torrey Oscillation will occur under high microwave power. This is why microwave power must be as low as possible. Moreover, the time profile of ESR signal must be analyzed by the Bloch equation indicated above.

As an example of the Torrey oscillation, CIDEP signal of the benzophenone and triethyamine system will be introduced here. Figure 2-2-1 shows TR-ESR spectrum of benzophenone ketyl and dehydrogenated radical of triethylamine obtained in the 308 nm laser photolysis, which is first reported by Miyagawa et. al.[6] To obtain the time profile of this CIDEP signal, difference between the signals of points A and B was measured where A is a position of resonance magnetic field of radical and B is an off resonance position. Time profile of this system is shown in Fig.2-2-2. CIDEP signal rose with pulse excitation and reached to its maximum value after 0.5 μs and then, decayed to the thermal equilibrium state. In this decay profile, remarkable differences are recognized with different microwave powers. At the higher microwave power like 50 or 100 mW, CIDEP signal decay with almost the same rate as that at lower microwave power but accompany the oscillation, which is the Torrey oscillation.

In general, the microwave power to avoid the Torrey oscillation is different in each system. Torrey oscillation depends on T_1 and T_2 of radicals, where T_2 are determined by concentration of radical as well as the character of radical itself.

c) Response Time

In the TR–ESR measurements, response time of an ESR cavity can not be ignored and signals must be corrected. Response time of an ESR spectrometer is determined by the Q value of the ESR cavity and frequency of microwave, $Q/2\pi\nu$. It is 0.134 μs for TE_{102} mode ESR cavity with the Q value of ca. 8000 and the microwave frequency of 9.52 GHz. An example of the response time effects is indicated in Fig.2-2-2: Reaction rate of the system is about 10 ns,[7] whereas the rise of CIDEP signals begins at 0.15 μs after laser pulse. In this system, electron spin polarization, M_z, would rise immediately just after the laser pulse, which is, then, transferred to the M_y component with the rate determined by the Bloch equation of the system. If the response of the cavity is rapid enough, the slow rise of M_y signal could be observed just after the laser pulse. Thus, this 0.15 μs is considered to be the response time of the ESR spectrometer system, which is consistent with the value estimated above from the Q value and microwave frequency. This response time must be considered in the analysis of CIDEP time profile.
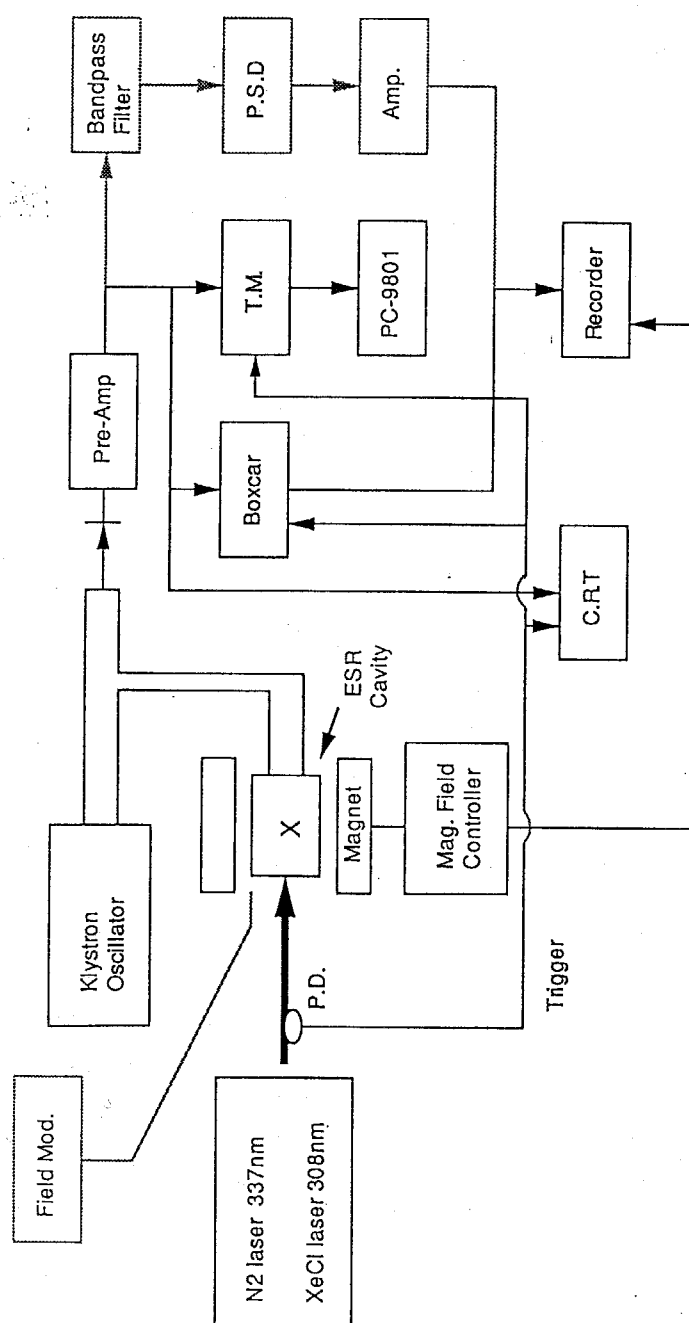
Fig.2-1-1 Schematic representation of the experimental apparatus.
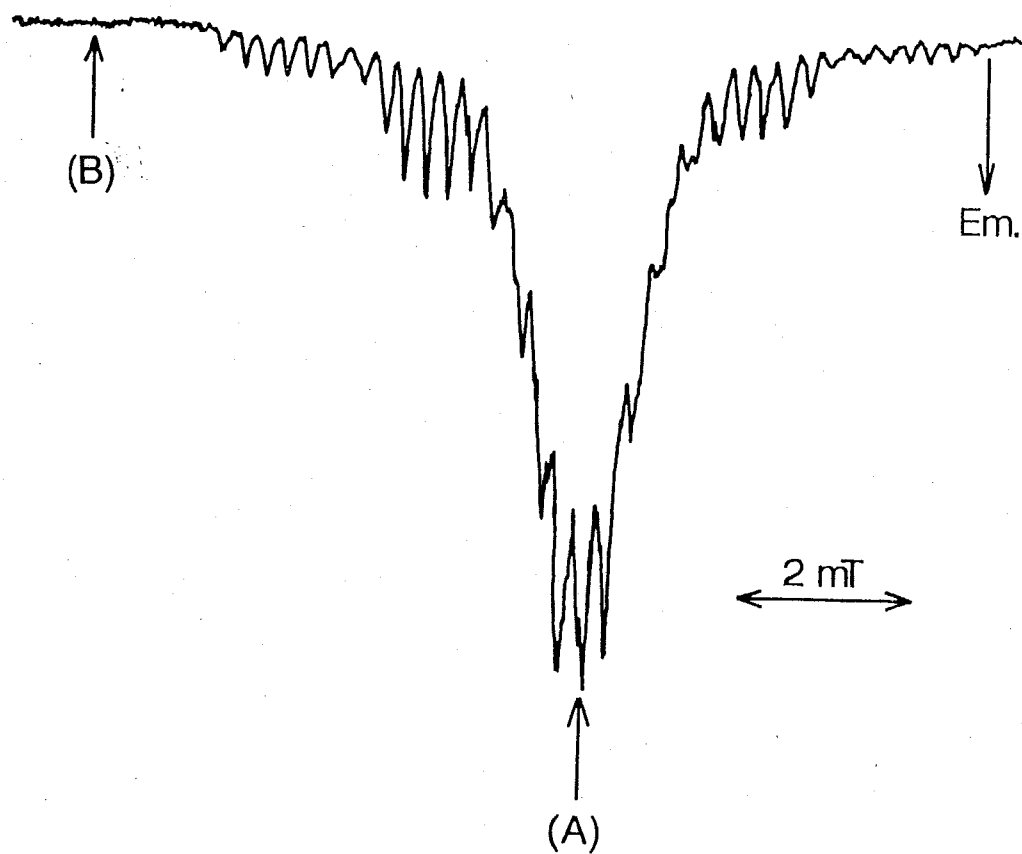
24

Fig.2-2-1 TR-ESR spectrum obtained in benzophenone-triethylamine (0.36 M) in benzene by 308 nm laser excitation. The gate is opened from 1.0 to 1.5 μs after excitation pulse.
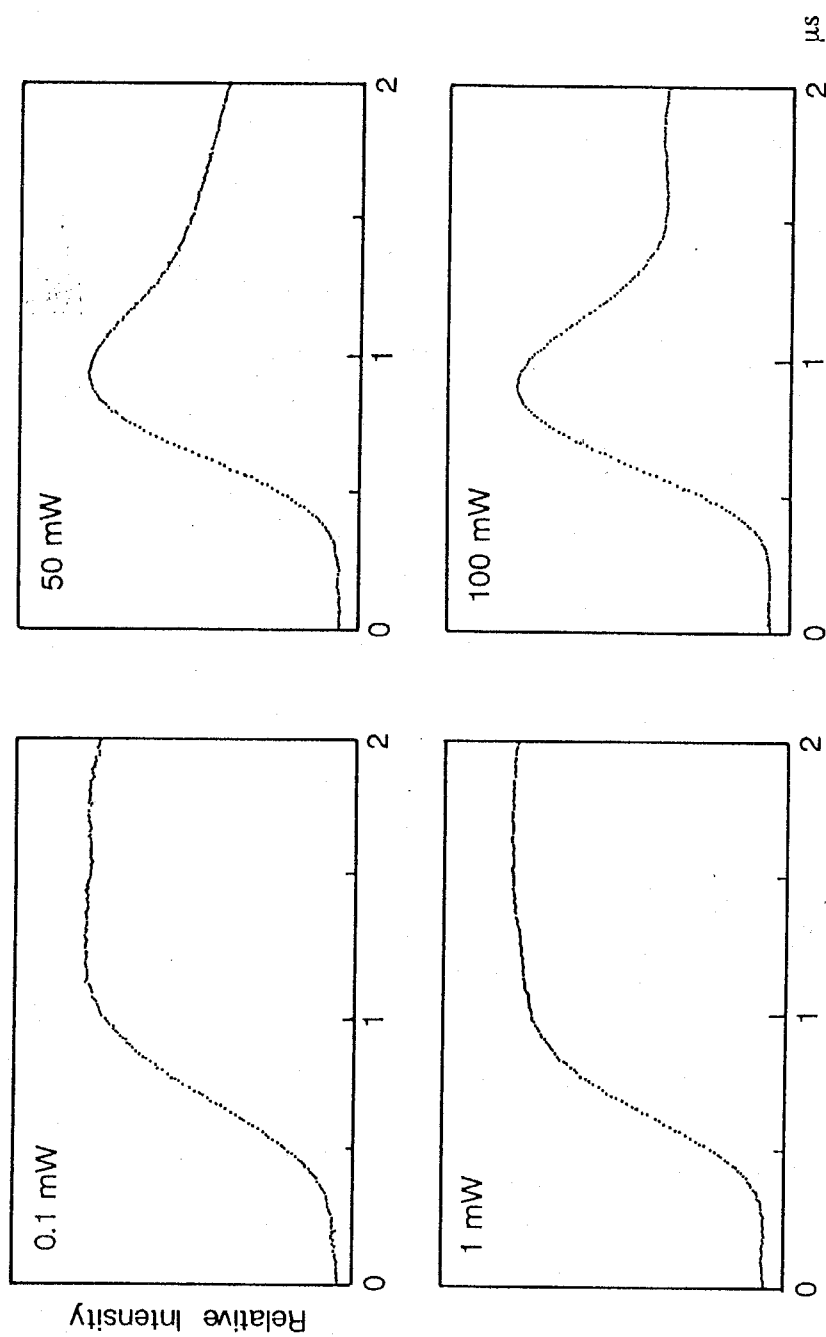
Fig.2-2-2 Microwave power dependence of the time profile of CIDEP signal obtained in benzophenone–triethylamine system.

References

[1] S.S Kim and S. I. Weissman, *J. Magn. Reson.*, **24**, 167, (1976).

[2] H. C. Torrey, *Phys. Rev.*, **76**, 1059, (1949).

[3] For examle, A. Carrington and A. D. McLauchlan, *Introduction to Magnetic Resonance with Applications to Chemistry and Chemical Physics*, Harper & Row, 1967.

[4] M. D. Smigel, L. R. Dalton, J. S. Hyde and L. A. Dalton, *Proc. Natl. Acad. Sci. USA*, **71**, 1925, (1974).

[5] P.J. Hore and K. A. McLauchlan, *J. Magn. Reson.*, **36**, 129, (1979).

[6] K. Miyagawa, Y. J. I'Haya and H. Murai, *Nippon Kagakukai-shi*, **8**, 1358, (1989).

[7] S. G. Cohen and A. D. Litt, *Tetrahedron Lett.*, 837, (1970).

CHAPTER III

Electron Spin Polarization in Radical and Triplet Molecule Systems

3-1 Introduction

Since the discovery of CIDEP by the Fessenden and Schular,[1] the mechanisms for the CIDEP in the initial photochemical stages had been constructed in 1970's.[2-4] There are two main mechanisms to generate CIDEP on free radicals : One is the triplet mechanism (TM)[2] in which the electron spin polarization of a reaction precursor, triplet state, is preserved in produced radicals and the other is radical pair mechanism (RPM)[3,4] which is caused by the mixing of spin states of a radical pair, mainly between S and T_0 states. As most CIDEP spectra were interpreted with a blend of these two mechanisms, the CIDEP generation rules were believed to be ready for every photochemical systems. However, generation of CIDEP is not peculiar to photochemically produced radicals from the excited state, but it is also seen in the interaction between doublet radicals and short-lived triplet molecules in liquid phase. In 1986, Imamura et al.[5] observed emissive electron spin polarized 4-amino-2,2,6,6-tetramethyl-1-piperidinyloxyl (ATEMPO) radical in laser photolysis of a benzene solution of benzophenone and ATEMPO and suggested that the CIDEP of ATEMPO was produced by electron spin polarization transfer (ESPT) from the spin polarized triplet molecules to ATEMPO, which was a similar mechanism to TM. On the other hand, a treatment similar to RPM was proposed by Blättler et al.[6] in 1990 for the triplet-doublet complex as the radical triplet pair mechanism (RTPM), where CIDEP of radicals was generated by the mixing of quartet and doublet spin states of triplet-doublet encounter complexes through the zero-field-splitting (zfs) interaction of the triplet molecule. They predicted the generation of net emissive electron spin polarization for the free radicals by RTPM. These two mechanisms predict only net polarization on free radicals, even if both mechanisms

contribute to CIDEP signals.

However, these mechanisms can not explain all signals obtained in radical and triplet molecule systems. In Section 3-3, the hyperfine dependent CIDEP signals of free radicals are shown as well as the net emissive signals, which is also generated by the quartet-doublet mixing in triplet-doublet complexes. These signals are superimposed on net electron spin polarization. As ESPT and RTPM can not interpret the hyperfine dependent CIDEP, a new mechanism which is obtained by a great modification of RTPM is proposed[7] in Section 3-4, in which the hyperfine interaction between triplet and doublet molecules is included to cause the mixing of quartet and doublet spin states. The hyperfine dependence in CIDEP spectra is successfully explained by introducing hyperfine interaction.

In Section 3-5, two main sources of CIDEP generation due to RTPM will be presented to show significant solvents effects. In RPM, Trifunac[8] reported the solvent viscosity effects on CIDEP signal pattern and interpreted them through the contribution of $S-T_{-1}$ mixing in high viscous solvents. Interaction between radicals is strongly affected by their circumstances, which is reflected in CIDEP signal pattern. In analogy with the RPM, such solvent effects are also expected to be reflected in RTPM signals. In the RPM, the $S-T_{-1}$ mixing generates CIDEP at a short distance of the pair whereas the $S-T_0$ mixing does at a long distance.[3,4] Actually the $S-T_{-1}$ mixing is known to be effective in viscous solvents. Considering these results in RPM, the solvent viscosity effects were investigated on RTPM signals.[9] Results obtained indicated the significant viscosity effects : Net polarization is enhanced in viscous solvents compared to hyperfine dependent polarization. Such tendency was also observed in micellar solutions.[9] These results give an important evidence for net and hyperfine dependent polarization sources in RTPM and are interpreted in terms of these two polarizations.

3-2 Experimental

The apparatus of the TR-ESR is described in Chapter II. In the CIDEP measurements, spectra were obtained at room temperature. The sample solutions were deoxygenized by the passage of nitrogen or Ar gases to avoid the broadening of ESR spectra and quenching of the excited states by the solved oxygen. The solutions were flowed through the quartz flat cell normally with 0.5 mm interior space in the ESR cavity. A Quartz flat cell of 0.3 mm interior space was also used especially for the high polarity samples like 1,2-ethanediol or water to avoid the loss of Q value. The flow rate of sample was ca. 2 ml/min.

2,2,6,6-tetramethyl-1-piperidinyloxyl (TEMPO), 4-oxo-2,2,6,6-tetramethyl-1-piperidinyloxyl (OTEMPO) and galvinoxyl [Aldrich] were used as received for the stable free radical. The other chemicals were used as supplied. GR-grade benzene, acetonitrile, 2-propanol and 1,2-ethanediol were used as solvent without further purification.

a) Net Emissive Polarization.

Figure 3-3-1a shows the TR-ESR spectrum of TEMPO obtained in the 308 nm laser photolysis of benzophenone-TEMPO system in benzene. The spectrum observed shows triplet hyperfine structure with net emissive CIDEP pattern. The hyperfine structure is the same as that of CW-ESR spectrum of TEMPO (Fig.3-3-1c) with three peaks of equivalent intensity corresponding to the nuclear spin states of nitrogen atoms. Therefore, the observed TR-ESR spectrum is attributed to TEMPO radical. As the S_1-T_1 ISC rate of benzophenone[10] is 10^{12} s^{-1} which is rapid enough to form the triplet state of benzophenone efficiently, it is appreciated that TEMPO and triplet benzophenone coexist in the system of Fig.3-3-1a in the period from submicro to microseconds after excitation pulse. In this system, reaction of triplet molecule and free radical is neglected because the intensity of CW-ESR spectrum of TEMPO does not change whether the benzophenone is contained in the system or not. As the origins of conventional CIDEP sources are associated with radical formation process or reactions between free radicals, it is impossible to interpret the net emissive signal obtained in benzophenone-TEMPO system by these CIDEP sources. The origin of this net polarization is likely associated with certain interactions between radical and triplet molecule.[2-4] Figure 3-3-1b shows the TR-ESR spectrum obtained in the pyruvic acid-TEMPO system of benzene solution, and net emissive CIDEP signals of TEMPO are also observed in this system. The S_1-T_1 intersystem crossing rate of pyruvic acid is also very fast and most excited molecules undergo triplet state immediately. Hence, this net polarization is also expected to be associated with interactions between radical and triplet molecule.

Table 3-I summarizes the CIDEP signals generated in systems containing nitroxide radical and many kinds of triplet molecules. The radicals used here was TEMPO. Electron spin polarization of triplet states which is caused by the anisotropic intersystem

crossing is also listed on Table 3-I. The spin polarization of triplet molecules is determined from the TM signals for reactive triplet molecules and from spin polarized ESR signals of triplet state for nonreactive molecules. It is noteworthy that the spin polarization of radicals is always emission regardless of the spin polarization of the triplet state.

Imamura et al.[5] proposed ESPT in doublet–triplet systems. Turro et al.[21] also reported the ESPT signal on the nitroxide radical which is chemically combined with photosensitive functional group. However, results obtained here can not be interpreted by this mechanism because all spin polarization would be lost due to spin lattice relaxation within the triplet state (normally 10^{-7} – 10^{-9} s^{-1}) at the radical concentration used here, 6 x 10^{-4} M, which corresponds to the triplet quenching rate of 6 x 10^{6} s^{-1} assuming diffusion controlled quenching. Actually, the triplet molecules with absorptive polarization yield emissive CIDEP radicals. Therefore, this emissive polarization should be attributed to an unknown CIDEP mechanism associated with radical and triplet molecule interactions.

b) Emission/Absorption (E/A) Multiplet Polarization

Figure 3-3-2 shows the TR–ESR spectra of phenazine–OTEMPO and acetone–OTEMPO systems. It is noteworthy that the relative intensity of the three hyperfine lines is different, especially the phase of CIDEP signal changes from emission at $M_I=1$ and 0 to absorption at $M_I=-1$ in acetone–OTEMPO system. Hyperfine dependent CIDEP was observed in various systems. The most intense line is hyperfine peak at $M_I=1$ nuclear spin state of nitrogen atom. The emissive CIDEP intensity diminishes with decrease in quantum number M_I. Several examples in triplet–TEMPO and –OTEMPO systems are summarized in Table 3-II. CIDEP signals were measured in many other triplet–doublet systems which are not shown in Table 3-II, but the hyperfine

dependence is not so strong for most molecules ; typical ratio $(M_1:M_0:M_{-1})$ of the CIDEP intensity is about 1:0.9:0.8 and acetone is only one example showing polarity inversion in hyperfine structure.

Generally, the decay profile of the CIDEP signal depends on the magnetic relaxation time and microwave power as well as the decay of radicals, themselves. Of course, decay of radicals does not affect relative intensity in hyperfine structure but only the integrated intensity of CIDEP. Magnetic relaxation time may depend on M_1.[22] If the decay rate of CIDEP signal of $M_1=-1$ peak is faster than that of $M_1=1$ peak, the CIDEP signal of $M_1=-1$ would be weaker than that of $M_1=1$. Figure 3-3-3 shows CIDEP signals obtained with different delay times. The ratio of signal intensities of three hyperfine peaks does not change significantly in all gate times and hence it is concluded that magnetic relaxation time has no effect on the ratio of the CIDEP signal intensities in our system. CIDEP signals are reported to decay with beat where emissive and absorptive signals recur with time,[23] known as Torrey Oscillation.[24] However, as seen in Fig.3-3-3, no phase modulation with time was observed for all three hyperfine peaks within the first 2 μs after laser pulse. Thus, the hyperfine dependence of CIDEP signals must purely result from triplet-doublet interactions. These hyperfine dependent CIDEP spectra are very similar to E^*/A(Emission*/Absorption) signal pattern of CIDEP in typical RPM.[3] Thus, it is concluded that this E^*/A type signal consists of total emissive and E/A signals. The latter may be generated by some type of hyperfine dependent interaction in the radical-triplet pair.

Table 3-I   Electron spin polarization of free radicals generated
by the interaction of triplet and doublet molecules

Triplet molecule	CIDEP of radical	Spin polarization of triplet state	Ref.
benzophenone	Em.	Em.	[11,12]
phenanthrene	Em.	Em.	[5]
naphthalene	Em.	Em.	[14]
1-nitronaphthalene	Em.	Em.	[15]
4-amino acetophenone	Em.	Em.	[16]
phenazine	Em.	Em.	[17]
biacetyl	Em.	Abs.	[17]
benzil	Em.	Abs.	[18]
9,10-acenaphthene - quinone	Em.	Abs.	[19]
acetone	Em.	Abs.	[19,20]
pyruvic acid	Em.	Abs.	[5,13]

Table 3-II Hyperfine dependence of CIDEP intensity

Triplet molecule	Ratio of the CIDEP intensity for each hyperfine peak $(M_{+1} : M_0 : M_{-1})^a$
benzophenone	1.00 : 0.95 : 0.92
4-aminoacetophenone	1.00 : 0.93 : 0.78
4-benzoylbiphenyl	1.00 : 0.89 : 0.79
benzil	1.00 : 0.89 : 0.78
1-naphthol	1.00 : 0.89 : 0.69
1-chloronaphthalene	1.00 : 0.76 : 0.42
phenazine	1.00 : 0.70 : 0.50
1-nitronaphtalene	1.00 : 0.65 : 0.44
biacetyl	1.00 : 0.59 : 0.18
9,10-acetonaphthene--quinone	1.00 : 0.50 : 0.14
acetone	1.00 : 0.41 : -0.24

a. M_i repesents the hyperfine peak due to M_I = i nuclear spin state of nitroxide radical. A positive sign indicates emissive polarization while a negative sign indicates absorptive one. The ratio of CIDEP intensity include about 5% experimental error.
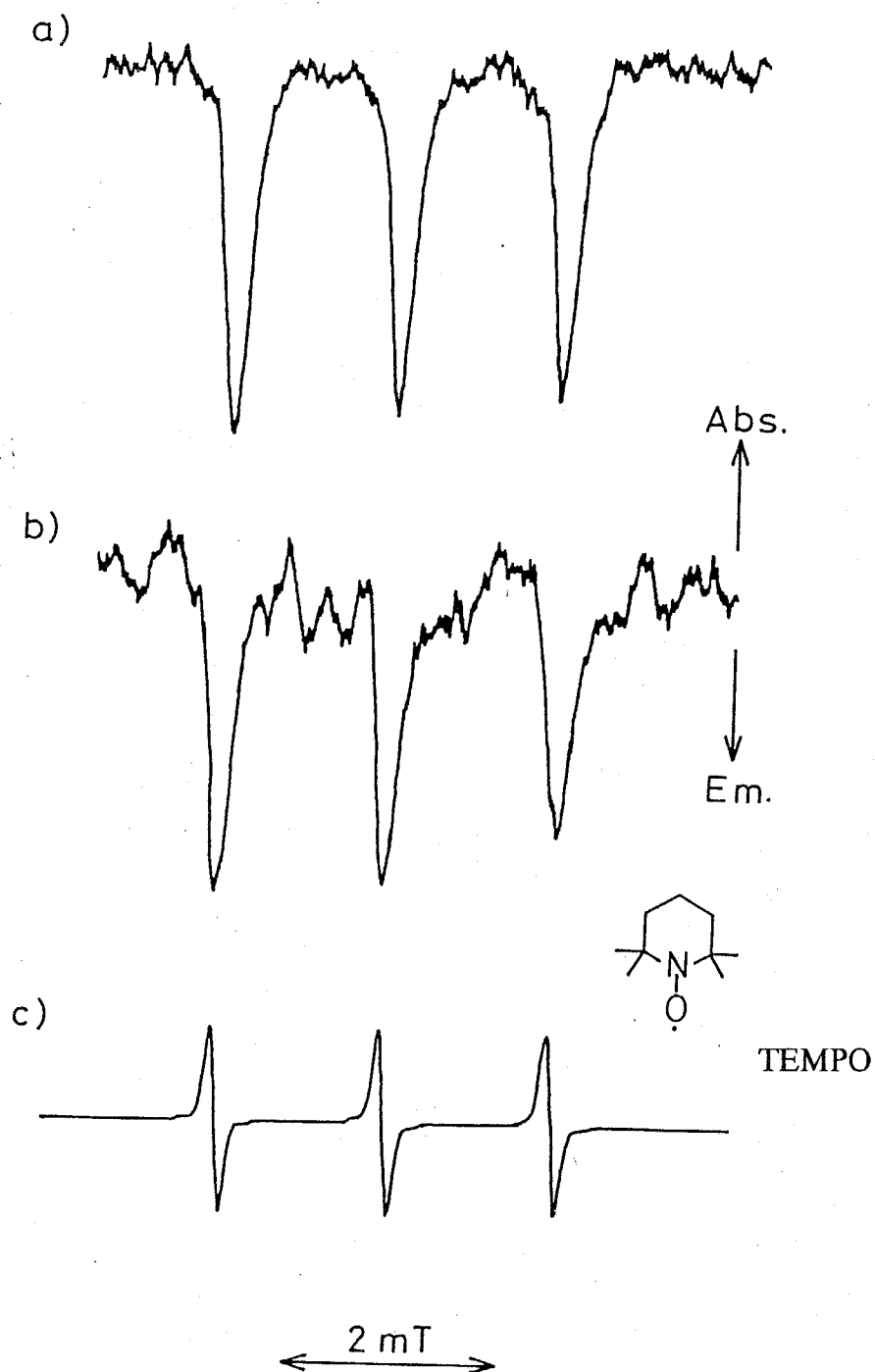
Fig.3-3-1 TR-ESR spectra of TEMPO (0.60 mM) in a) TEMPO and

benzophenone (55 mM) mixture and b)TEMPO and pyruvic acid (72 mM)

in benzene by 308 nm excitation. c)cw-ESR spectrum of TEMPO.

The gate is opened from 1.0 to 1.5 μs after excitation pulse.
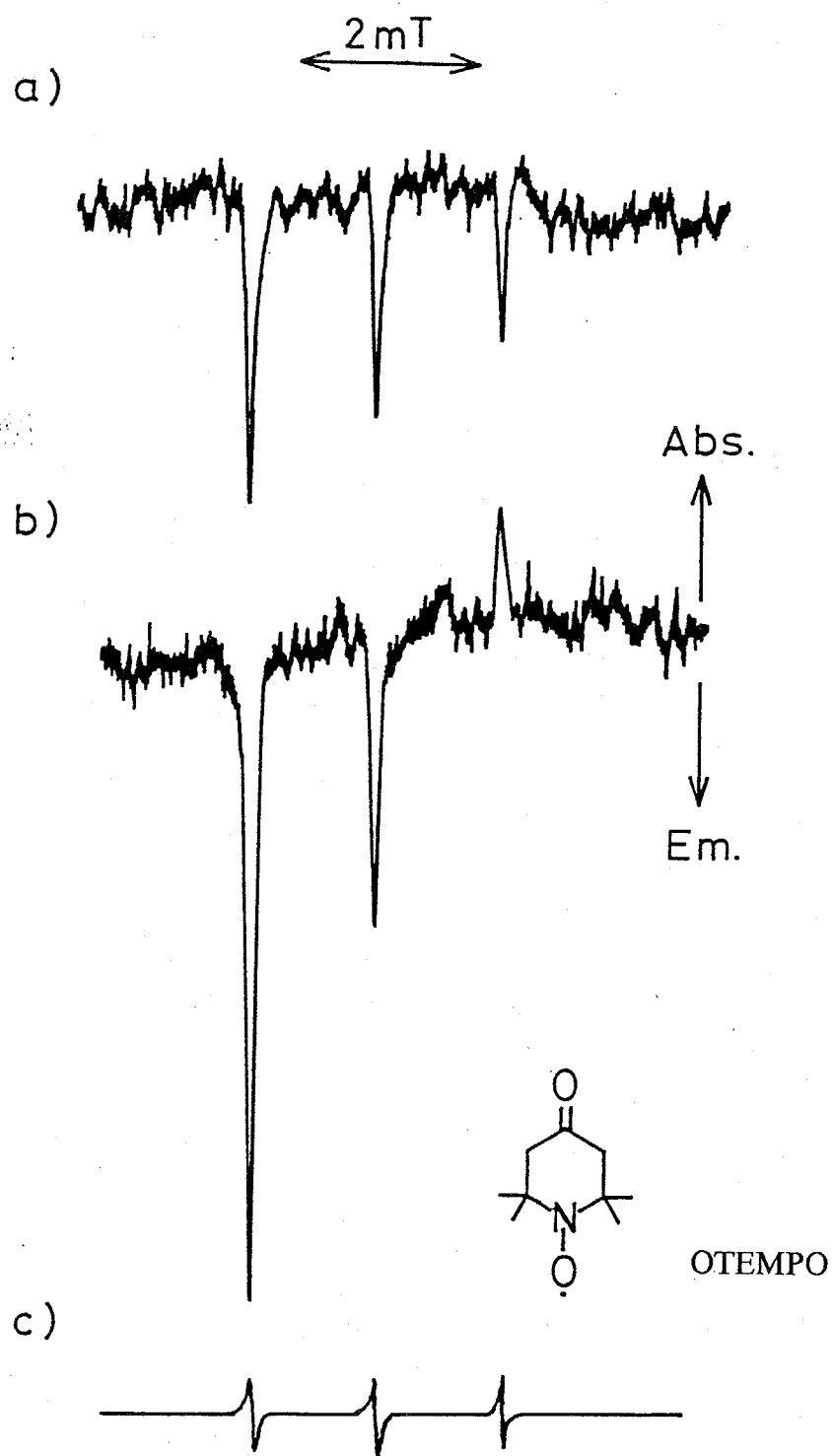
Fig.3-3-2 Hyperfine dependent CIDEP spectra of OTEMPO (0.60 mM) in the
systems of OTEMPO and triplet molecules in benzene. The systems are
a) phenazine (8.3 mM)–OTEMPO and b) acetone (0.68 M)–OTEMPO.
The gate is opened from 1.0 to 1.5 μs after excitation pulse.

37
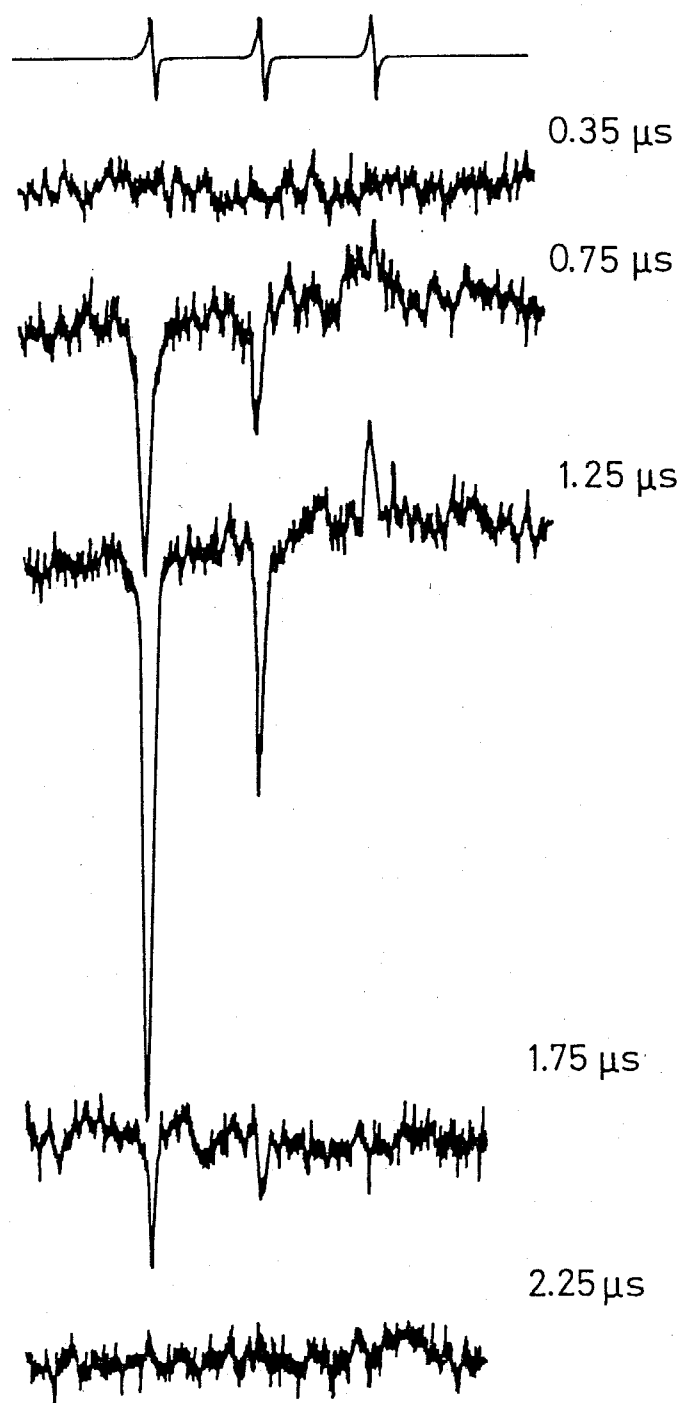
Fig.3-3-3 TR-ESR spectra of OTEMPO (0.60 mM) in the system of
acetone (0.68 M)-OTEMPO in benzene.

3-4 Theory of Radical Triplet Pair Mechanism (RTPM)

a) A Design for RTPM.

New CIDEP generations observed here must be explained by a certain new mechanism which includes the interactions between radical and triplet molecule. Recently Blattler et al.[6] reported the net emissive electron spin polarization on radicals in radical-triplet systems and proposed the radical-triplet pair mechanism for the origin of this polarization. Hence, there is some possibility to explain the net emissive polarization observed here by their mechanism. However, E/A multiplet polarization can not be explained by this mechanism. As the E/A multiplet polarization is hyperfine dependent, it seems to be necessary to include hyperfine interactions in RTPM. Such calculations were easily carried out using the RTPM, and hyperfine dependent polarization was obtained. Results show, however, opposite phase of spin polarization; A/E multiplet polarization. According to this calculation, the RTPM proposed by Blattler et al.[6] is hard to be mainly operative for the spin polarization in radical-triplet systems. As the radical concentration of 6 x 10^{-4} M is high enough to encounter the triplet molecule within microsecond region, and well known F pair RPM[3,4] is based on the interactions between paramagnetic species after the encounter of free radicals, the foundamental concept of RTPM itself seems to be reasonable, in which CIDEP is welling out from the interacting radical and triplet molecule. Therefore, the RTPM should be reexamine to be conformable to both net and multiplet polarization generations.

RTPM has three fundamental old ideas, which have been known well and been used for the discussion of the triplet quenching by free radicals. These ideas are also useful for constructing the mechanism of CIDEP generation in radical-triplet interactions. One is the assumption that the radical and triplet molecule make pairs and they split into doublet and quartet pair states through the electron exchange interaction.[25] Second is that the zero-field-splitting and hyperfine interactions work on the pair as the

perturbations.[25] The last one is the spin selective quenching of triplet state by radical,[26,27] in which only doublet pair states correlate to radical and ground state molecule pair. In RTPM, quartet pair states are initially generated by spin selective quenching and then, perturbations as zfs and hf interactions operate on these pair to generate net emissive and E/A multiplet polarization on radical. The purpose of following sections is to introduce calculation process for the generation of CIDEP of radical through RTPM.

b) Basis Spin Functions and Spin Hamiltonian of Radical–Triplet Pair.

In the radical–triplet molecule pair, one electron of radical and two electrons of triplet molecule are involved in the radical–triplet interactions. Hence, spin states of the pair are described using three electron spin wave functions. Spin wave functions of the pair depend on the separation between radical and triplet molecule. When the pair is separated to zero electron exchange interaction region, eigen states of the pair are represented by the combination of spin states of radical and triplet or ground state molecule. Totally eight spin wave functions are described as follows.

$$T_1 + D_{1/2} \, ,$$
$$T_1 + D_{-1/2} \, , \quad T_0 + D_{1/2} \, , \quad S + D_{1/2} \, ,$$
$$T_{-1} + D_{1/2} \, , \quad T_0 + D_{-1/2} \, , \quad S + D_{-1/2} \, ,$$
$$T_{-1} + D_{-1/2} \, ,$$

Here, these states are rewritten using the one electron spin functions α and β,

$$3/2 \quad : \quad |\alpha\alpha\alpha\rangle$$
$$1/2 \quad : \quad |\alpha\alpha\beta\rangle \, , \quad (|\alpha\beta\alpha\rangle + |\beta\alpha\alpha\rangle)/\sqrt{2} \, , \quad (|\alpha\beta\alpha\rangle - |\beta\alpha\alpha\rangle)/\sqrt{2}$$
$$-1/2 : \quad |\beta\beta\alpha\rangle \, , \quad (|\alpha\beta\beta\rangle + |\beta\alpha\beta\rangle)/\sqrt{2} \, , \quad (|\alpha\beta\beta\rangle - |\beta\alpha\beta\rangle)/\sqrt{2}$$

$$-1/2: \quad | \beta\beta\beta \rangle$$

where numbers at top are magnetic quantum number, and | > means the three electron spin function and first two electron represent the spin state of electrons in HOMO and LUMO of triplet or two HOMO electrons of ground state molecule, whereas the last one represents the SOMO electron of radical.

On the other hand, in the presence of electron exchange interaction between radical and triplet molecule, spin wave functions are obtained as the eigen functions of electron exchange interaction, $H_{ex} = -2J(r)(S_T \cdot S_R)$,[25] where S_T and S_R mean spin angular momentum operators of triplet and radical, respectively, and r is the distance between radical and triplet molecule. Results are as follows.

$$| Q\ 3/2 \rangle = |\alpha\alpha\alpha\rangle$$

$$| Q\ 1/2 \rangle = (|\alpha\alpha\beta\rangle + |\alpha\beta\alpha\rangle + |\beta\alpha\alpha\rangle) /\sqrt{3}$$

$$| Q\ {-1/2} \rangle = (|\beta\beta\alpha\rangle + |\beta\alpha\beta\rangle + |\alpha\beta\beta\rangle) /\sqrt{3}$$

$$| Q\ {-3/2} \rangle = |\beta\beta\beta\rangle$$

$$| D\ 1/2 \rangle = (2|\alpha\alpha\beta\rangle - |\alpha\beta\alpha\rangle - |\beta\alpha\alpha\rangle) /\sqrt{6}$$

$$| D\ {-1/2} \rangle = (2|\beta\beta\alpha\rangle - |\beta\alpha\beta\rangle - |\alpha\beta\beta\rangle) /\sqrt{6}$$

$$| {}^s D\ 1/2 \rangle = (|\alpha\beta\alpha\rangle - |\beta\alpha\alpha\rangle) /\sqrt{2}$$

$$| {}^s D\ {-1/2} \rangle = (|\alpha\beta\beta\rangle - |\beta\alpha\beta\rangle) /\sqrt{2}$$

where Q and D indicate quartet and doublet states of the pairs and $\pm 3/2$, $\pm 1/2$ are magnetic quantum numbers of each state. | ^{s}D> means radical and ground state molecule pair and the others correspond to radical-triplet pair.

According to these spin wave functions, the potentials of each pair state are drawn as shown in Fig.3-4-1 for the distance of radical and triplet molecule in the presence of external magnetic field. In this potential, sign of J(r) is assumed to be negative and

exponential function of r is assumed for J(r) according to usual manner. In RTPM, these pair states are defined as zeroth-order states.

In the radical-triplet pairs, spin sensitive interactions are zfs and hf interactions. These interactions are represented as follows.

$$H_{zfs} = D(S_{Tz}^2 - S_T^2/3) + E(S_{Tx}^2 - S_{Ty}^2) \tag{1}$$

$$H_{hf} = \beta(g_T S_T + g_R S_R) H_0 + \Sigma_i A_{Ti} I_i^{(k)} S_T + \Sigma_j A_{Rj} I_{Rj}^{(l)} S_R \tag{2}$$

where subscripts R and T represent the radical and triplet molecule, respectively. g is the g-tensor, β is the Bohr magneton and H_0 is the external magnetic field. A_{Ri} and A_{Tj} are hyperfine tensors of the ith and jth nuclei. I_{Ri} and I_{Tj} are the nuclear spin angular momentum operator of the ith and jth nuclei. k and l represent nuclear spin states of triplet and radical, respectively. D and E are the zfs constants of the triplet molecule and $T_{x,y,z}$ are the zfs axis of the triplet molecule. As there are several spin operators in these Hamiltonians, the matrices of the operators are summarized in Table 3-III. Density matrix, ρ, used here is defined as follows.

$$\rho = \begin{pmatrix} c_{Q3/2}^* \\ c_{Q1/2}^* \\ c_{D1/2}^* \\ c_{D-1/2}^* \\ c_{Q-1/2}^* \\ c_{Q-3/2}^* \end{pmatrix} \begin{pmatrix} c_{Q3/2} & c_{Q1/2} & c_{D1/2} & c_{D-1/2} & c_{Q-1/2} & c_{Q-3/2} \end{pmatrix}$$

C) Spin Selective Quenching in Radical–Triplet Pairs.

Triplet quenching by free radicals is one of the interesting subjects in the excited states dynamics. Experimental and theoretical studies have been reported on this subject.[28-30] In the RTPM, quenching of triplet state with free radical especially the spin selective quenching is important. Razi Naqvi[26] calculated the matrix elements of triplet-doublet quenching process and evaluated the selection rules of the quenching by electron exchange based on the spin angular momentum. In his treatment, $| Q>$ and $| D>$ states of radical–triplet pair were used as wavefunctions. The initial and final wave functions are represented as follows,

$$^4\psi_i = <Q\pm3/2 | , <Q\pm1/2 | \qquad ^2\psi_i = <D\pm1/2 |$$

$$^2\psi_f = | \, ^sD\pm1/2>$$

The matrix elements between initial and final states are, then given by

$$<^4\psi_i | H_{int} | \, ^2\psi_f> = 0, \qquad <^2\psi_i | H_{int} | \, ^2\psi_f> = - 3/2 \, Q_c \qquad (4)$$

where, H_{int} denotes the interaction energy of initial and final states of the pair and Q_c is the two electron Coulomb integral. Hence, under the weak spin–orbit interaction, selection rule of triplet quenching can be obtained by the above results ; total spin angular momentum of the pair is conserved during the quenching process. At present, this result has not been proved by the direct experimental evidence but indirectly examined by the magnetic field effect of triplet–triplet annihilation rate in the presence of free radicals as triplet quencher.[25,29]

According to the results obtained above, triplet quenching with free radical makes the

doublet states of the radical–triplet pair be less populated than quartet states. After all, in RTPM, quartet spin states of radical–triplet pair are expected to be initially populated through spin selective triplet quenching process.

d) Origin of Net Emissive Polarization.

In this section, origin of net emissive polarization will be explained by introducing the modified RTPM based on the knowledge discussed in the former sections.

In initial stages just after pulsed laser irradiation, triplet molecules are efficiently generated within 10 ns for all systems studied here. As the free radical used is stable and the reactions are hardly observed, the main process of triplet deactivation is the quenching by the free radical due to the energy transfer or enhanced intersystem crossing.[30,31] This process is easily visualized by the potential of radical–triplet pairs (Fig.3-4-1). First, nitroxide radical and photogenerated triplet molecule come across and encounter to split into quartet and doublet states due to the electron exchange interaction weighted with spin statistics. Internal conversion from radical–triplet pairs to radical–ground state molecule pairs occurs selectively in doublet pair states,[26,27] which results in the formation of remaining radical–triplet pair with mainly quartet states. This quartet states will, then, dissociate to free radical and triplet state molecule along the potential surfaces.

In the zeroth–order potential surface, free radicals escaping from the pair have no electron spin polarization because the four unpaired radical–triplet states are equally populated after dissociation. However, on the first–order potential caused by the zfs or hf interactions, population ratios between the four unpaired states are expected to be different. It will be discussed how perturbation affects on the pair potential in the following parts.

Generally, it is estimated to be short time to stay in the none–zero exchange

interaction region for the pair because of the steep slope of the potential curves.[3,4]   The time to stay in this region is estimated to be about 10 ns in normal solvents like benzene. Actually, for the radical pairs, remarkable perturbation effects on CIDEP intensity are hardly observed in none-zero exchange interaction region, except for the pairs with large hyperfine interaction[32] or in the high viscous solvents.[8]   Large hf interaction (>10 mT, which corresponds to the mixing rate of faster than 3×10^8 s^{-1} even in case of degenerated levels) causes the rapid state mixing during the very short time of the pair staying in none-zero exchange interaction and generates the CIDEP on radicals.   High viscosity restricts the diffusion motion of the pair and remarkable state mixing occurs with the weak hf interaction.   Most radical pairs, however, have small hf interaction (10 mT>) and it is almost impossible to generate the state mixing in effective J region.   On the other hand, radical-triplet pair has the zfs interaction as well as hf interaction.   The zfs interaction is able to cause the state mixing, even in the non-zero J region because its maximum value is normally about 100 mT which corresponds to a state mixing rate of 3 $\times 10^9$ s^{-1}.   Therefore, the state mixing by the zfs interaction[25] is considered to be important in RTPM.   In the following discussion, only zfs interaction is considered and hf interaction is extracted.

The zfs interaction has two parameters, D and E values.   These values are summarized in Table 3-IV for the molecules used here.   Generally, E value is small compared to D value.   Thus, it can be safely omitted in the zfs interaction to simplify the mixing model.   By this approximation, the zfs interaction is represented as follows,

$$H_{zfs} = D(S_{Tz}^2 - S_T^2/3) \qquad (5)$$

In this interaction, x y and z axis of triplet molecule are in the molecular flame and are different from experimental coordinate.   Orientation between molecular and experimental axis depends on the rotation of triplet molecule.   As it is too complicate to

consider the random rotation of triplet molecule for the mixing magnitude, three ideal rotations are selected in the calculation ; triplet molecule rotates around the x, y, or z experimental axis. This is the same treatment with RTPM by Blättler et. al.[6] The matrix elements for each case are calculated with H_{zfs} as Table 3-III and results are summarized in Table 3-V. According to the Table 3-V, state mixing is allowed within | Q-3/2>, | Q1/2> and | D1/2> states and also allowed within | Q3/2>, | Q-1/2> and | D-1/2> states. It is noticeable that $<Q3/2 \mid H_{zfs} \mid D-1/2>$ is the same with $<Q-3/2 \mid H_{zfs} \mid D1/2>$ and $<Q1/2 \mid H_{zfs} \mid D1/2>$ is also same with $<Q-1/2 \mid H_{zfs} \mid D-1/2>$. According to these matrix elements, the potential surfaces should be modified in the first order like Fig. 3-4-2 assuming J<0. The crossing region of | Q-3/2> and | D1/2> states is considered to be the avoided crossing.

In this potential, the dissociation of quartet pairs to the free radical and triplet molecule yields the different results from that in zeroth-order shown in Fig.3-4-1. In this case, | Q-3/2> state is converted to the | D1/2> due to the avoided crossing. Hence the spin polarization will be generated because of the lack of | Q-3/2> state which correlates to the β spin state of radical. Assuming that the main perturbation operates on the | Q-3/2> and | D1/2> states and the other mixing can be ignored because of the Zeeman splitting, spin polarization of the free radical dissociated from the pair is calculated using the spin operator, S_{Rz} and density matrix, ρ, which is represented as follows.

$$\rho = \begin{pmatrix} 1 & 0 & 0 & 0 & 0 & 0 \\ 0 & 1 & 0 & 0 & 0 & 0 \\ 0 & 0 & p^2 & 0 & 0 & (1-p)p \\ 0 & 0 & 0 & 0 & 0 & 0 \\ 0 & 0 & 0 & 0 & 1 & 0 \\ 0 & 0 & p(1-p) & 0 & 0 & (1-p)^2 \end{pmatrix}$$

46

where p is the parameter and $p/\{(1-p)^2+p^2\}$ means the probability of transmittance from the $|$ Q–3/2> to $|$ D1/2> state. Then, spin polarization of radical is obtained as follows,

$$P_{sp} = tr(S_{Rz}\rho) = p/3 \qquad (6)$$

Positive sign means emissive polarization in which α spin state is more populated than β spin state. This result shows that the free radical will be net emissively polarized through the interactions between radical–triplet pair.

If the J value of this pair is positive, spin polarization must be opposite phase of above result and free radical shows net absorptive polarization. This is against the experimental results and, thus, the J value should be negative according to this mechanism.

e) Origin of the E/A Multiplet Polarization

The zfs interaction produces net emissive polarization as discussed above but it can not generate the E/A multiplet polarization. On the other hand, the hyperfine interaction could yield the hyperfine dependent CIDEP on radicals. Thus, the state mixing by hf interaction should be discussed. Selection rules of Q–D mixing by isotropic hf interaction is summarized in Table 3–VI. If the hf interaction acts on the mixing of the $|$ Q–3/2> and $|$ D1/2> states in addition to the zfs interaction, hyperfine lines of net emissive CIDEP have different relative intensity. However, the matrix element of hf interaction between the $|$ Q–3/2> and $|$ D1/2> states is zero and hence hf interaction does not contribute this state mixing. As for the mixing of $|$ Q–1/2> and $|$ D1/2> and that of $|$ Q–3/2> and $|$ D–1/2>, hf interaction is effective but its magnitude is thought to be small because the encounter pair exists for short time in the crossing region compared to the mixing time due to hf interaction. Therefore, another mechanism should be

examine for E/A multiplet polarization.

It is well known that spin polarization by RPM results from $S-T_0$ mixing followed by a fast electron exchange interaction.[3] The similar process is expected for triplet–doublet system. First, two couples of degenerated levels are considered as the mixing states, which are | Q1/2> − | D1/2> states and | Q−1/2> − | D−1/2> states. In RPM, if J is constant for the period of $S-T_0$ mixing with its rate of ω_{ab}, paired radicals must exist at separation of $J=\omega_{ab}$ for 10^{-7}–10^{-9} s, which is almost improbable.[3] Mixing rates of | Q1/2> − | D1/2> states and | Q−1/2> − | D−1/2> states were estimated to be about the same order with ω_{ab} as discussed above. Therefore, on the analogy of RPM, it is possible to assume that the triplet–doublet pair experiences an initial period of Q–D mixing by H_{hf} from t = 0 to t_1 and then, exchange interaction acts on the pair during the reencounter of the pair caused by diffusion in the period from t_1 to t_2. This process is illustrated in Fig.3–4–3 together with the potential of the pair. In this model, anisotropic terms of g tensors and hyperfine tensors are omitted because the rapid free rotations of doublet and triplet molecules would average the effect of anisotropic interaction in the period of slow Q – D mixing and do not contribute to the state mixing. The mixing among different Zeeman levels is considered to have a much smaller mixing rate compared to | Q1/2> − | D1/2> and | Q−1/2> − | D−1/2> mixing because of the large energy difference of the states under experimental condition of high magnetic field (about 340 mT) compared to the matrix elements of interaction. Thus, the mixing among different Zeeman levels is also neglected.

As discussed before, the doublet pairs mainly disappear through triplet quenching and the quartet pairs remain in the initial spin state. The time evolution of density matrix is obtained using the Liouville equation as follows

$$\partial\rho(t)/\partial t = [\rho(t), H] \qquad (7)$$

48

In this case, Hamiltonians are written as follows,

$$
H(t=0-t_1) = \begin{pmatrix} 0 & 0 & 0 & 0 & 0 & 0 \\ 0 & 0 & \omega_{kl} & 0 & 0 & 0 \\ 0 & \omega_{kl} & 0 & 0 & 0 & 0 \\ 0 & 0 & 0 & 0 & -\omega_{kl} & 0 \\ 0 & 0 & 0 & -\omega_{kl} & 0 & 0 \\ 0 & 0 & 0 & 0 & 0 & 0 \end{pmatrix}
$$

and

$$
H(t=t_1-t_2) = \begin{pmatrix} -J+\frac{3}{2}g\beta H_0 & 0 & 0 & 0 & 0 & 0 \\ 0 & -J+\frac{1}{2}g\beta H_0 & 0 & 0 & 0 & 0 \\ 0 & 0 & 2J+\frac{1}{2}g\beta H_0 & 0 & 0 & 0 \\ 0 & 0 & 0 & 2J-\frac{1}{2}g\beta H_0 & 0 & 0 \\ 0 & 0 & 0 & 0 & -J-\frac{1}{2}g\beta H_0 & 0 \\ 0 & 0 & 0 & 0 & 0 & -J-\frac{3}{2}g\beta H_0 \end{pmatrix}
$$

where ω_{kl} is obtained by the hf interaction (2) as

$$
\omega_{kl} = <Q1/2 \mid H_{hf} \mid D1/2>
$$
$$
= \sqrt{2/3} \; X \; \{(g_T-g_R)\beta H_0 + \Sigma_i a_{Ti}^{(k)} - \Sigma_j a_{Rj}^{(l)}\}. \tag{10}
$$

Electron spin polarization of radical is obtained as the results of $\text{tr}\{S_{Rz}\,\rho(t_2)\}$ which is written as follows,

$$
<S_{Rz}(t_2)> = 2 \; 2/3 \; x \; \sin\{3J(t_2-t_1)\} \; x \; \{\sin(2\omega_{kl}t_1)\} \tag{11}
$$

49

In the fluid media, molecular motions are described by the diffusion theory and hence, time averaged value of $<S_{Rz}(t_2)>$ must be calculated due to the diffusion theory. According to the diffusion theory,[35] the probability of reencounter is represented as follows,

$$dP(R \rightarrow R\sigma, t \mid R_0, 0) = 1/3 \times (t/\tau)^{-3/2} d(t/\tau) \qquad (12)$$

where R is the distance of the pair, R_0 is the initial separation of the pair, R_σ is the limited distance of the pair under effective exchange interaction, and τ is the time between diffusive displacements of molecules.

Therefore, time averaged spin polarization by equation (12) is given by

$$<S_{Rz}(t_2)>_t = 1/3 \times \int_0^\infty <S_{Rz}(t_2)> \times (t_1/\tau)^{-3/2} d(t_1/\tau)$$

$$= 4\sqrt{2}\pi/9 \times <\sin\{3|J|(t_2 - t_1)\}> \times \omega_{kl}J/|\omega_{kl}J| \times \sqrt{|\omega_{kl}|\tau} \qquad (13)$$

where $<\sin\{3 \mid J \mid (t_2-t_1)\}>$ is the averaged value of $\sin\{3 \mid J \mid (t_2-t_1)\}$. As this crude result includes ω_{kl}, it is predicted that the magnitude of CIDEP intensity depends on each hyperfine line, which is considered to be the origin of the E/A multiplet polarization.

Now, origins of two electron spin polarization are clarified, and in next section, these mechanisms will be examined with the aid of computer simulation.

f) Test of Theory.

According to the above discussion, two sources of CIDEP are revealed. Net emissive polarization is easily understood but the mechanism of multiplet polarization must be ensured by reproducing the observed spectra by the theory because the results for

50

E/A multiplet polarization are too complicated to understand directly.

Relative magnitude of electron spin polarization of k nuclear spin state of radical is obtained by the following equation

$$P_R(k) = \Sigma_l(C_l \times P_R(kl)) \tag{14}$$

where C_l is the relative population of l nuclear state of triplet molecule and $P_R(kl)$ is the electron spin polarization generated by the interaction of k and l nuclear states of radical and triplet molecule, respectively, which is calculated by equation (13). In the TR–ESR spectra, the intensity of the line is proportional to the relative population, C_k, of k nuclear spin state as well as the electron spin polarization of the state. Hence, the relative intensity of k nuclear state of radical is finally given by

$$I_R(k) = C_k \times P_R(k) \tag{15}$$

From this equation, one can obtain the simulated spectra of radical caused by the RTPM.

Unfortunately, the hyperfine coupling constant of most triplet molecules has not been reported. Thus, hyperfine structure of triplet state was assumed to be concentrated on the g center as shown in Fig.3–4–4. ω_{kl} can be obtained from the ESR spectra as indicated in the Fig.3–4–4. The g center of the triplet molecule is generally 2.0030, and that of TEMPO is measured to be 2.0058. Using these parameters, simulated spectrum of TEMPO is obtained as shown in Fig.3–4–5a. This spectrum shows E/A multiplet pattern with weak net emissive polarization. The latter is attributed to the Δg effect of radical and triplet molecule and is different from the net emissive polarization generated by zfs interaction. The observed spectrum in the acetone–OTEMPO system is similar to the simulated one. Addition of net emissive polarization due to zfs interaction makes the

simulated spectrum well fitted with the observed one. The observed spectra of many radical–triplet systems can be also reproduced by the sum of these two simulated spectra with proper ratios.

Table 3-III

$$S_{T_z}^2 = \begin{pmatrix} 1 & 0 & 0 & 0 & 0 & 0 \\ 0 & \dfrac{1}{3} & \dfrac{\sqrt{2}}{3} & 0 & 0 & 0 \\ 0 & \dfrac{\sqrt{2}}{3} & \dfrac{2}{3} & 0 & 0 & 0 \\ 0 & 0 & 0 & \dfrac{2}{3} & \dfrac{\sqrt{2}}{3} & 0 \\ 0 & 0 & 0 & -\dfrac{\sqrt{2}}{3} & \dfrac{1}{3} & 0 \\ 0 & 0 & 0 & 0 & 0 & 1 \end{pmatrix}$$

$$S_{T_x}^2 = \begin{pmatrix} \dfrac{1}{2} & 0 & 0 & \dfrac{\sqrt{6}}{6} & \dfrac{\sqrt{3}}{6} & 0 \\ 0 & \dfrac{5}{6} & -\dfrac{\sqrt{2}}{6} & 0 & 0 & \dfrac{\sqrt{3}}{6} \\ 0 & -\dfrac{\sqrt{2}}{6} & \dfrac{2}{3} & 0 & 0 & \dfrac{\sqrt{6}}{6} \\ \dfrac{\sqrt{6}}{6} & 0 & 0 & \dfrac{2}{3} & -\dfrac{\sqrt{2}}{6} & 0 \\ \dfrac{\sqrt{3}}{6} & 0 & 0 & -\dfrac{\sqrt{2}}{6} & \dfrac{5}{6} & 0 \\ 0 & \dfrac{\sqrt{3}}{6} & \dfrac{\sqrt{6}}{6} & 0 & 0 & \dfrac{1}{2} \end{pmatrix}$$

$$S_{T_y}^2 = \begin{pmatrix} \dfrac{1}{2} & 0 & 0 & -\dfrac{\sqrt{6}}{6} & -\dfrac{\sqrt{3}}{6} & 0 \\ 0 & \dfrac{5}{6} & -\dfrac{\sqrt{2}}{6} & 0 & 0 & -\dfrac{\sqrt{3}}{6} \\ 0 & -\dfrac{\sqrt{2}}{6} & \dfrac{2}{3} & 0 & 0 & -\dfrac{\sqrt{6}}{6} \\ -\dfrac{\sqrt{6}}{6} & 0 & 0 & \dfrac{2}{3} & -\dfrac{\sqrt{2}}{6} & 0 \\ -\dfrac{\sqrt{3}}{6} & 0 & 0 & -\dfrac{\sqrt{2}}{6} & \dfrac{5}{6} & 0 \\ 0 & -\dfrac{\sqrt{3}}{6} & -\dfrac{\sqrt{6}}{6} & 0 & 0 & \dfrac{1}{2} \end{pmatrix}$$

Table 3-III (continued)

$$S_{R_z} = \begin{pmatrix} \frac{1}{2} & 0 & 0 & 0 & 0 & 0 \\ 0 & \frac{1}{6} & -\frac{\sqrt{2}}{3} & 0 & 0 & 0 \\ 0 & -\frac{\sqrt{2}}{3} & -\frac{1}{6} & 0 & 0 & 0 \\ 0 & 0 & 0 & \frac{1}{6} & \frac{\sqrt{2}}{3} & 0 \\ 0 & 0 & 0 & \frac{\sqrt{2}}{3} & -\frac{1}{6} & 0 \\ 0 & 0 & 0 & 0 & 0 & -\frac{1}{2} \end{pmatrix}$$

$$S_{R_x} = \begin{pmatrix} 0 & \frac{\sqrt{3}}{6} & \frac{\sqrt{6}}{6} & 0 & 0 & 0 \\ \frac{\sqrt{3}}{6} & 0 & 0 & -\frac{\sqrt{2}}{6} & \frac{1}{3} & 0 \\ \frac{\sqrt{6}}{6} & 0 & 0 & \frac{1}{6} & -\frac{\sqrt{2}}{6} & 0 \\ 0 & -\frac{\sqrt{2}}{6} & \frac{1}{6} & 0 & 0 & \frac{\sqrt{6}}{6} \\ 0 & \frac{1}{3} & -\frac{\sqrt{2}}{6} & 0 & \frac{1}{3} & \frac{\sqrt{3}}{6} \\ 0 & 0 & 0 & \frac{\sqrt{6}}{6} & \frac{\sqrt{3}}{6} & 0 \end{pmatrix}$$

$$S_{R_y} = \begin{pmatrix} 0 & \frac{\sqrt{3}}{6}i & \frac{\sqrt{6}}{6}i & 0 & 0 & 0 \\ -\frac{\sqrt{3}}{6}i & 0 & 0 & -\frac{\sqrt{2}}{6}i & \frac{1}{3}i & 0 \\ -\frac{\sqrt{6}}{6}i & 0 & 0 & \frac{1}{6}i & -\frac{\sqrt{2}}{6}i & 0 \\ 0 & \frac{\sqrt{2}}{6}i & -\frac{1}{6}i & 0 & 0 & \frac{\sqrt{6}}{6}i \\ 0 & -\frac{1}{3}i & \frac{\sqrt{2}}{6}i & 0 & 0 & \frac{\sqrt{3}}{6}i \\ 0 & 0 & 0 & -\frac{\sqrt{6}}{6}i & -\frac{\sqrt{3}}{6}i & 0 \end{pmatrix}$$

Table 3-IV zfs parameters of organic compounds

	$\mid D \mid$ cm^{-1}	$\mid E \mid$ cm^{-1}
benzophenone	0.1581	0.0211
phenanthrene	0.0998	0.0438
naphthalene	0.0994	0.0154
phenazine	0.07509	0.01112
biacetyl	0.2048	0.0167
benzil	0.1191	0.0253
acetone	0.158	0.0449

All data from reference 33 except acetone from 20.

Table 3-V

matrix elements of zfs interaction

< case1 > rotate along Z axis

$$
H_{zfs} = \begin{pmatrix}
0 & 0 & 0 & 0 & 0 & 0 \\
0 & 0 & \frac{\sqrt{2}}{3}D & 0 & 0 & 0 \\
0 & \frac{\sqrt{2}}{3}D & 0 & 0 & 0 & 0 \\
0 & 0 & 0 & 0 & \frac{\sqrt{2}}{3}D & 0 \\
0 & 0 & 0 & \frac{\sqrt{2}}{3}D & 0 & 0 \\
0 & 0 & 0 & 0 & 0 & 0
\end{pmatrix}
$$

< case2 > rotate along Y axis

$$
H_{zfs} = \begin{pmatrix}
0 & 0 & 0 & \frac{\sqrt{6}}{18}D & 0 & 0 \\
0 & 0 & -\frac{\sqrt{2}}{6}D & 0 & 0 & 0 \\
0 & -\frac{\sqrt{2}}{6}D & 0 & 0 & 0 & \frac{\sqrt{6}}{18}D \\
\frac{\sqrt{6}}{18}D & 0 & 0 & 0 & -\frac{\sqrt{2}}{6}D & 0 \\
0 & 0 & 0 & -\frac{\sqrt{2}}{6}D & 0 & 0 \\
0 & 0 & \frac{\sqrt{6}}{18}D & 0 & 0 & 0
\end{pmatrix}
$$

< case3 > rotate along X axis

$$
H_{zfs} = \begin{pmatrix}
0 & 0 & 0 & \frac{\sqrt{6}}{6}D & 0 & 0 \\
0 & 0 & -\frac{\sqrt{2}}{6}D & 0 & 0 & 0 \\
0 & -\frac{\sqrt{2}}{6}D & 0 & 0 & 0 & \frac{\sqrt{6}}{6}D \\
\frac{\sqrt{6}}{6}D & 0 & 0 & 0 & -\frac{\sqrt{2}}{6}D & 0 \\
0 & 0 & 0 & -\frac{\sqrt{2}}{6}D & 0 & 0 \\
0 & 0 & \frac{\sqrt{6}}{6}D & 0 & 0 & 0
\end{pmatrix}
$$

Table 3-VI

Selection rule of Q-D mixing by hyperfine interaction

	Q3/2	Q1/2	D1/2	D-1/2	Q-1/2	Q-3/2
Q3/2	allowed	allowed	allowed	forbidden	forbidden	forbidden
Q1/2	allowed	allowed	allowed	allowed	allowed	forbidden
D1/2	allowed	allowed	allowed	allowed	allowed	forbidden
D-1/2	forbidden	allowed	allowed	allowed	allowed	allowed
Q-1/2	forbidden	allowed	allowed	allowed	allowed	allowed
Q-3/2	forbidden	forbidden	forbidden	allowed	allowed	allowed
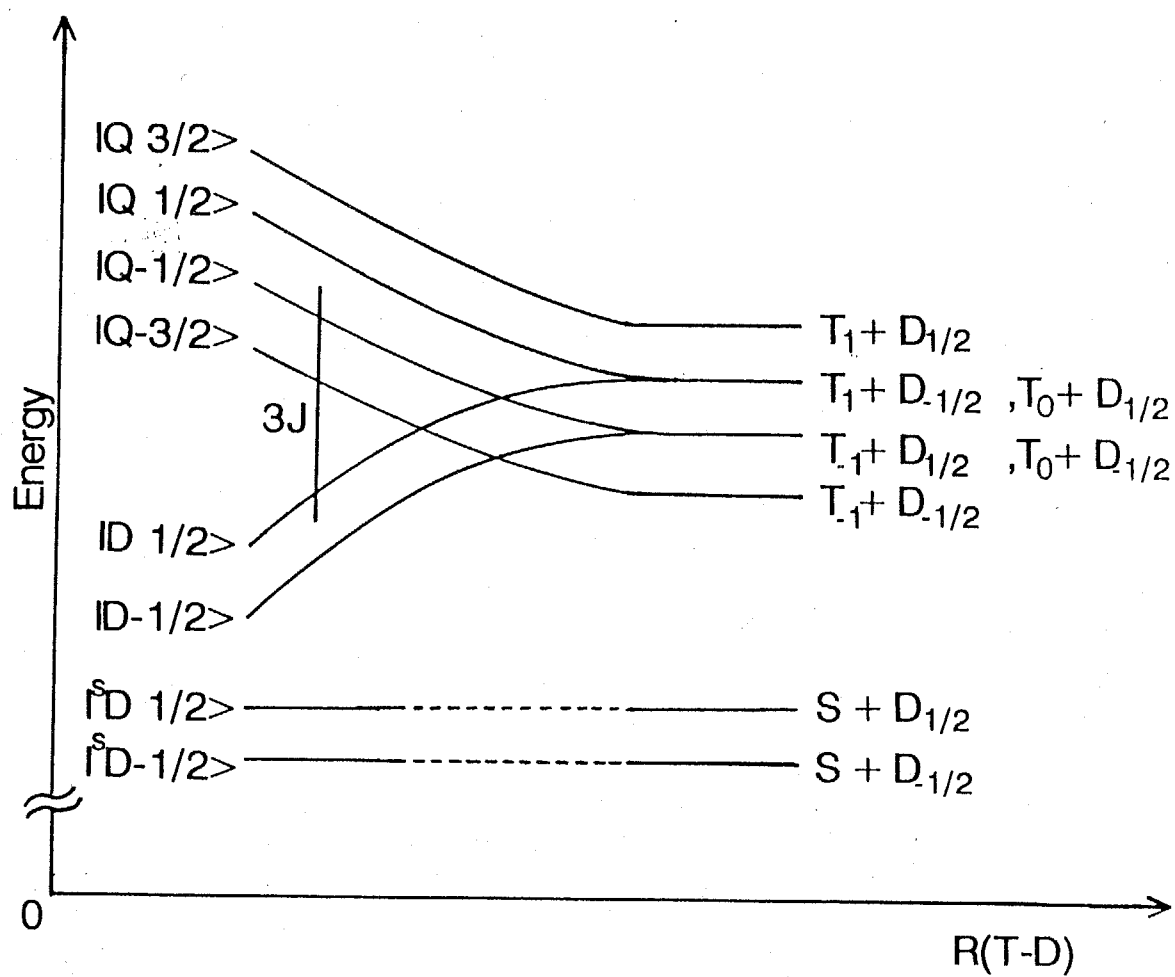
Fig.3–4–1 Energy diagram of the spin states of the
triplet–doublet encounter complex assuming J<0.

58
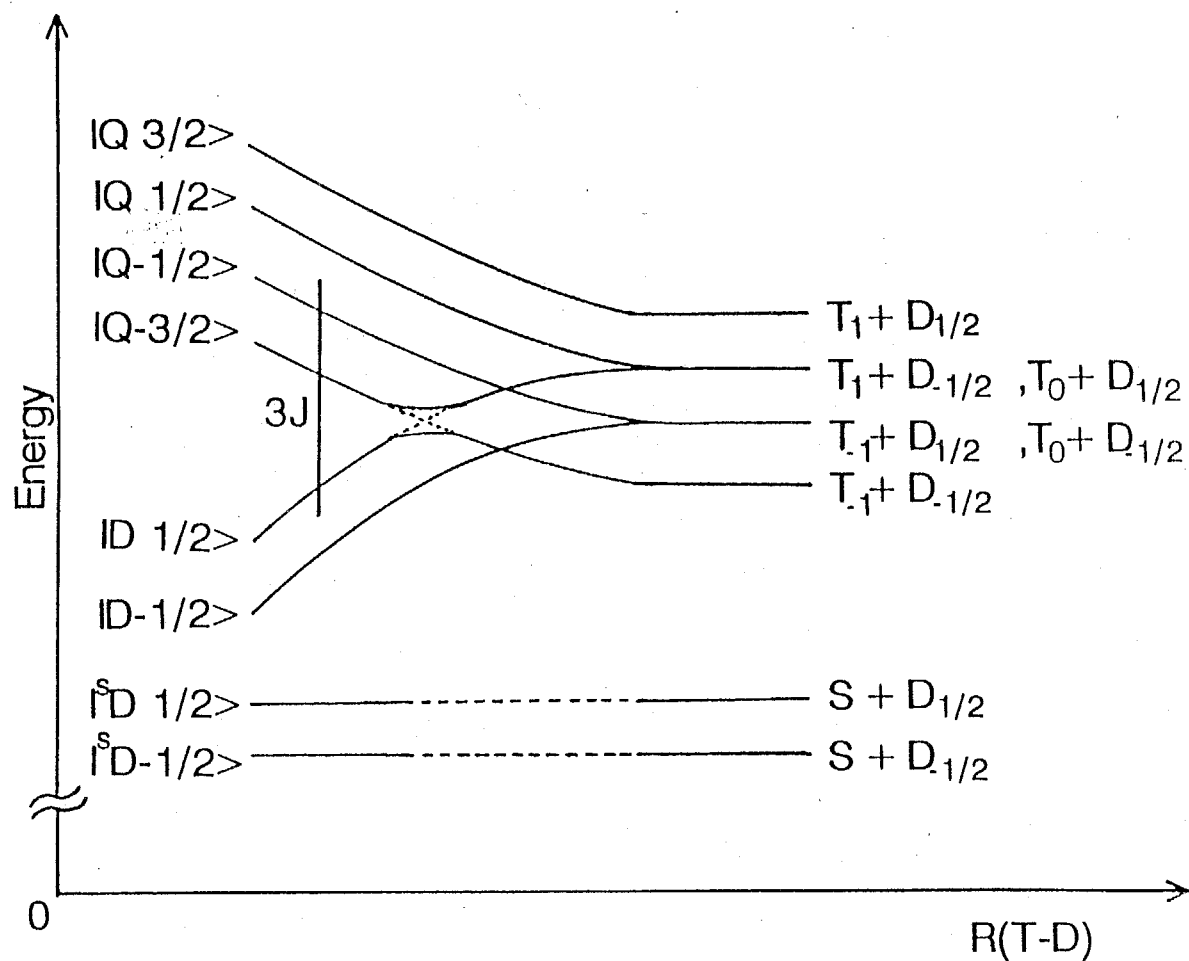
Fig.3–4–2 Energy diagram and state mixing of spin states of the

triplet–doublet encounter complex by zfs interaction assuming J<0.

escape

re-encounter

$t=t_1$

$t=t_2$

R_σ (T)

(R) $t=0$

first collision

electron exchange (3J)

Q-D mixing (hyperfine interaction)

Q3/2>
Q1/2>
Q-1/2>
Q-3/2>

D1/2>
D-1/2>

Energy

0

R_σ

R(T-D)
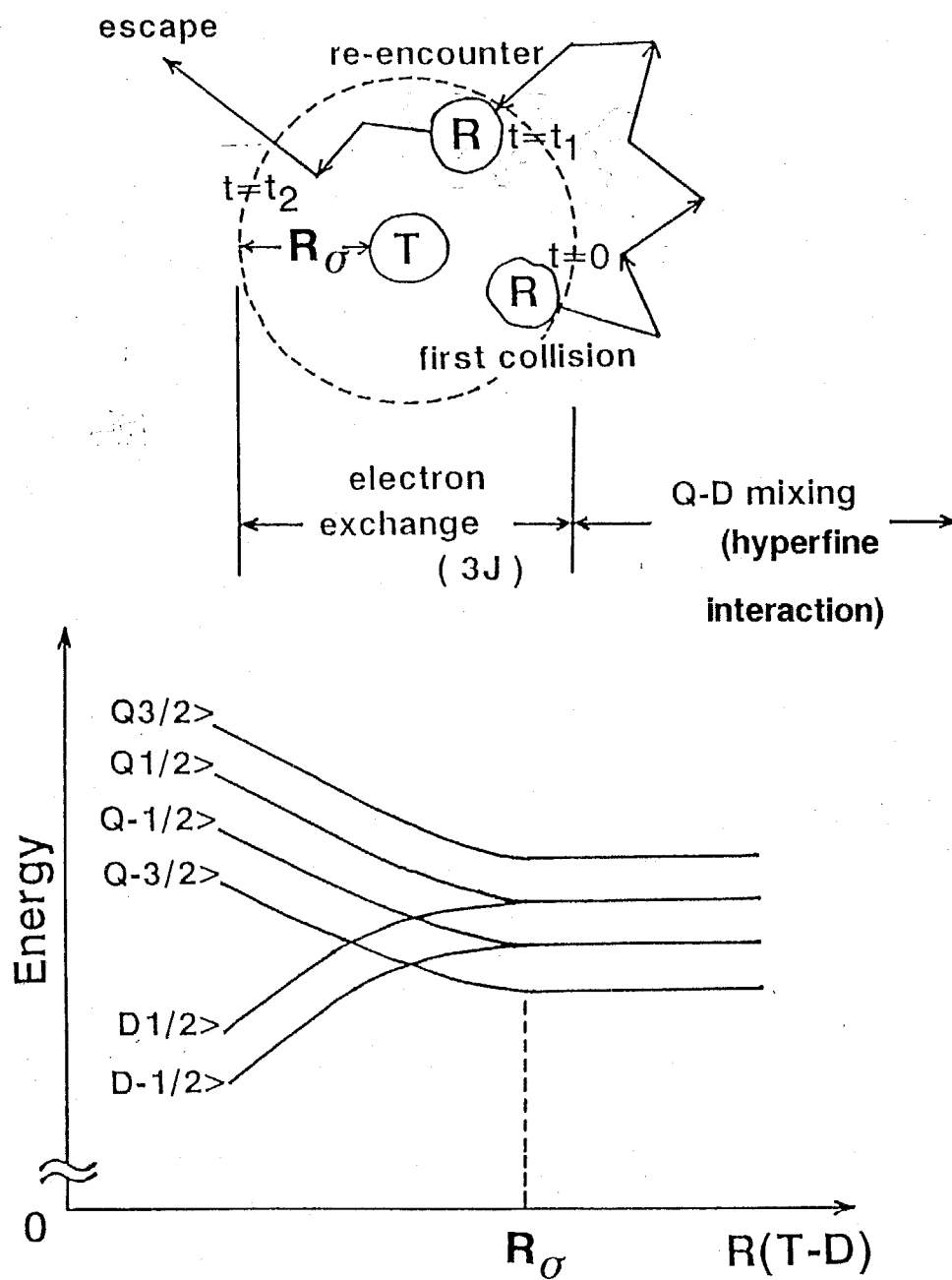
Fig.3-4-3 Diffusion controlled radical triplet pair separation and re-encounter.

Fig.3–4–4 g value of triplet state is assumed to be 2.003. Lower is the CIDEP

spectrum of OTEMPO obtained in acetone–OTEMPO system.

hf interaction energy, ω_{kl}, is measured from the spectrum.
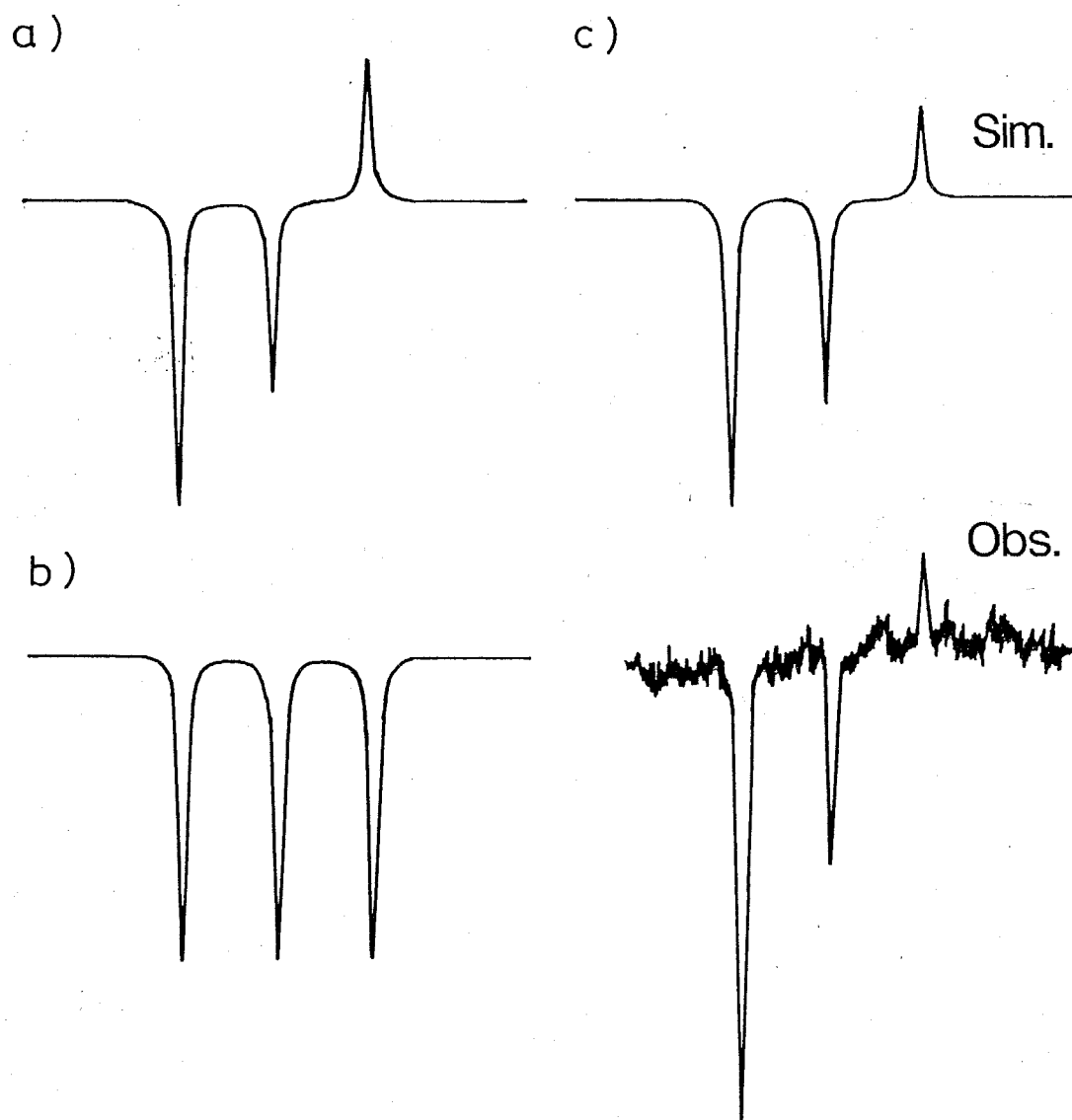
Fig.3-4-5 a) Simulated spectra of OTEMPO obtained by eq.(13), b) assuming net

emissive polarization and c) by a sum of a) and b) with a ratio of 3 : 2

and observed spectrum of acetone–OTEMPO system.

3–5 Solvent Effects on Net and Multiplet Polarization.

a) Viscosity Dependence of RTPM Signals.

In the above discussion, the new mechanism of CIDEP generation in the radical and triplet pair was constructed and the simulation for the observed spectrum was demonstrated. To confirm this new mechanism, solvent effects on CIDEP signals are studied in the following sections.

Figure 3–5–1 shows the CIDEP spectra of the 1–chloronaphthalene–TEMPO system in various solvents. The spectra obtained were assigned to spin polarized TEMPO from its triplet hyperfine structure. The spectrum in benzene solution shows remarkable hyperfine dependence, which is interpreted as the superposition of E/A multiplet pattern and net emissive polarization. However, the CIDEP spectrum in 2–propanol solution is different from that in benzene, in which hyperfine dependent polarization is relatively reduced. This tendency was also observed in 1,2–ethanediol solution and each emissive line ap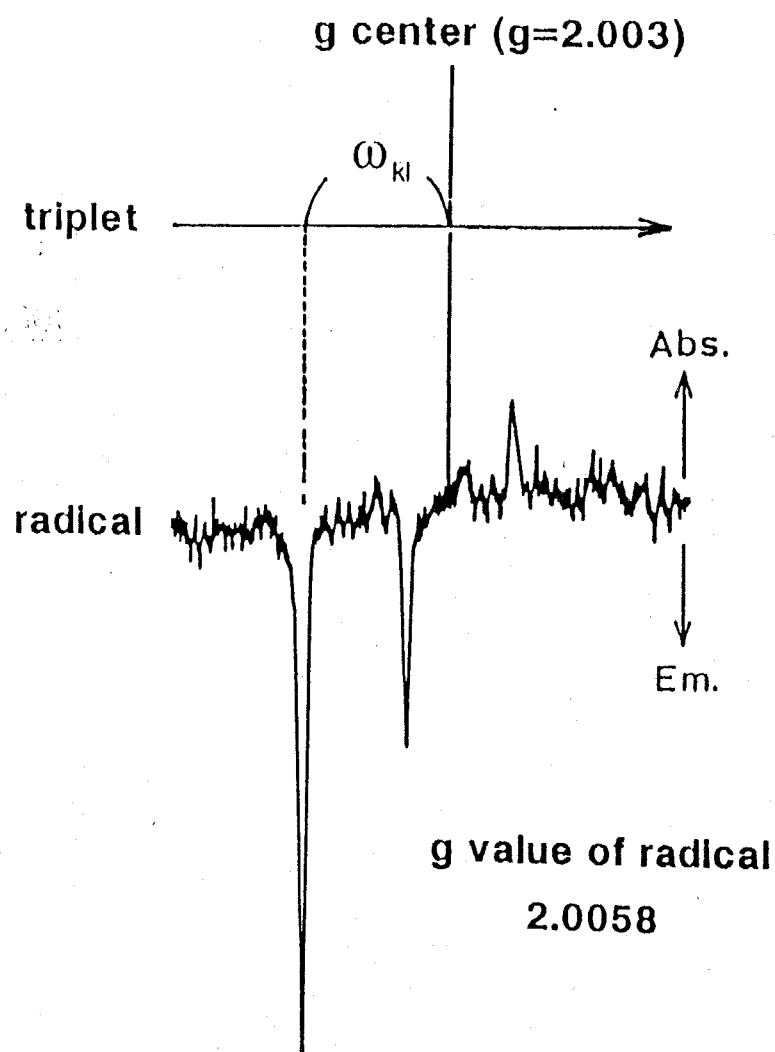peared with almost the same intensities. On the other hand, in acetonitrile solution, net emissive polarization was reduced and the hyperfine peak of $M_I=-1$ is almost vanished. The ratios of net and multiplet polarization are determined by the simulation of the spectra obtained according to the method introduced in section 3–4–f) and summarized in Table 3–VII. The solvents used have different viscosity; η(acetonitrile)=0.345, η(benzene)=0.649, η(2–propanol)=2.869 and η(1,2–ethanediol)=26.09 [CP].[36] The following rule is found for the results : net emissive polarization is enhanced with the increase in solvent viscosity compared to hyperfine dependent polarization. Similar results were obtained in the 9,10–acenaphthenequinone(ANQ)–TEMPO system(Fig.3–5–2) : Hyperfine dependence is also reduced in this system with the increase in solvent viscosity. The trace of the alcoholic radical was observed in 2–propanol solution, which was generated by the hydrogen abstraction reaction of ANQ. The similar experiments were carried out in other triplet–

TEMPO systems and the decrease in hyperfine dependent CIDEP was also observed in these systems with increase in solvent viscosity.

b) RTPM Signals in Micellar Solution

The continuous wave ESR spectrum of TEMPO was measured in aqueous SDS micellar solution as shown in Fig.3-5-3a, which shows triplet hyperfine peaks with different intensity, though the remarkable M_I dependence was not observed in other solutions like benzene and 2-propanol. Line width of the ESR spectra generally depends on the M_I and is determined by the following equation,[22]

$$\Delta H = \tau(a + bM_I + cM_I^2) \qquad (16)$$

where τ is the correlation time of the rotational motion of radical. Therefore, the relative rotational correlation time of radical is obtained from the M_I dependence of ESR spectrum. According to the M_I dependence of the spectrum, the rotational motion of TEMPO in SDS micellar solution is estimated to be ca. 50 times slower than that in benzene. Figure 3-5-3b shows CIDEP signal of TEMPO obtained in an aqueous SDS micellar solution of the 1-chloronaphthalene-TEMPO system. The observed small hyperfine dependence is explained with the restriction of the molecular motion of TEMPO and the spectrum consists of almost net emissive polarization. In this system, each triplet hyperfine line becomes the same intensity and the net emissive polarization is enhanced in comparison with benzene solution. Such a tendency was observed in other excited molecule-TEMPO systems in SDS micellar solutions. The enhancement of net emissive polarization is similar to viscosity effect in normal solvent systems.

c) Solvent Effects on RTPM Signals

Remarkable solvent viscosity effects were observed on RTPM signal pattern. This phenomenon is considered to be associated with the origin of RTPM, but before discuss this point, another plausible mechanism must be examined to interpret the solvent effects, that is ESPT.[5] In ESPT, triplet molecules must encounter doublet molecules with rate of 10^7–10^9 s^{-1} because the spin relaxation of triplet states reduces the magnitude of ESPT. This condition for the encounter rate is similar to that for CIDEP generation through triplet mechanism. The concentration of TEMPO is 6 x 10^{-4} M in benzene and it results in the encounter rate of 6 x 10^{-6} s^{-1} assuming diffusion control. Hence, it is hard to observe the ESPT signal under this condition. The diffusion rate constant decrease with increase in solvent viscosity; 10^{10} M^{-1}s^{-1} in benzene and reduced to 3 x 10^9 M^{-1}s^{-1} in 2–propanol.[10] Hence, more frequent encounter is anticipated in benzene than in 2–propanol. The relative intensity of net polarization is, however, weaker in benzene than in 2–propanol as seen in Fig.3–5–1. This is inconsistent with ESPT.

In RTPM, net emissive polarization is generated when the pair passes through the avoided crossing of | Q-3/2> and | D1/2> states after the triplet quenching through doublet states of encounter pair, where the avoided crossing is caused by zero–field–interaction of triplet molecule. Therefore, its magnitude depends on both mean time of the pair to pass through the crossing region and the effective D value (this value is represented as D_{zfs}) to produce the avoided crossing. These points will be discussed below.

The effect of the avoided crossing is similar to that in S–T$_{-1}$ mixing of RPM. In S–T$_{-1}$ mixing mechanism, avoided crossing of S and T$_{-1}$ states is caused by hyperfine interaction. The mixing rate between S and T$_{-1}$ states is not rapid enough to generate net emissive CIDEP in the solvents with low viscosity like benzene. It is necessary for the pair to stay for long time in the crossing region enough to mix the S and T$_{-1}$ states. The

higher viscosity restricts the rapid diffusion motion and the radicals go through the crossing region more slowly. Trifunac first reported[8] the enhancement of net emissive polarization in high viscous solvents. Adrian et al.[37] calculated the electron spin polarization due to $S-T_{-1}$ mixing, $\rho(S-T_{-1})$, for various molecular diffusion constant, D, and derived the relation $\rho(S-T_{-1})$ 1/D. On the other hand, according to the treatment of Pedersen and Freed,[38] electron spin polarization of $S-T_0$ mixing does not change drastically with D. (CIDEP intensity changed only 10–20 times with the variation of D = 10^{-3}–10^{-8} cm^2s^{-1}). This implies why total net emissive CIDEP due to RPM gives major contribution to CIDEP signal in high viscous solvents. The same principle is expected for the RTPM signal : CIDEP intensity of net polarization is in proportion to 1/D whereas that of hyperfine dependent polarization does not change considerably with variation of D. According to this viscosity dependency, net polarization is more enhanced than hyperfine dependent polarization in high viscous solvent, which is consistent with the experimental results. It was demonstrated from continuous wave ESR spectra that radical motion was restricted in the micellar solution. The motion of excited molecules also ought to be restricted in the micellar solution. The slack motion due to narrow micellar structure might have influence on CIDEP generation with the similar manner to viscosity effect. Though the exchange interaction is large in crossing region of | Q–3/2> and | D1/2> states, micellar structure makes the mean distance of radical–triplet pair closer than that in normal solvents and hence, the net emissive polarization is enhanced.

Next point discussed here is the avoided crossing caused by D_{zfs}. The avoided crossing between | Q–3/2> and | D1/2> states is generated by the effective magnitude of D_{zfs} value. The effective D_{zfs} value is related to the frequency of molecular rotation. If the radical–triplet pair passes through the crossing region much slower than the correlation time of the molecular rotation, effective D_{zfs} value of the triplet state is

reduced to zero by the rotational modulation. On the other hand, if the pair passes through the crossing region faster than the correlation time of the molecular rotation, the D_{zfs} value is not averaged to be zero, which generates the net polarization on the radicals. Under the experimental condition, the frequency of the molecular rotation in benzene is estimated to be 6 times faster than that in 2-propanol from the line width of TEMPO. The restriction of molecular rotation also enhances net polarization in the radicals. The same idea is also acceptable for the results of micellar solution experiments.

As discussed above, there are two possible mechanisms to interpret the enhancement of net polarization in viscous solvents and micellar solutions. At present, there is no evidence which mechanism is mainly operative on the enhancement of net polarization. However, the viscosity effects on net and hyperfine dependent polarizations are in any event well explained with the RTPM. The experimental results given in this study are the evidence for the RTPM of net and hyperfine dependent polarizations.

Table 3-VII   Ratio of net and multiplet polarizations

solvent	multiplet	net	η [cp]
acetonitrile	100	250	0.345
benzene	100	510	0.649
2-propanol	100	1870	2.859
1,2-ethanediol	$\fallingdotseq$ 0	100	26.09

g value of 1-chloronaphthalene is assumed to be 2.0003.   g value of TEMPO is 2.00586 from its ESR spectrum. Hyperfine coupling constants a_N of TEMPO is 1.65 mT.
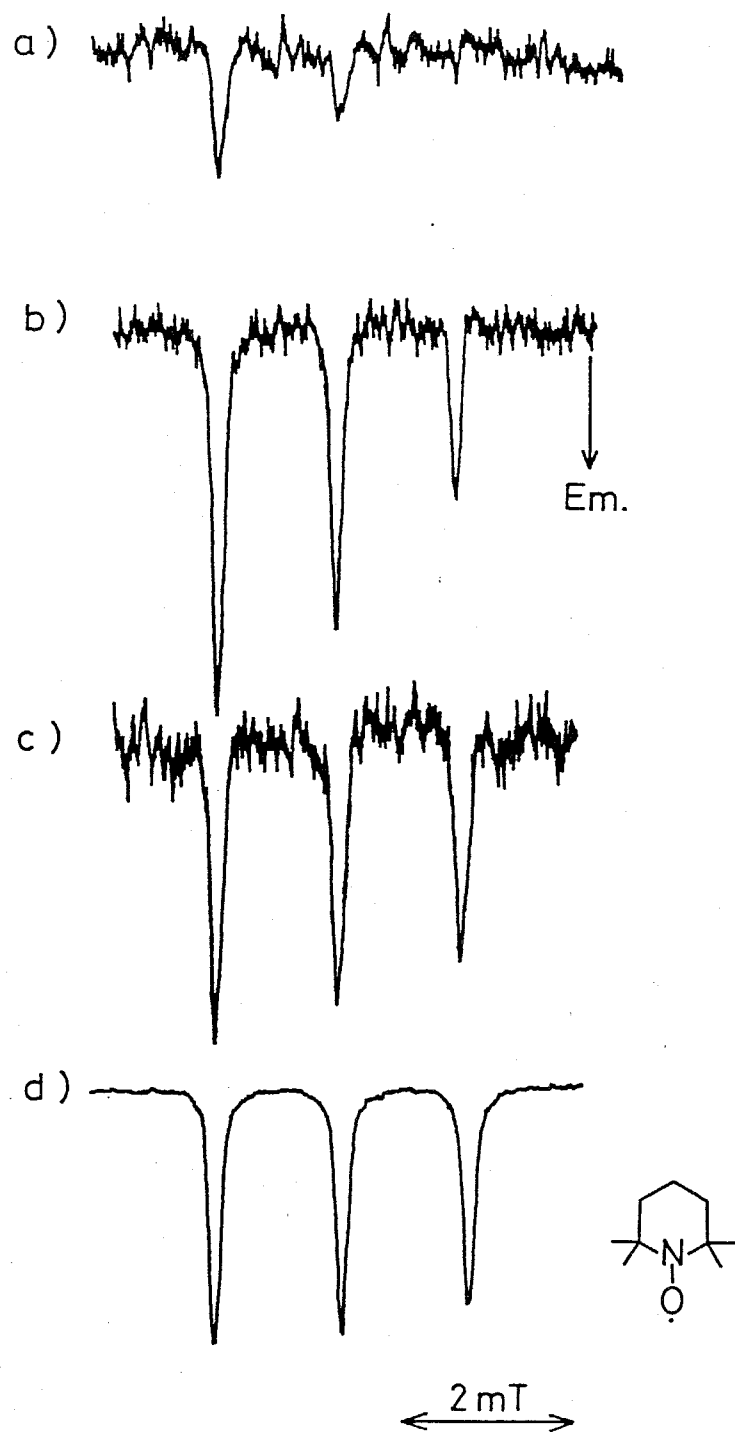
Fig.3-5-1 TR-ESR spectra of TEMPO (0.6 mM) in the 1-chloronaphthalene-TEMPO

system in a) acetonitrile, b) benzene, c) 2-propanol and d) 1,2-ethanediol.
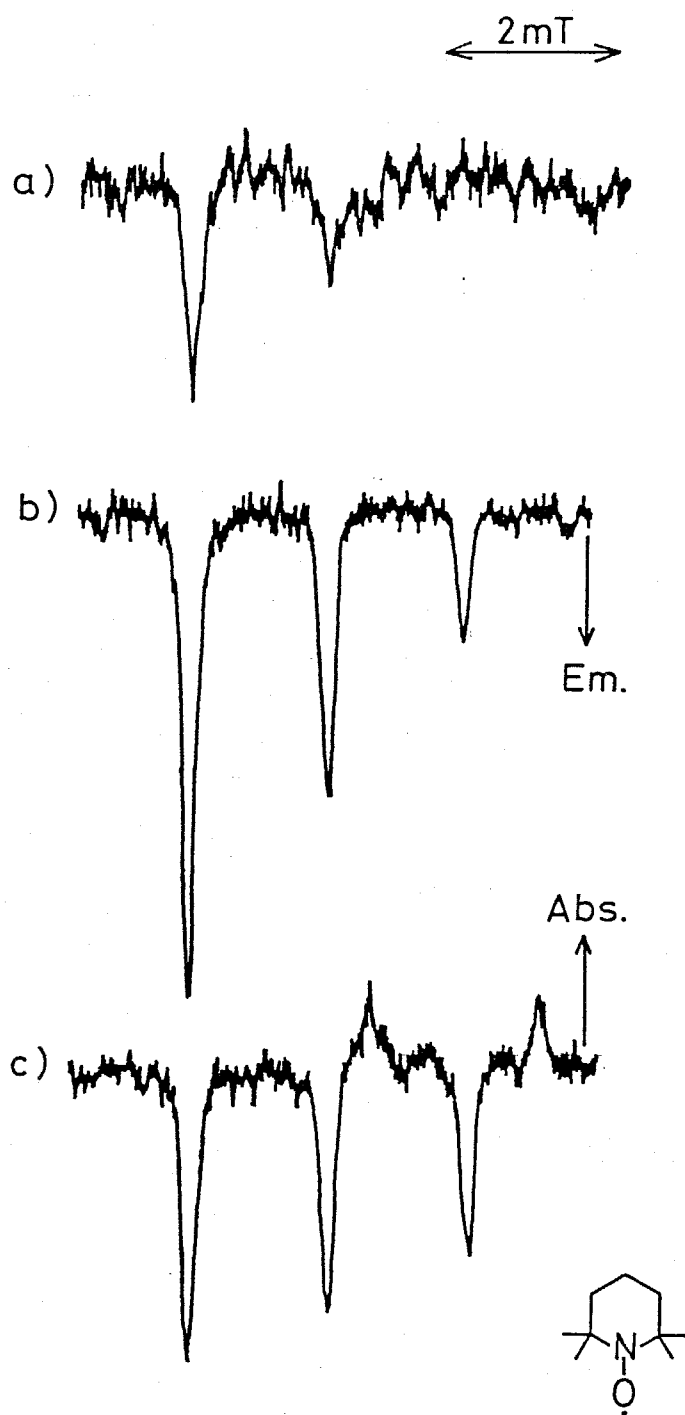
Fig.3-5-2 TR-ESR spectra of TEMPO (0.60 mM) in the 9,10-acenaphthenequinone
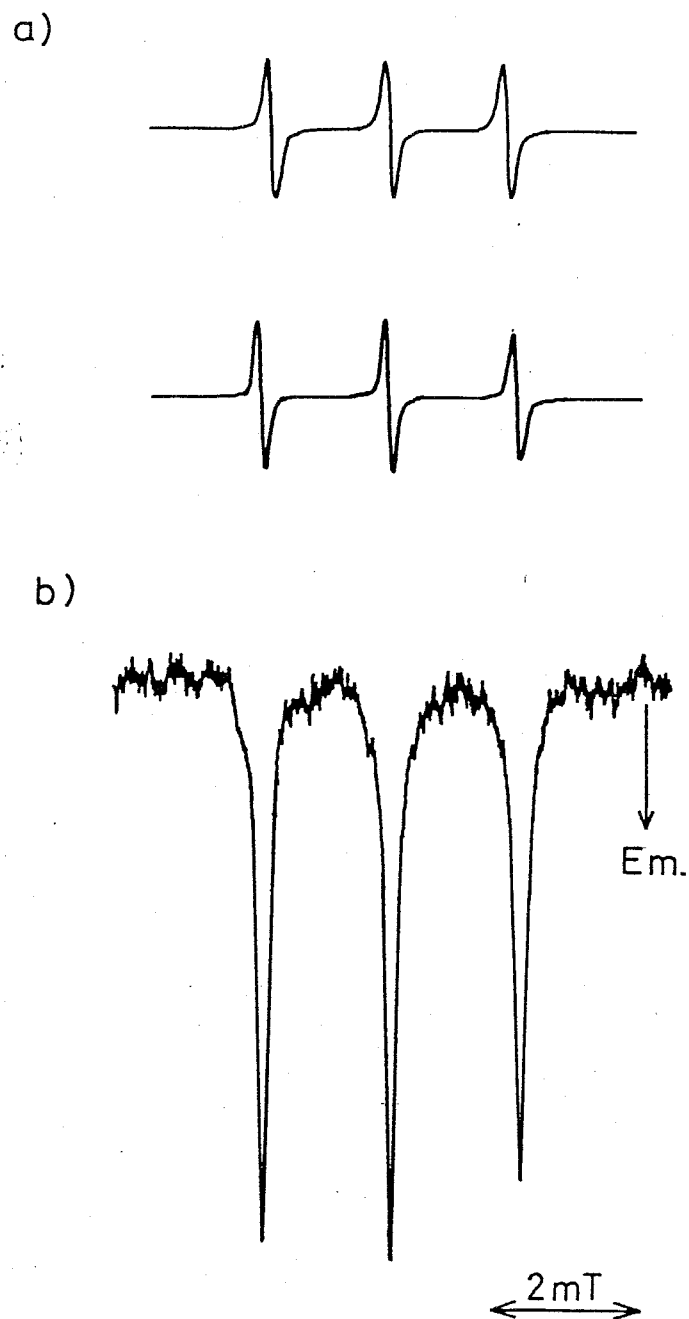-TEMPO system in a) acetonitrile, b) benzene and c) 2-propanol.

Fig.3-5-3 a) CW-ESR spectra of TEMPO (0.60 mM) in benzene (upper) and
0.1 M SDS aqueous micellar solution (lower). b) TR-ESR spectra of
TEMPO (0.60 mM) in the 1-chloronaphthalene-TEMPO system
in SDS aqueous micellar solution (0.1 M).

71

References

[1] R. W. Fessenden and R. H. Schuler, *J. Chem. Phys.*, **39**, 2147, (1963).

[2] S. K. Wong and J. K. S. Wan, *J. Am. Chem. Soc.*, **94**, 7197, (1972).

[3] F. J. Adrian, *Rev. Chem. Intermediates*, **3**, 3. (1979).

[4] L. T. Muss, P. W. Atkins, K. A. McLauchlan and J. B. Pedersen,
Chemically Induced Magnetic Polarization, Reidel, Dordrecht, (1977).
; K. M. Salikhov, Yu, N. Molin, R. Z. Sagdeev and A. L. Buchachenko,
Spin Polarization and Magnetic Field Effects in Radical Reactions,
Elsevier, New York, (1984).

[5] T. Imamura, O. Onitsuka and K. Obi, *J. Phys. Chem.*, **90**, 6741, (1986).

[6] C. Blättler, F. Jent and H. Paul, *Chem. Phys. Lett.*, **166**, 375, (1990).

[7] A. Kawai, T. Okutsu and K. Obi, *J. Phys. Chem.*, **95**, 9130, (1991).

[8] A. D. Trifunac, *Chem. Phys. Lett.*, **49**, 457, (1977).

[9] A. Kawai and K. Obi, *J. Phys. Chem.*, submitted for publication.

[10] N. J. Turro, *Modern Molecular Photochemistry*, Benjamin/Cummings, (1978).

[11] H. Murai, T. Imamura and K. Obi, *Chem. Phys. Lett.*, **87**, 295, (1982).

[12] K. Miyagawa, Y. J. I'Haya and H. Murai, *Nippon Kagaku Kaishi*, 1365, (1989).

[13] A. I. Grant and K. A. McLauchlan, *Chem. Phys. Lett.*, **101**, 120, (1983).

[14] M. A. El–Sayed, W. R. Moomaw and J. B. Chodak,
Chem. Phys. Lett., **20**, 11, (1973).

[15] Y. Shioya, M. Yagi and J. Higuchi, *Chem. Phys. Lett.*, **154**, 25, (1989).

[16] K. Akiyama, S. Tero–Kubota, T. Ikoma and Y. Ikegami,
Nippon Kagaku kaishi, 1463 (1989).

[17] S.Yamauchi and N. Hirota, *J. Phys. Chem.*, **88**, 4631, (1984).

[18] I. Y. Chan and B. N. Nelson, *J. Chem. Phys.*, **65**, 4080, (1975).

[19] S. Basu, A. I. Grant and K. A. McLauchlan, *Chem. Phys. Lett.*, **94**, 517, (1983).

[20] M. Gehrtz, Chr. Brauchle, J. Voitlander, *Chem. Phys. Lett.*, **91**, 217, (1982).

[21] W. S. Jenks and N. J. Turro, *J. Am. Chem. Soc.*, **112**, 9009, (1990).

[22] D. Kivelson, *J. Chem.Phys.*, **33**, 1107, (1960).

[23] P. J. Hore and K. A. McLauchlan, *J. Magn. Reson.*, **36**, 129, (1980).

[24] H. C. Torrey, *Phys. Rev.*, **76**, 1059,(1949).

[25] P. W. Atkins and G. T. Evans, *Mol. Phys.*, **29**, 921, (1975).

[26] K. Razi Naqvi, *J. Phys. Chem.*, **85**, 2303, (1981).

[27] K. Schulten, *J. Chem. Phys.*, **80**, 3668, (1984).

[28] J. B. Birks, *Photophysics of Aromatic Molecules*, New York, Wiley, (1970).

[29] L. R. Faulkner and A. J. Bard, *J. Am. Chem. Soc.*, **91**, 6495, (1969).

; L. R. Faulkner, H. Tachikawa and A. J. Bard, *J. Am. Chem. Soc.*,**94**, 691, (1972).

[30] O. L. J. Gijzeman, F. Kaufman and G. Porter, *J. Chem. Soc. Faraday Trans. 2*,

69, 727, (1973).

[31] V. A. Kuzumin and A. S. Tatikolov, *Chem. Phys. Lett.*, **53**, 606, (1978).

[32] A. D. Trifunac, D. J. Nelson and C. Mottley, *J. Magn. Reson.*, **30**, 263, (1978)

; T. J. Burkey, J. Lusztyk, K. U. Ingold, J. K. S. Wan and F. J. Adrian,

J. Phys. Chem., **89**, 4286, (1985).

[33] E. G. Brame, Jr., (Eds.) *Applied Spectroscopy Reviews*,

Marcel Dekker, Inc., New York and Basel, **17**, 1,(1981).

[34] R. M. Noyes, *Progr. React. Kin.*, **1**, 129, (1961); *J. Am. Chem. Soc.*,

78, 5486, (1956); *J. Chem. Phys.*, **22**, 1349, (1954).

[35] F. J. Adrian, *J. Chem. Phys.*, **53**, 3374, (1970); *ibid.*, **54**, 3912, (1971).

[36] S. L. Murov, *Handbook of Photochemistry*, Marcel Dekker INC. New York (1973).

[37] F. J. Adrian and L. Monchick, *J. Chem. Phys.*, **71**, 2600, (1979);

J. Chem. Phys., **72**, 5786, (1980).

[38] J. B. Pedersen and J. H. Freed, *J. Chem. Phys.*, **58**, 2746, (1973).

CHAPTER IV

Electron Spin Polarization in Radical and Singlet Molecule System

4-1 Introduction.

Singlet and triplet excited molecules and intermediate radicals coexist in the early photochemical stage. Interactions between these species have extensively been investigated and many interesting phenomena have been well known, such as S_1 and T_1 quenching by radicals, triplet–triplet annihilation and so on.[1] Photochemistry and photophysics of these species have been discussed based on the electron spin multiplicities because the spin angular momentum of these intermediate molecules is a good quantum number. For example, quenching of excited states by free radicals and radical recombination reactions selectively occur according to the conservation rule of the spin angular momentum, which are confirmed by magnetic field effects.[2,3]

CIDEP of radicals is generated through the radical pair mechanism (RPM),[4] the triplet mechanism (TM)[5] and the radical triplet pair mechanism (RTPM).[6,7] These mechanisms are also discussed based on the spin angular momentum. RPM and RTPM are explained by magnetic interaction acting on the potential surface of spin states of radical pair and radical triplet pair, respectively.

RPM and RTPM are so far the only CIDEP mechanisms due to the interaction among the species of initial photochemical processes, but it is still unknown whether CIDEP is generated or not via radical–excited singlet and triplet–triplet pairs. As for the interaction between the lowest excited singlet molecule and radical, quenching of fluorescence is well known and is interpreted as the enhanced ISC of singlet molecule due to radical perturbation.[8,9] Just after this event, pairs of radical and generated triplet molecule are formed. Magnetic interactions are expected in these pairs of paramagnetic species and RTPM will operate. In this chapter, it is demonstrated that the radical–

74

singlet pairs generate an A*/E polarization in the coronene–, fluoranthene–, pyrene– and naphthalene–TEMPO systems by time resolved ESR. Obtained CIDEP signal pattern is explained by an extended RTPM in which the initial spin state of the radical–singlet pair is assumed to be converted into the doublet spin states of radical–triplet pair. In this chapter, it is concluded that there are two types of CIDEP generation in RTPM : one is the doublet precursor RTPM which shows A*/E pattern and the other is the quartet precursor RTPM that shows E*/A pattern. These two types of CIDEP generation are expected to be simultaneously operative in the early stage of photochemical processes and the CIDEP signal of naphthalene–TEMPO system is demonstrated as a typical example of simultaneous operation of these RTPMs.

4–2 Experimental.

An equipment of TR–ESR measurements was described in Chapter II. The width of the gate time of the boxcar integrator was usually 0.5 μs after 1.0 μs of the laser pulse. The fluorescence was measured by the quartz flat cell with 0.5 mm interior space because of the high concentration of the sample.

Fluoranthene and pyrene (Tokyo Kasei) were recrystallized from n–hexane. Coronene (Tokyo Kasei) and naphthalene (Kanto Chemicals) were recrystallized from benzene and ethanol, respectively. The other reagents are used as received. GR grade benzene and 2–propanol (Kanto Chemicals) were used as solvents without further purification in room temperature experiments. Spectrograde 2–methylbutane (Tokyo Kasei) was used as a solvent for the measurement of fluoranthene triplet state. In the room temperature experiments, the solution was deaerated by bubbling nitrogen gas and flowed through the quartz flat cell (0.5 mm interior space) in ESR cavity. In the low temperature experiments, dissolved oxygen in the sample solution was degassed by freeze–pump–thaw cycles. Afterwards the glasses of sample solution were prepared in 5 mm diameter quartz ESR tube by quick cooling to 77 K.

4–3 Net Absorptive and Absorption/Emission (A/E) Multiplet Polarization.

Figure 4–3–1 shows the CIDEP spectra obtained in the fluoranthene–, pyrene– and coronene–TEMPO systems by 308 nm laser excitation, together with CW–ESR spectrum of TEMPO. Hyperfine peaks appear at the same positions with those of TEMPO, which shows triplet hyperfine structure due to the nitrogen atom. Hence, the signals of these CIDEP spectra are assigned to spin polarized TEMPO radicals. CIDEP patterns of these spectra show two characteristic points: One is the total absorptive spin polarization, and the other is the hyperfine dependence. The signal of $M_I = +1$ peak is the most intense and the magnitude of absorptive signal diminishes with decrease in the quantum number M_I. The CIDEP spectra in Fig.4–3–1 are represented as sum of the total absorption and the hyperfine dependent A/E(Absorption/Emission) pattern, which results in A^*/E pattern. The hyperfine dependence is weak in the coronene–TEMPO system and enhanced in pyrene–TEMPO.

In Chapter III, the generation of total emissive and hyperfine dependent (E/A type) CIDEP signals of nitroxide radicals were observed in the solution of many organic compounds–radical systems, which were interpreted by triplet–doublet interaction. But the results obtained here show completely opposite phase of CIDEP signals to those in these systems. RTPM predicts the generation of E^*/A type CIDEP signals in the triplet–doublet interaction for J<0 system. The sign of spin polarization due to RTPM depends on the sign of J value and thus, J>0 is simply considered for an answer of A^*/E type CIDEP signals in these systems. Generally, neutral radical pairs show negative J value though some ionic radical pairs exceptionally show positive value.[4,10] According to RTPM proposed in Chapter III, all neutral radical–triplet pairs studied previously should have negative J value. It is, therefore, hard to consider exceptionally opposite sign of J value for the neutral radical–triplet pairs studied here.

Electron spin polarization transfer(ESPT) is another plausible mechanism to explain

total absorptive CIDEP.[11] If the triplet states of fluoranthene, coronene and pyrene have β spin enhanced population, radicals would show absorptive spin polarization due to ESPT. Fig.4-3-2 shows TR-ESR spectrum of the triplet state of fluoranthene obtained in 2-methylbutane at 77 K. The sharp H_{min} signal appeared around 150 mT with emissive polarization. If ESPT is effective in this system, radical should have emissive polarization which is opposite to the experimental result. The α spin enhanced population in the triplet state of coronene is also demonstrated with microwave induced delayed phosphorescence.[12] Hence, ESPT can not explain the results of CIDEP.
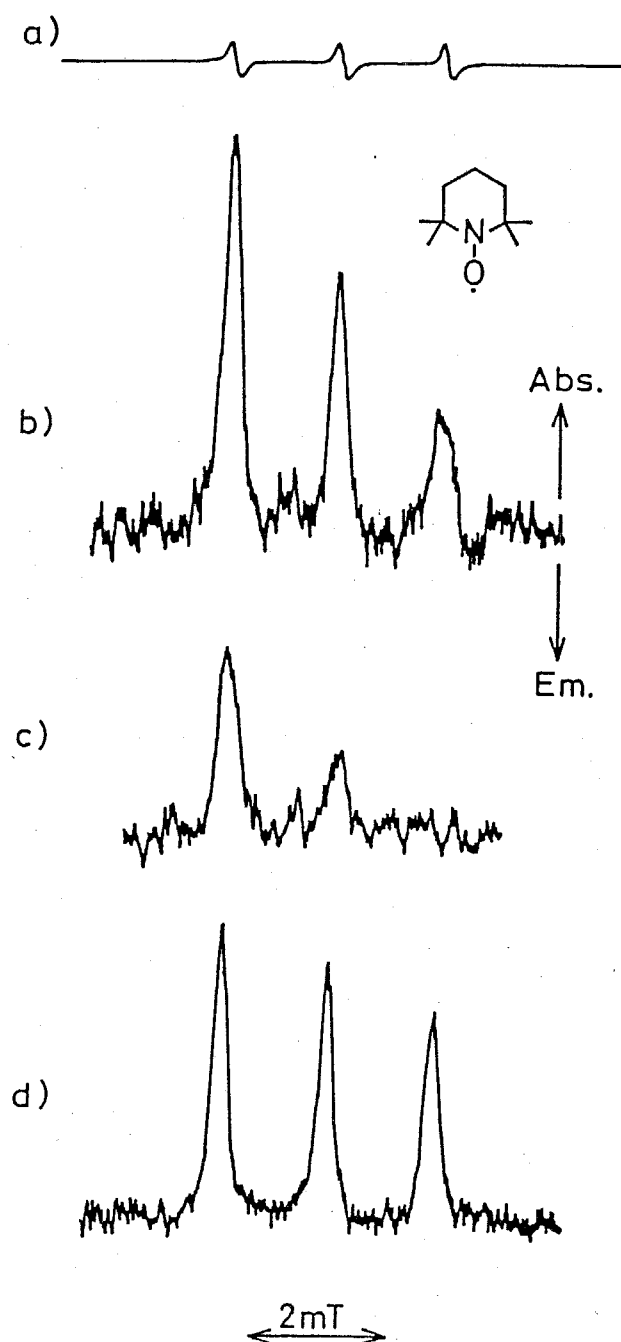
Fig.4-3-1 CW-ESR spectrum of TEMPO (0.60 mM) in benzene a) and TR-ESR

spectra of TEMPO in the systems of b) TEMPO-fluoranthene (12 mM),

c) TEMPO-pyrene (8.2 mM) and (d) TEMPO-coronene (1.1 mM)
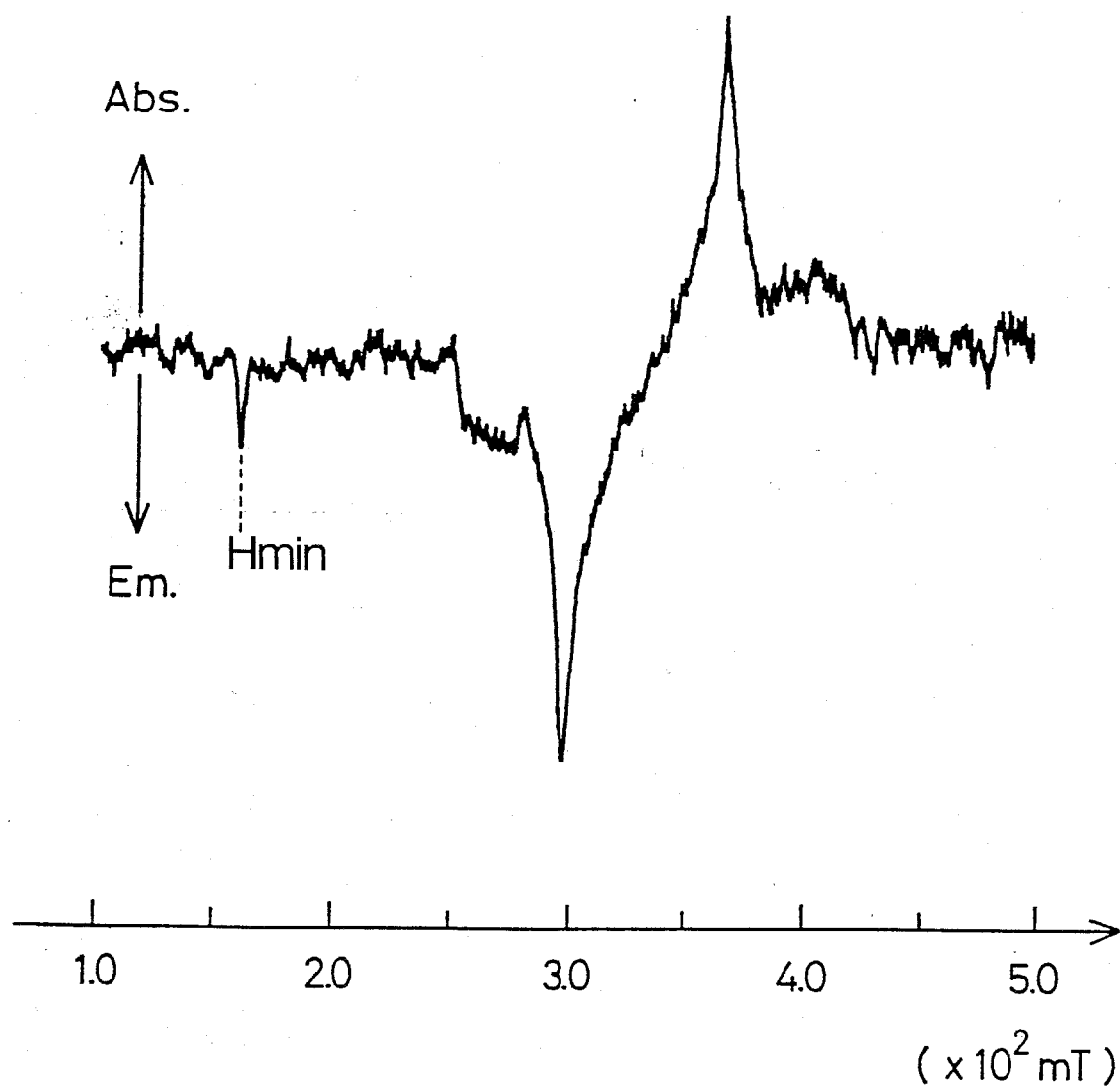
at room temperature.

Fig.4-3-2 TR-ESR spectrum of fluoranthene (0.6 mM)

obtained in 2-methylbutane glass at 77 K.

4−4 RTPM with Doublet Precursor.

As the conventional theories are hard to explain the A^*/E signal of TEMPO, a new theory based on the RTPM is proposed to interpret the signals observed here, in which A^*/E signal is caused by the state mixing of quartet and doublet spin states originating from the doublet state spin pair. This is different from that of RTPM discussed above. Hoytink and Birks reported that intersystem crossing (ISC) from the lowest excited singlet state was enhanced in the presence of free radicals.[13] As for the pyrene− and coronene−radical systems, the enhanced S_1−T_1 ISC occurred with the quenching rate[14] of about 10^{10} $M^{-1}s^{-1}$, which indicated that the triplet state was formed with the rise time of 0.1 μs in radical concentration of 10^{-3} M. The relative fluorescence quantum yield of fluoranthene was measured for various radical concentrations which is shown in Fig.4−4−1. It is obvious that the S_1 state of fluoranthene was quenched by TEMPO. Under the experimental condition of Fig.4−3−1b, fluorescence intensity was reduced to about 0.65 compared to that in the absence of free radical. Fluoranthene, coronene and pyrene have long S_1 lifetimes (50 ns<)[15] and thus, the enhanced ISC of these molecules makes a major contribution to the generation of triplet state. The radical−triplet pair formed through the S_1−T_1 enhanced ISC from the S_1−radical complex should have the same spin states as the complex,[16] that is, | D±1/2>. Thus, the doublet spin states are selectively populated in the radical−triplet pair with this mechanism, and quartet−doublet mixing in the generated radical−triplet pair will start under the initial condition where only the doublet states are populated but no quartet states. If this initial condition is applied to RTPM,[7] A^*/E type of CIDEP is predicted to be generated on radicals. The experimental results are consistent with this prediction and thus, this A^*/E signal is attributed to doublet precursor RTPM.

RTPM shows the solvent viscosity effects on the CIDEP pattern[17] as discussed in Chapter III. In more viscous solvents, the net polarization is enhanced compared to

multiplet polarization. Hence, the same tendency must also appear in doublet precursor RTPM. Figure 4-4-2 shows the CIDEP spectra of pyrene- and fluoranthene-TEMPO systems in benzene and 2-propanol. As is seen in the spectra, the net absorptive polarization is enhanced in 2-propanol solution. These results are consistent with the viscosity effect of RTPM.

The CIDEP signals obtained here are the first observation of doublet precursor RTPM. In the CIDEP studies, the concept has been well accepted that the CIDEP generation needs the magnetic interactions between paramagnetic species which are often free radicals or triplet molecules in conventional photochemical stages. However, in this new RTPM, non-paramagnetic species, S_1 molecules, are really included to generate A^*/E spin polarization. This is, in a way, considered to give a surprising concept to the CIDEP studies.
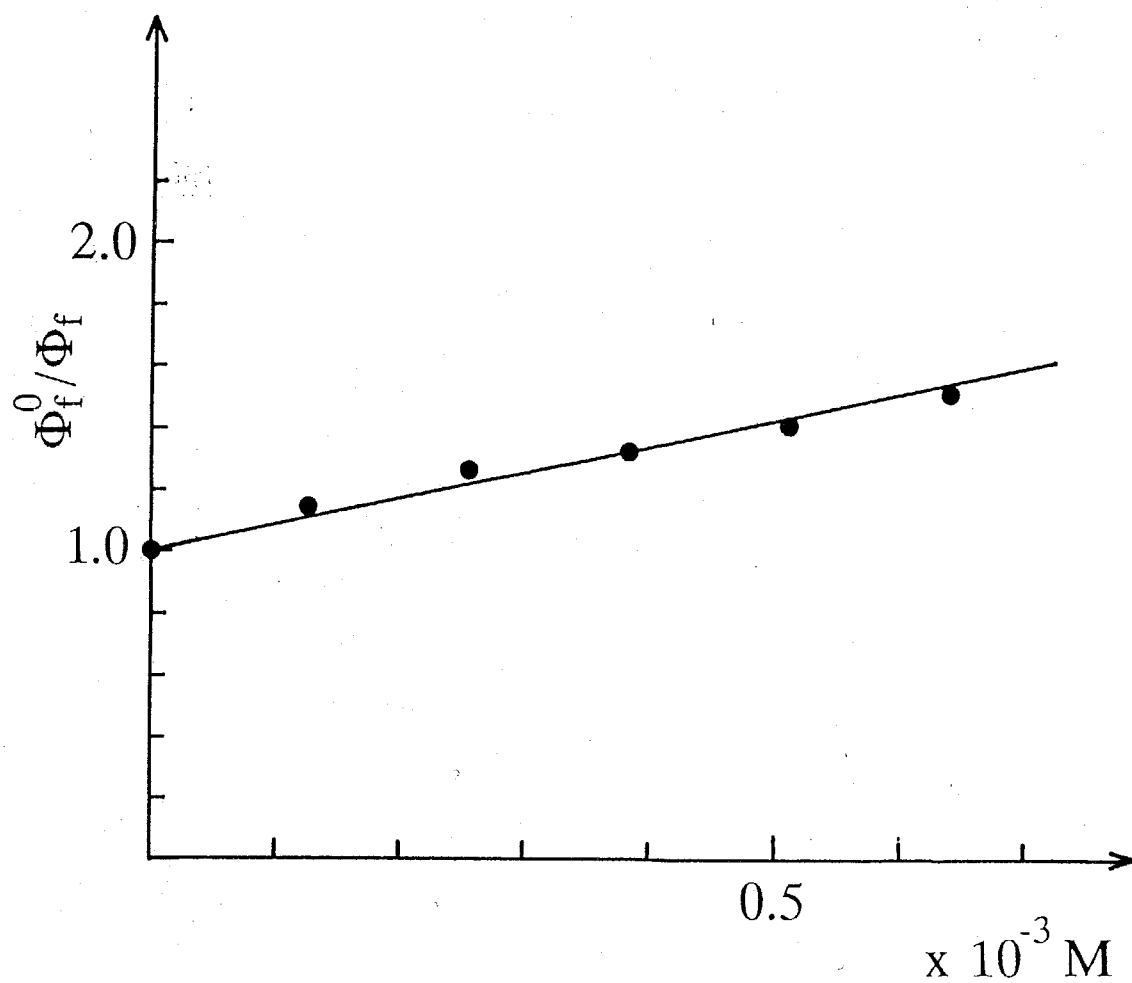
Fig.4-4-1 Stern-Volmer plot of relative fluorescence quantum yields of fluoranthene
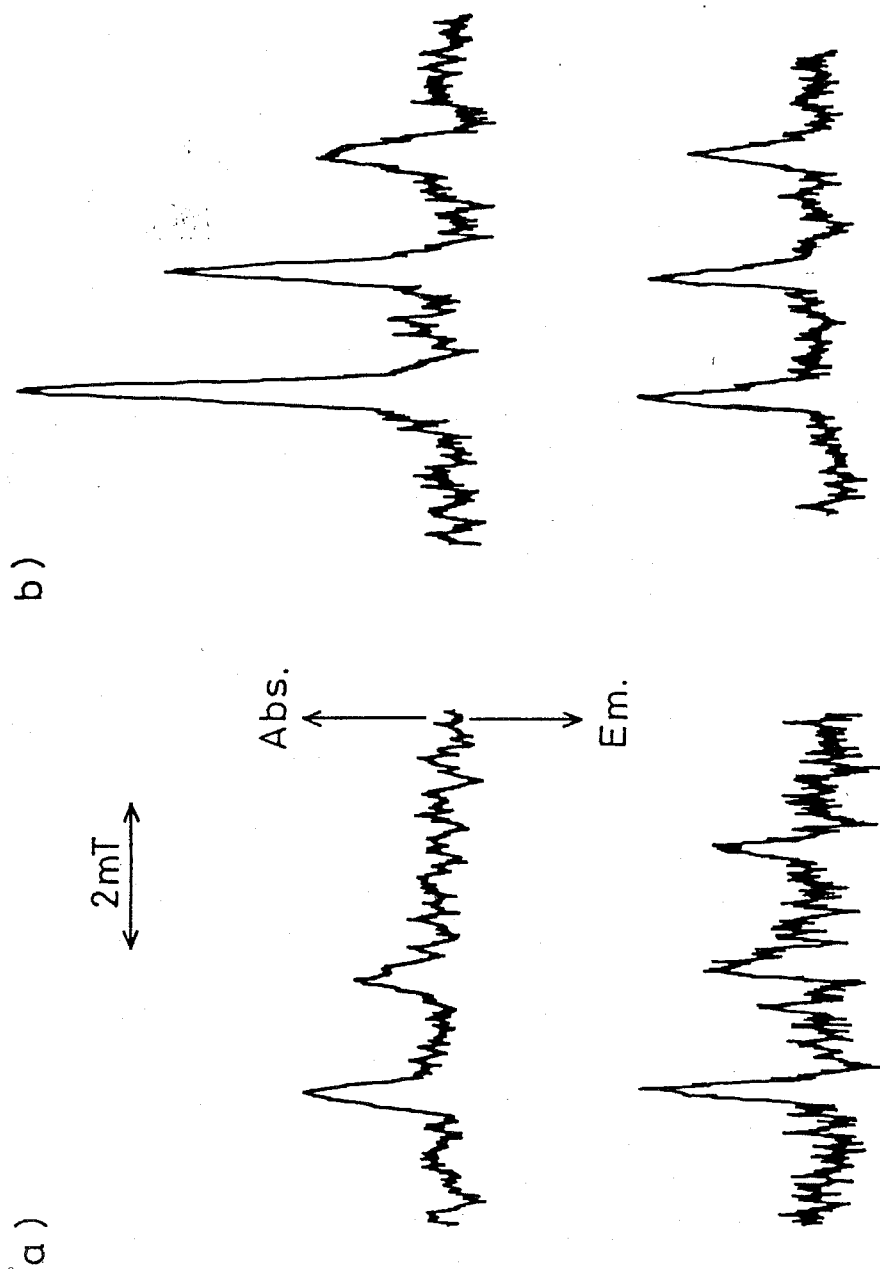via several radical concentrations.

Fig.4–4–2 TR–ESR spectra of TEMPO (0.60 mM) in a) pyrene–TEMPO and b) fluoranthene–TEMPO systems. Upper spectra are in benzene and the lower are in 2–propanol. The gate is opened from 0.5 to 1.0 µs after laser pulse.

a) Time Profiles of RTPM Signal.

CIDEP generations are observed through the quartet precursor RTPM in the previous chapter and also through the doublet precursor RTPM in this chapter. Thus, both RTPMs are expected to be simultaneously operative to generate CIDEP in a system where the rate of S_1-T_1 ISC is comparable with that of enhanced ISC. A good example of such a case is naphthalene ; the rate of enhanced ISC becomes comparable with the rate[18] of S_1-T_1 ISC, 10^6 s^{-1}, at the radical concentration of about 10^{-4} M. The CIDEP spectra of TEMPO in the naphthalene–TEMPO system were obtained at different gate times as shown in Fig.4–5–1. Phase of CIDEP signal changes from absorption in early gate time(Fig.4–5–1a) to emission in late gate time(Fig.4–5–1b). Hyperfine dependence of CIDEP is also observed in this system and is almost the same between former and latter spectra. These facts indicate that the absorptive CIDEP signals are generated in the course of enhanced ISC and emissive signals results from the interaction of radicals with the triplet naphthalene molecules produced by ISC.

In order to investigate details of transient CIDEP, time profiles were measured in various systems, as shown in Fig.4–5–2. Decay profiles of CIDEP in 1–chloronaphthalene–TEMPO and benzophenone–TEMPO systems are typical in the quartet precursor RTPM ; the phase of CIDEP is emissive throughout the profile. The S_1-T_1 ISC rates of benzophenone and 1–chloronaphthalene are reported[18] to be 10^{11} and 10^8 s^{-1}, respectively, which are too fast to generate the doublet precursor RTPM signal. This is why only emissive CIDEP is observed in these systems. A little difference in decay rates between these profiles would be caused by the difference in magnetic relaxation time due to spin–spin interaction between triplet and radical. This is supported by the broad linewidth of TEMPO in the benzophenone–TEMPO system

which is twice as broad as that of the 1-chloronaphthalene-TEMPO system. On the other hand, in the time profile of the naphthalene-TEMPO system shown in Fig.4-5-2c, phase of CIDEP is absorption for the first 0.3-0.8 μs and is turned to emission after 0.8 μs which continues to end of its decay. Such kind of phase change has not been seen for other triplet-TEMPO systems observed before. The maximum intensity of absorptive signal is much weaker than that of emissive signal. If such a waving decay profile is due to the magnetic relaxation process known as Torrey oscillation,[19] intensity of the first maximum absorptive signal should be stronger than that of the first maximum emissive signal. This is also excluded from the microwave power dependence of CIDEP signals shown in Fig.4-5-3. Time profiles of CIDEP spectra do not changed in the microwave power range from 1 mW to 100 mW. Therefore, the phase turning due to magnetic relaxation process is ruled out.

From the kinetic consideration discussed above, the phase change is interpreted by the switching of the CIDEP generation mechanism from doublet precursor RTPM to quartet one with time. The magnitude of spin polarization, $<S_z(t)>$, at $M_I=+1$ peak is determined by the equation,

$$<S_z(t)> = (- k_{qs}[S_1(t)]I_s + k_{qt}[T_1(t)]I_t)[R] \qquad (1)$$

Positive sign means emissive polarization. k_{qs} and k_{qt} are quenching rate constants of S_1 and T_1 by radicals, respectively. I_s and I_t are the enhancement factor of CIDEP generation. As TEMPO is stable free radical, its concentration, [R], is constant. In early gate time, doublet precursor RTPM is dominant because the S_1 state of naphthalene is first quenched by radicals and forms the doublet spin states of radical-triplet pair, which corresponds to the first term of equation (1). In late stage, radicals encounter the triplet state of naphthalene generated through direct or enhanced ISC. The triplet molecules formed through enhanced ISC loose their spin correlation with the counter

radicals due to separation of the pair. The quartet spin states survive in triplet–radical pair during triplet quenching, which results in E^*/A type CIDEP observed in the late gate time after 0.8 μs.

Abnormal decay profiles like that in the naphthalene–TEMPO system are also observed in the fluoranthene– and coronene–TEMPO systems as shown in Fig.4–5–4. In these systems, maximum intensity of absorptive signal is much stronger than that of emissive signal appearing in later time, which is different from the naphthalene–TEMPO system. If the emissive decay signal is generated as the result of Torrey oscillation of the initial absorptive signal, the decay profile should oscillate with a specific frequency. This is not the case in our systems. Moreover, no phase change is observed in other systems with short lived S_1 and efficient ISC. The phase change of CIDEP is, thus, accounted with switching of the doublet precursor RTPM at early stage to the quartet precursor RTPM at late stage.

b) Triplet Quenching Effects on Transient RTPM Signals.

To confirm RTPM with doublet precursor, 1,3–pentadiene is added to the naphthalene–TEMPO system as a triplet quencher, where selective quenching of the T_1 state must reduce the quartet precursor RTPM signal. The T_1 state of 1,3–pentadiene is 20700 cm^{-1}, which is 600 cm^{-1} lower than that of naphthalene. Hence, the effective triplet quenching is expected in this system. Figure 4–5–5 shows the time profile of CIDEP signal generated in the naphthalene–TEMPO systems without the triplet quencher (a) and with 1,3–pentadiene (b). The absolute intensity in Fig.4–5–5 is not calibrated but the relative intensity of emissive signals is reduced in decay profile (b) as predicted above. In the case of 1–chloronaphthalene–TEMPO system, the same reduction of quartet precursor RTPM signal was observed by addition of 1,3–pentadiene, which is shown in Fig.4–5–6. The T_1 lifetime of 1,3–pentadiene is not reported, but could be

short due to its free rotor structure. The 1,3-pentadiene-TEMPO interaction is, therefore, considered to give minor contribution to whole CIDEP signal.

Triplet quenching experiment was also carried out in the coronene-TEMPO system to confirm the switching mechanism. Fig.4-5-7 shows decay profiles of CIDEP signal in the coronene-TEMPO system by 337 nm laser excitation. In the absence of triplet quencher, phase change was observed as shown in fig.4-5-7a, which is almost the same with Fig.4-5-4b, whereas when trans-stilbene was added in this system as a triplet quencher, only absorptive signal was observed without phase change. This result strongly supports the switching mechanism in the coronene-TEMPO system.

The dual spin polarization observed in these systems is another evidence for the idea that the sign of J value is negative in all radical-triplet systems as discussed before, because the phase change is accounted by switching of RTPM and net emissive polarization is observed at later gate time due to quartet precursor RTPM.
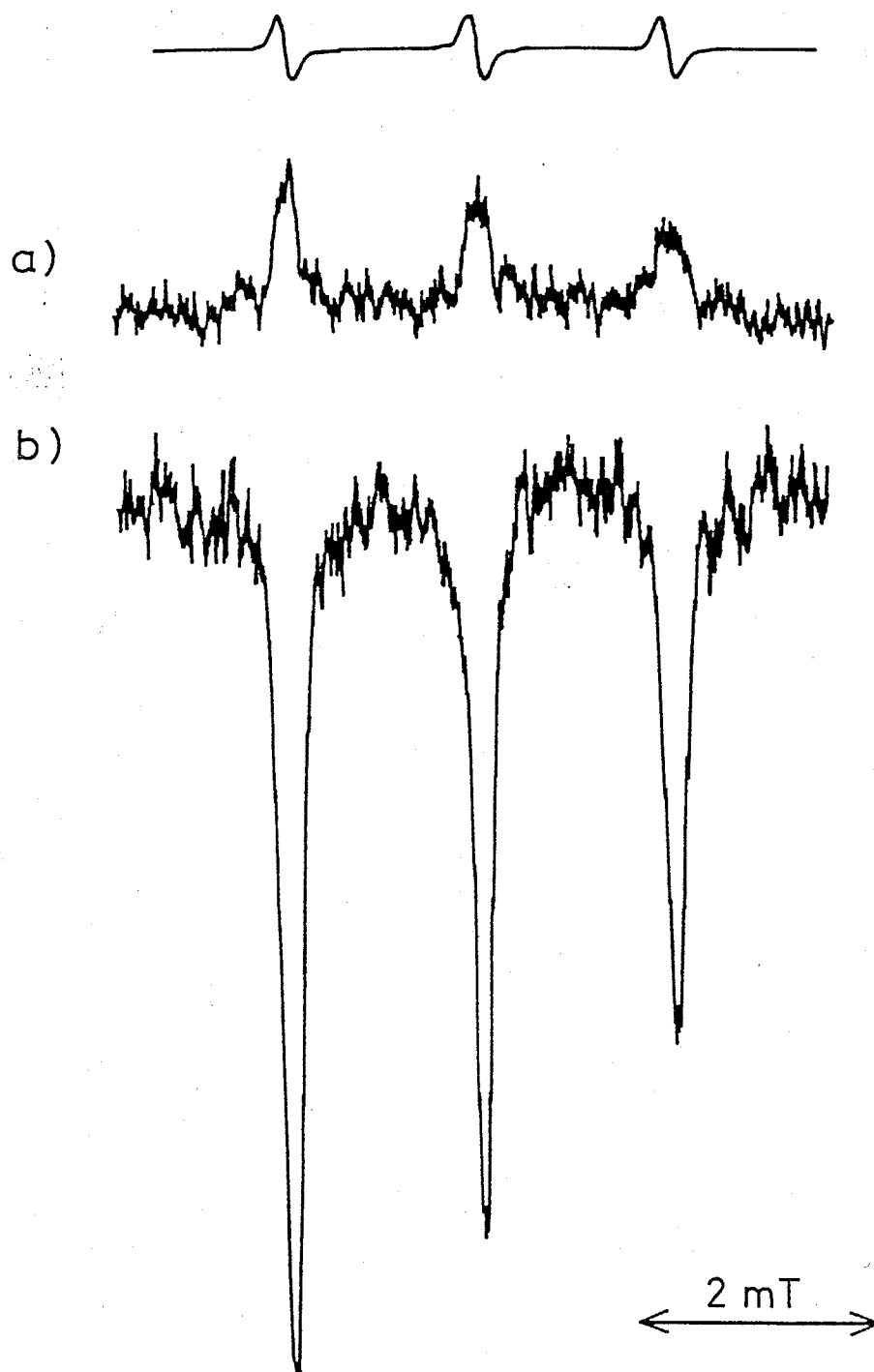
Fig.4-5-1 TR-ESR spectra of TEMPO (0.60 mM) in the TEMPO-naphthalene

(39 mM) system in 2-propanol solution. The gate is

opened from (a) 0.3 to 0.8 μs, and (b)1.5 to 2.0 μs.
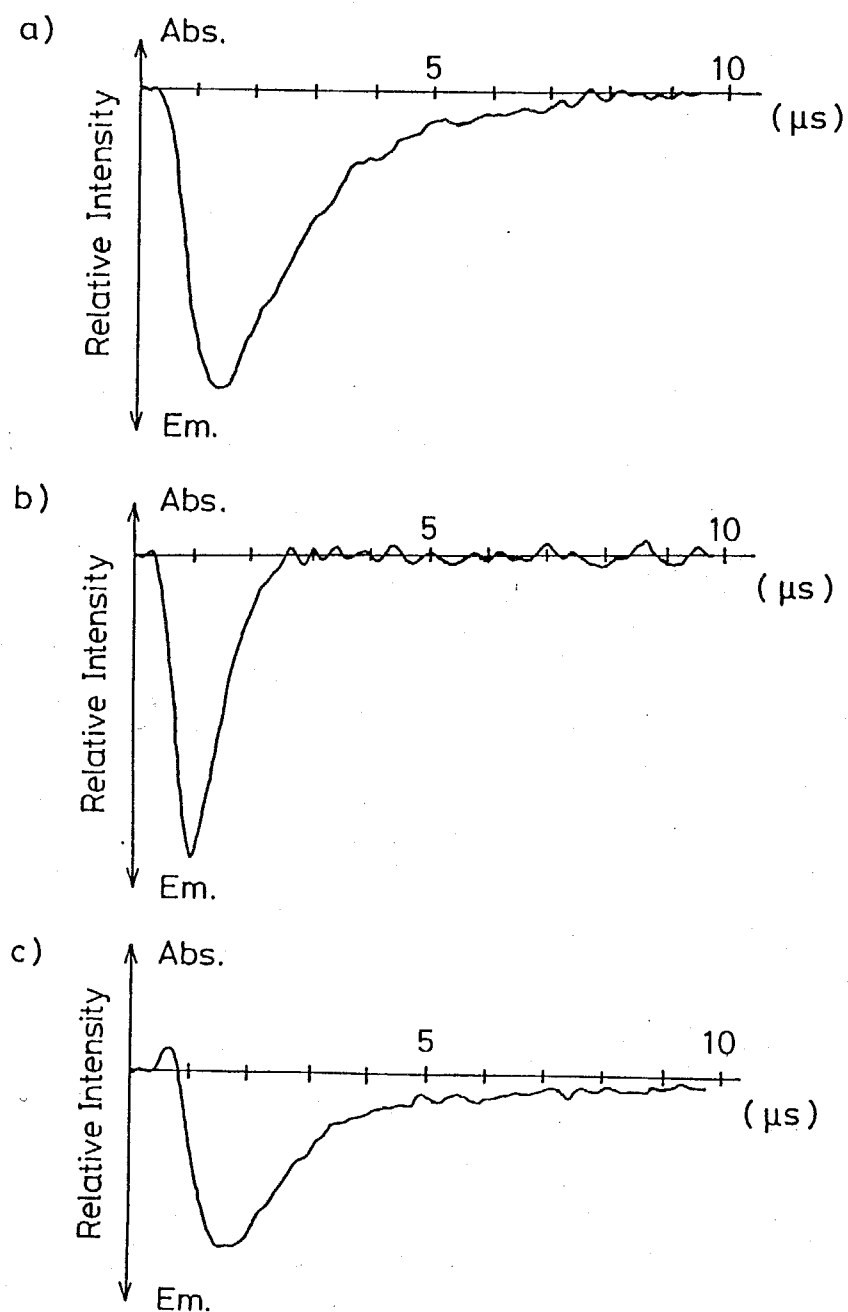
Fig.4-5-2 Time profiles of CIDEP signal of TEMPO (0.60 mM) at the $M_I=-1$ peak

in (a) TEMPO-1-chloronaphthalene (37 mM) in 2-propanol,

(b) TEMPO-benzophenone (55 mM) in benzene and

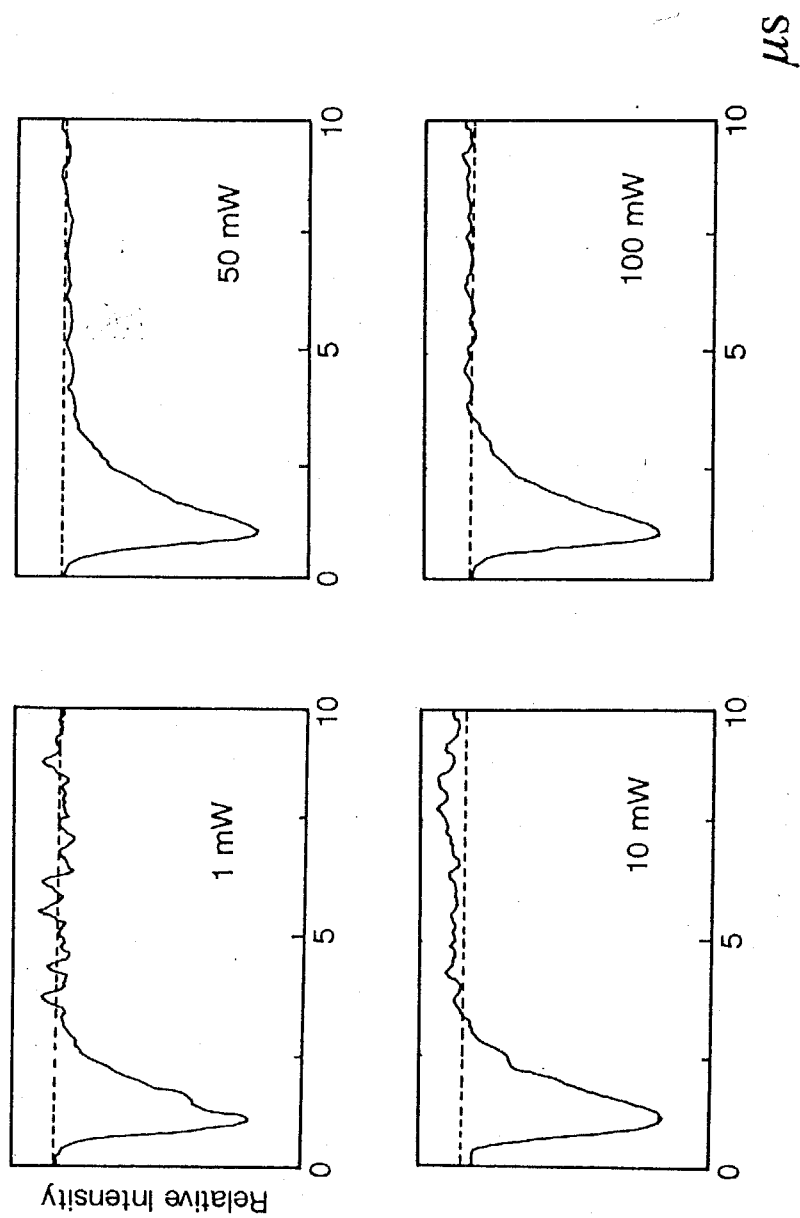(c) TEMPO-naphthalene (39 mM) in 2-propanol. Microwave power is 1 mW.

Fig.4–5–3a Microwave power dependence of the time profiles of RTPM signal in 1–chloronaphthalene–TEMPO system.
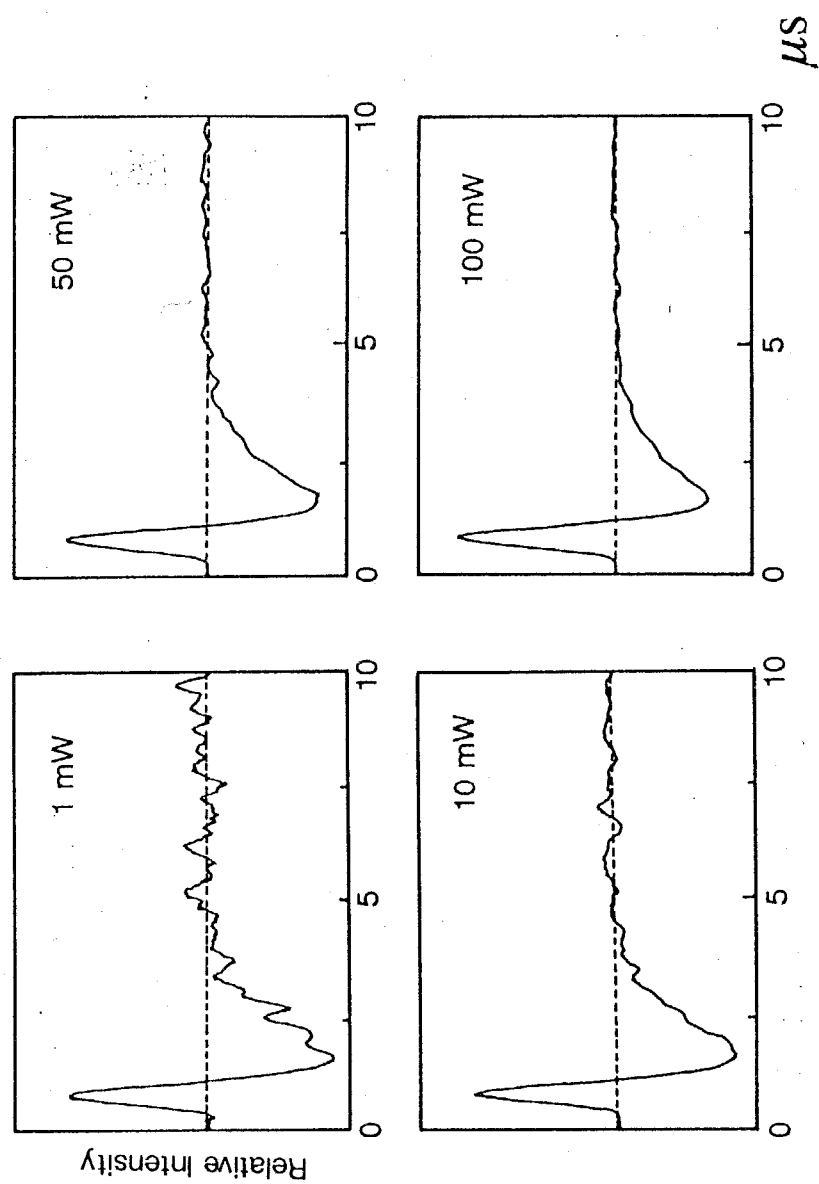
Fig.4–5–3b Microwave power dependence of the time profiles of RTPM signal in coronene–TEMPO system.
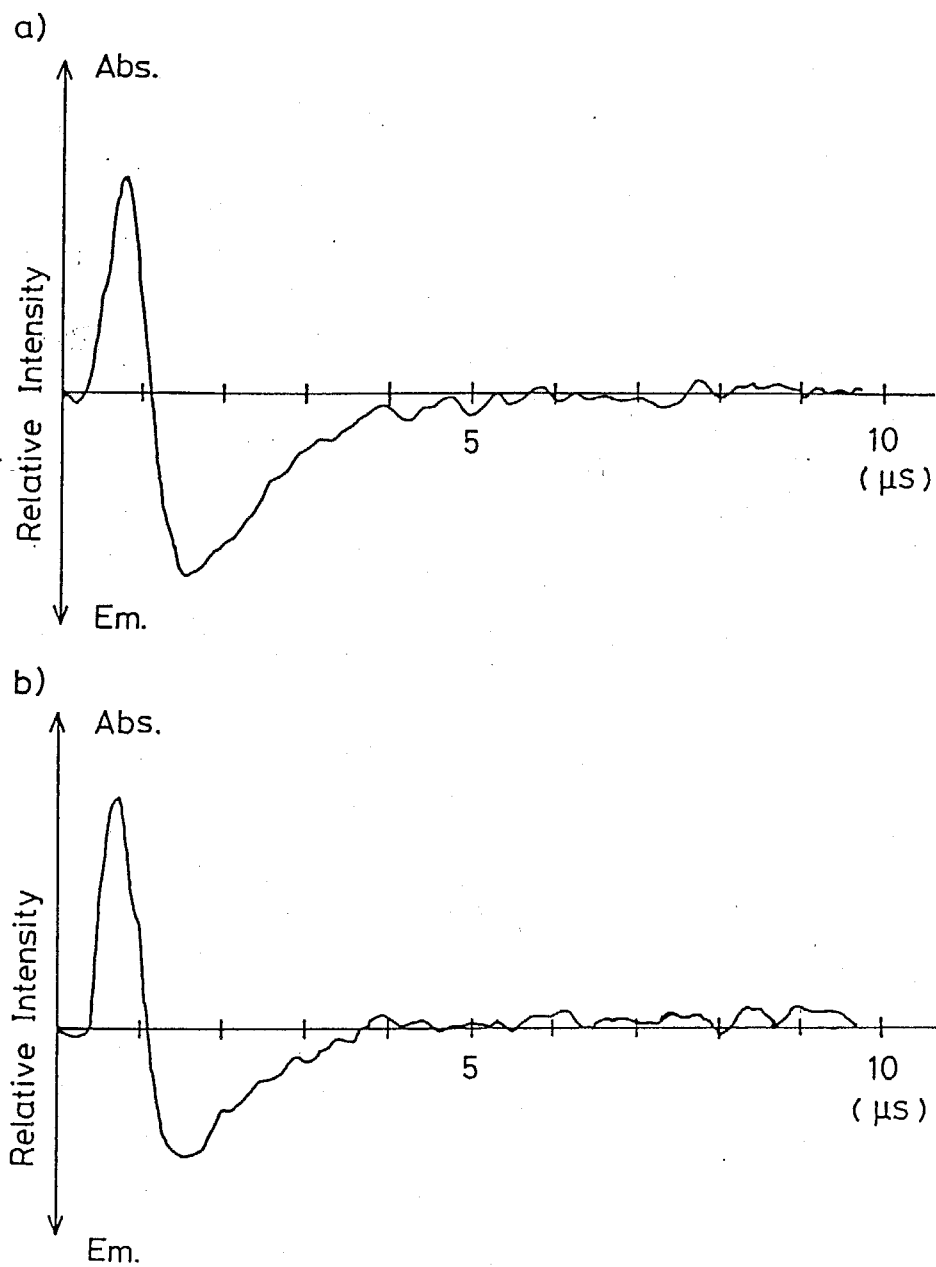
Fig.4-5-4 Time profiles of CIDEP signal of TEMPO (0.60 mM) at the $M_I=+1$ peak in

(a) TEMPO-fluoranthene (12 mM) and (b) TEMPO-coronene (1.1 mM)
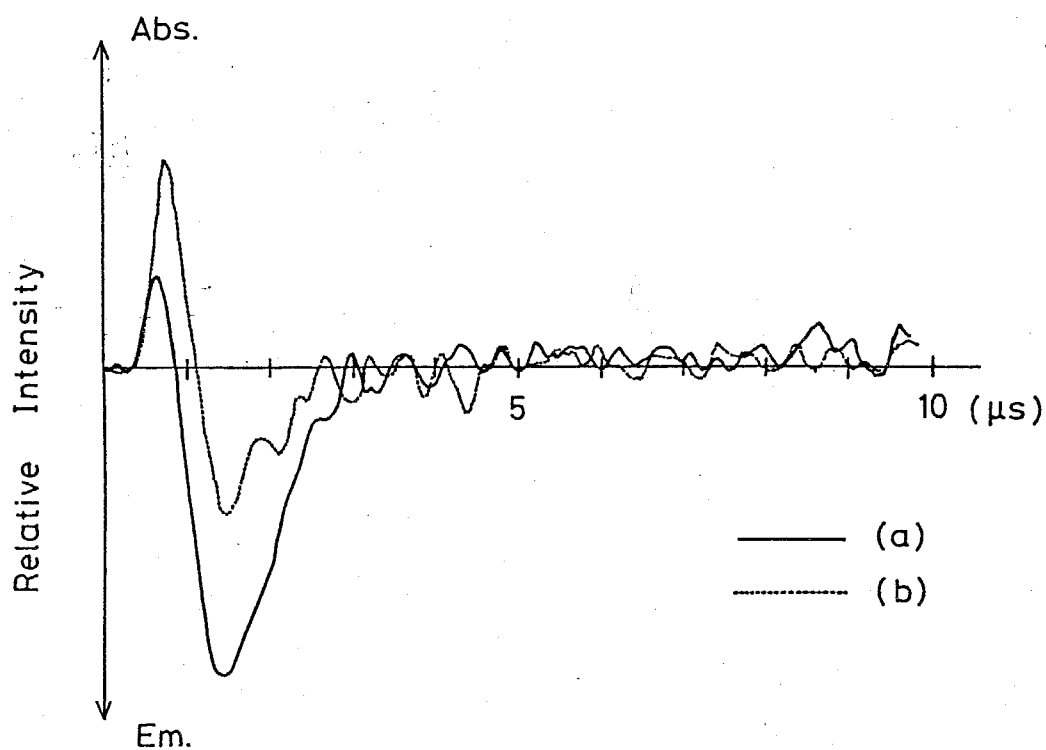
in benzene.   Microwave power is 1 mW.

Fig.4–5–5 Time profiles of CIDEP signal of TEMPO (0.60 mM) at the M_I=+1 peak

in the TEMPO–naphthalene (39 mM) system (a) without triplet quencher and

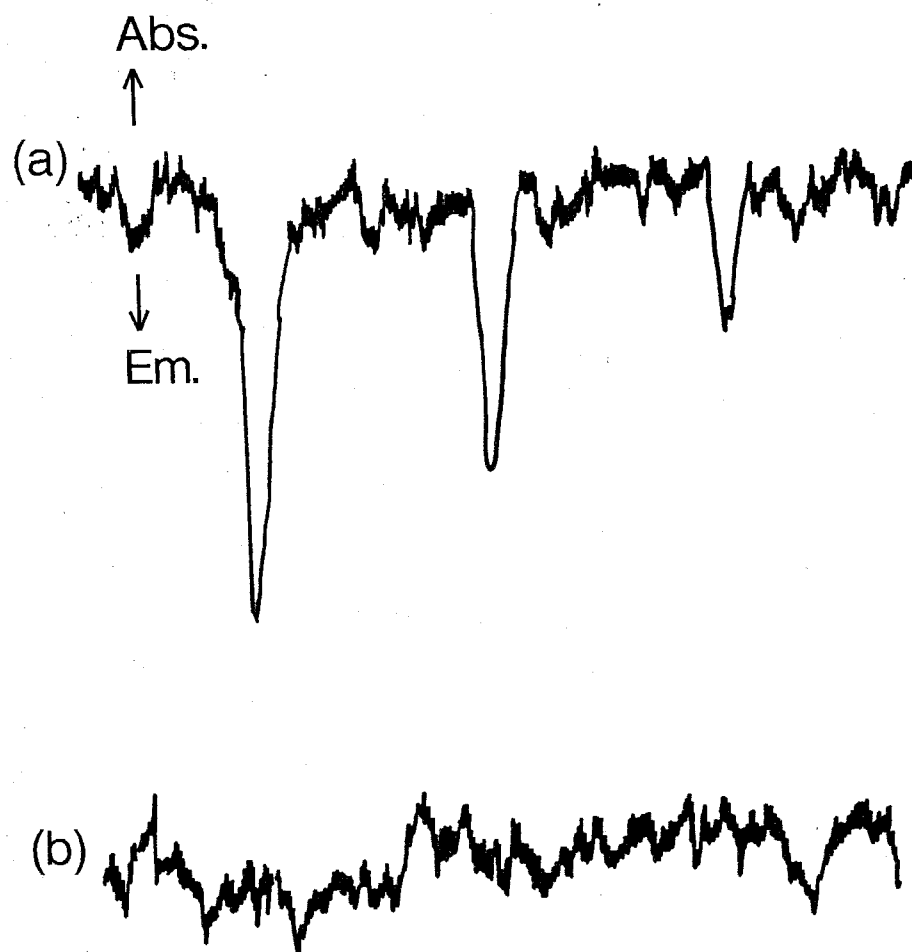(b) with 1,3–pentadiene (35 mM). Microwave power is 1 mW.

Fig.4-5-6 RTPM signal of a) 1-chloronaphthalene-TEMPO (0.60 mM) system and

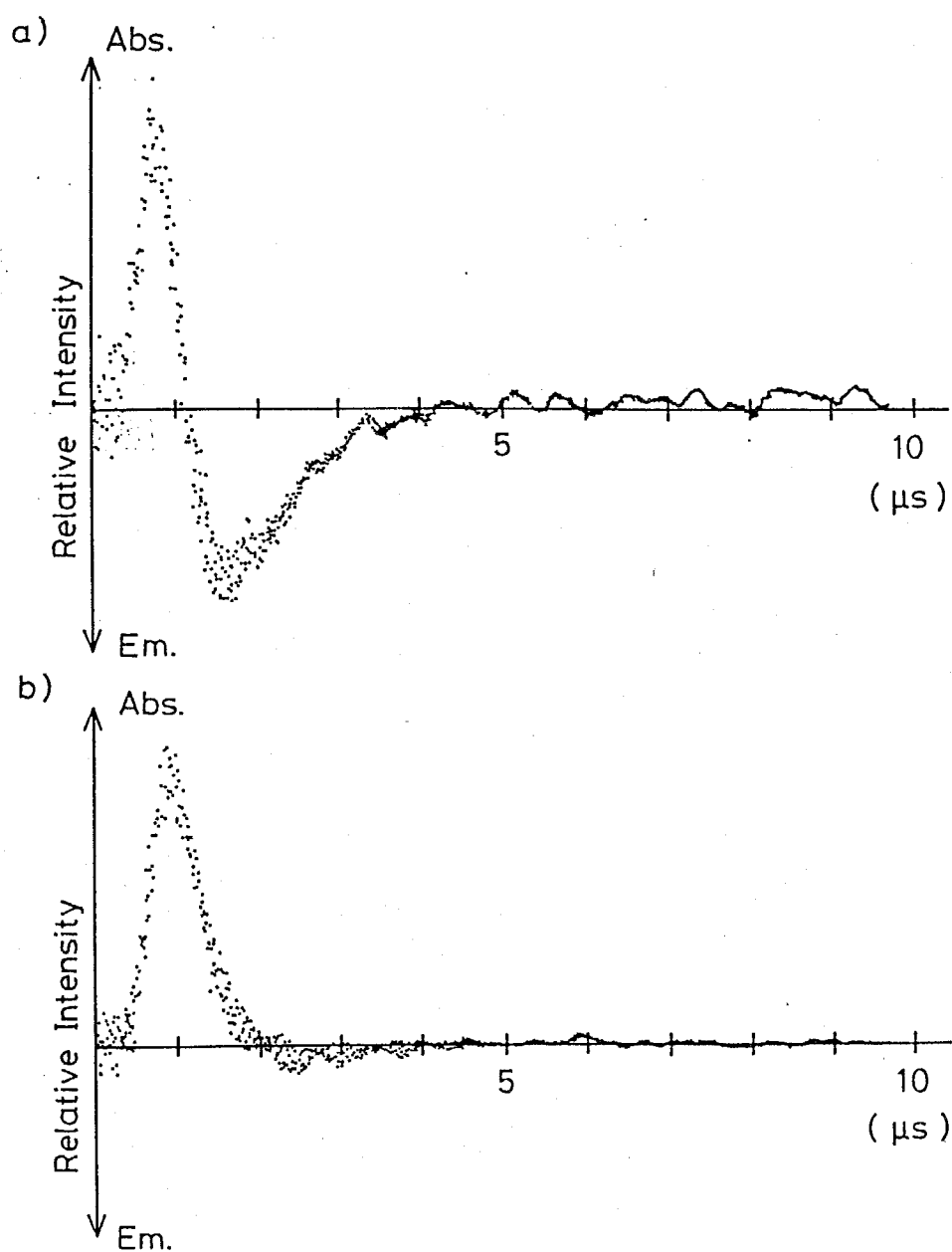b) a)+ 1,3-pentadiene (50 mM) as the triplet quencher.

Fig.4-5-7 Time profiles of CIDEP signal of TEMPO (0.60 mM) at the $M_I=+1$ peak in
TEMPO-coronene (1.1 mM) system (a) without quencher and
(b) with trans-stilbene (83 mM). Microwave power is 50 mW.

References

[1] J. B. Birks, *Photophysics of Aromatic Molecules*, New York, Wiley, (1970).

[2] K. Razi Naqvi and T. Gillbro. *Chem. Phys. Lett.*, **49**, 160, (1977).

[3] Y. Sakaguchi, S. Nagakura, H. Hayashi, *Chem. Phys. Lett.*, **72**, 420, (1980) and references therein; N. Yu, Molin, (Eds.), *Spin polarization and magnetic effect in radical reactions*, Elsevier Amsterdam, (1984).

[4] F. J. Adrian, *Rev. Chem. Intermediates*, **3**, 3, (1979)
; L. T. Muus, P. W. Atkins, K. A. McLauchlan and J. B. Pedersen,
Chemically Induced Magnetic Polarization, Reidel, Dordrecht, (1977).

[5] S. K. Wong and J. K. S. Wan, *J. Am. Chem. Soc.*, **94**, 7197, (1972).

[6] C. Blättler, F. Jent and H. Paul, *Chem. Phys. Lett.*, **166**, 375, (1990).

[7] A. Kawai, T. Okutsu and K. Obi, *J. Phys. Chem.*, **95**, 9130, (1991).

[8] A. J. Watkins, *Chem. Phys. Lett.*, **29**, 526, (1974).

[9] J. A. Green, L. A. Singer and J. H. Parks, *J. Chem. Phys.*, **58**, 2690, (1973).

[10] H. Murai and K. Kuwata, *Chem. Phys. Lett.*, **164**, 567, (1989).

[11] T. Imamura, O. Onitsuka and K. Obi, *J. Phys. Chem.*, **90**, 6741, (1986).

[12] K. Ohno, N. Nishi, M. Kinoshita and H. Inokuchi,
Chem, Phys. Lett., **33**, 293, (1975).

[13] G. J. Hoytink, *Acc. Chem. Res.*, **2**, 114, (1969)
; J. B. Birks, *J. Lumin.*, **1–2**, 154, (1970).

[14] T. Suzuki, K. Obi, (to be published).

[15] S. L. Murov, *Handbook of Photochemistry*,
Marcel Dekker INC., New York, (1973).

[16] K. Razi Naqvi, *J. Phys. Chem.*, **85**, 2303, (1981).

[17] A. Kawai and K. Obi, *J. Phys. Chem.*, submitted for publication.

[18] N. J. Turro, *Modern Molecular Photochemistry*, Benjamin/Cummings, (1978).

[19] P. J. Hore and K. A. McLauchlan, *J. Magn. Reson.*, **36**, 129, (1979).

CHAPTER V

Relation of RTPM and Radical–Excited State Molecule Interactions

According to the discussion in chapter III and IV, it is apparent that there is a new CIDEP generation mechanism by the interactions between free radical and excited molecule. These CIDEP signals were successfully classified according to the quartet and doublet precursor RTPMs. Here, both RTPMs are visuallized by the illustration of Fig.5-1. In case of triplet quenching (1), randomly encountered pairs of radical and triplet molecule become quartet and doublet spin states and the latter states undergo the pair of radical and ground state singlet molecule through triplet quenching.[1] Through this quenching process, quartet spin states are populated much more than doublet spin states. This enhanced population on quartet states produces the E + E/A type CIDEP on radicals due to the quartet–doublet mixing in quartet precursor through magnetic interaction. Therefore, I named this mechanism quartet precursor RTPM. This type of CIDEP is often observed in the systems with fast S_1-T_1 ISC rates, such as ketones and azaaromatics.

On the other hand, in case of singlet quenching, the random encounter of the lowest excited singlet molecule and radical yields the doublet spin states of the pair. In this pair, enhanced ISC by radicals[2] occurs and doublet spin states of radical and triplet molecule are formed. Hence, the doublet spin states of the pair is initially populated much more than quartet states, which is opposite condition to quartet precursor RTPM, and CIDEP generated on radical in this mechanism is A + A/E type. Therefore, I named this mechanism doublet precursor RTPM. Doublet precursor RTPM is operative under the following conditions: (1) Long lifetime of lowest excited singlet state, (2) slow S_1-T_1 ISC rate, and (3) radical concentrations high enough to enhance ISC.

Table 5-I summarizes S_1 lifetime,[3] triplet quantum yield, Φ_{ISC}[4] and generated CIDEP

pattern due to RTPM. As seen in this table, if S_1 has a lifetime longer than 50 ns, it is possible to detect the A^*/E type CIDEP. On the other hand, if its lifetime is shorter than 50 ns, it is almost impossible to detect A^*/E and only E^*/A type is observed. The S_1 lifetime and ISC rate under the experimental condition in such as the naphthalene–TEMPO system are just appropriate to observe both A^*/E and E^*/A type CIDEP depending on the gate time.

RTPM is a newborn CIDEP source and is expected to have many possibility to play a role in the research of the interactions of radical and excited molecules with a new sight as electron spin polarization. Moreover, it may be the key to dissolve the unknown CIDEP pattern of conventional systems. Recent developments of laser equipments make possible to generate the higher concentration of the photochemical intermediates and RTPM signal is becoming easy to appear in TR–ESR measurements. Therefore, scientists should have always RTPM in mind as well as TM and RPM when they investigate the photochemistry by TR–ESR method.

Table 5-I S$_1$ lifetime [ns], Φ_{isc} and CIDEP patterns generated in TEMPO radicals

excited molecule	S$_1$ lifetime[ns]	Φ_{isc}	CIDEP pattern
pyrene	450	0.38	A˙/E
coronene	302	0.56	A˙/E → E˙/A
fluoranthene	53	-	A˙/E → E˙/A
naphthalene	96	0.70	A˙/E → E˙/A
1-naphthol	10.6	-	E˙/A
acetone	2.0	1.00	E˙/A
benzophenone	0.005	1.00	E˙/A

1) Quartet Precursor RTPM

(Triplet quenching)

$$T_1 + D$$

$$^4(T_1 + D) \Longrightarrow {}^2(T_1 + D)$$

$$^2(S_0 + D) \longrightarrow S_0 + D$$

E + E/A
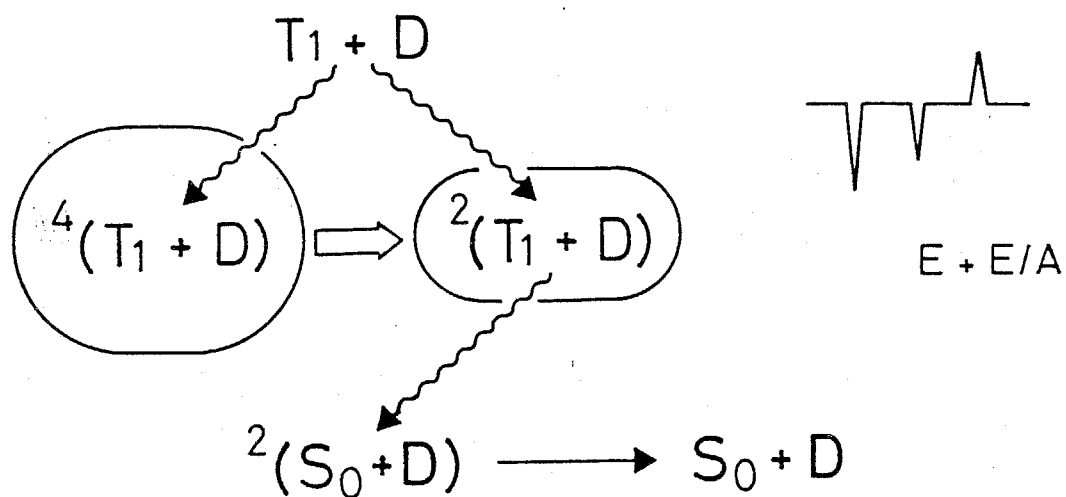
2) Doublet Precursor RTPM

(Singlet quenching)

$$S_1 + D$$

$$^2(S_1 + D)$$

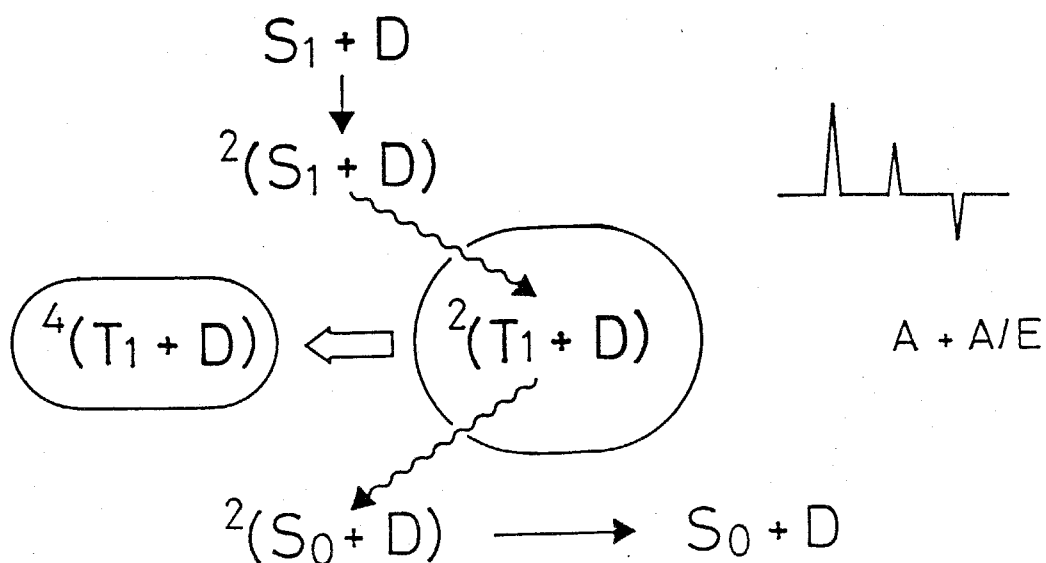$$^4(T_1 + D) \Longleftarrow {}^2(T_1 + D)$$

$$^2(S_0 + D) \longrightarrow S_0 + D$$

A + A/E

Fig.5-1　Schematic representations of doublet and quartet precursor RTPM's.

102

References

[1] P. W. Atkins and G. T. Evans, *Mol. Phys.*, **29**, 921, (1975)

; K. Razi Naqvi, *J. Phys. Chem.*, **85**, 2303, (1981).

; K. Schulten, *J. Chem. Phys.*, **80**, 3668, (1984).

[2] G. J. Hoytink, *Acc. Chem. Res.*, **2**, 114, (1969)

; J. B. Birks, *J. Lumin.*, **1–2**, 154, (1970).

[3] S. L. Murov, *Handbook of Photochemistry*, Marcel Dekker INC. New York (1973).

; N. J. Turro, *Modern Molecular Photochemistry*, Benjamin/Cummings, (1978).

[4] C. Blättler, F. Jent and H. Paul, *Chem. Phys. Lett.*, **166**, 375, (1990).

[5] K. N. Murrell and J. Tanaka, *Mol. Phys.*, **7**, 363, (1964).

[6] A. Kawai, T. Okutsu and K. Obi, *J. Phys. Chem.*, **95**, 9130, (1991).

; A. Kawai and K. Obi, *J. Phys. Chem.*, (1992), in press.

CHAPTER VI

Application of RTPM

6-1 RTPM in Conventional Photochemical Systems

a) Introduction.

RTPM[1-3] is based on the interactions between free radical and triplet molecule and, thus, is expected to be operative in the initial photochemical stages with high photon flux which may produce high concentration of radicals and triplet molecules. Since the discovery of CIDEP, many photochemical systems have been studied by TR–ESR spectroscopy[4] and discussed based on the well known two mechanisms of CIDEP, that is RPM[4,5] and TM.[4,6] However, these spectra must be reconsidered under new sight of RTPM beside the RPM and TM. The good examples of these cases are presented and discussed in this section.

b) Benzil–Phenoxyl System.

Figure 6-1-1a shows TR–ESR spectra of benzil ketyl[7] and 2,6–ditertialbutylphenoxyl (DTBP) radicals[7,8] obtained by the 308 nm laser excitation of the benzil–2,6–ditertialbutylphenol (DTBPL) system in benzene. DTBP shows E/A multiplet polarization with weak net absorptive polarization at low laser power. The former polarization is generated by the geminate RPM with triplet precursor and the latter by TM from benzil triplet state. This interpretation is easily understood by the conventional CIDEP theories, and any scientists will conclude that the hydrogen abstraction occurs between triplet benzil and DTBPL. However, this system is not so simple and the CIDEP pattern of spectra change drastically with laser power. The spectra of both radicals changed to E/A with net emissive polarization in higher laser power (Fig.6-1-1b). If we try to interpret this CIDEP pattern with only RPM and TM, it is very hard to

attribute net emissive polarization of both radicals. This additional emissive polarization might be attributed to RTPM due to the interaction between triplet benzil and produced radical, that is, benzil ketyl and DTBP. As the laser power is higher in this system, concentrations of radicals and triplet molecule are increased compared to low laser power and RTPM should operate in this system.

c) Naphthol–Naphthoxyl System.

Photochemistry of the benzil–phenol system was shown as an example of RTPM operation. Next, another system, naphthol–naphthoxyl, will be discussed as the RTPM operation.

Photoexcited 1–naphthol is known to produce naphthoxyl radical[9] by the laser flash photolysis. TR–ESR spectrum of naphthoxyl was measured by the 308 nm laser excitation of 1–naphthol in benzene (Fig.6–1–2a) and assigned to 1–naphthoxyl radical.[10] CIDEP of 1–naphthoxyl shows E/A multiplet pattern which indicates that the dissociation channel is the triplet state.

In this system, the CIDEP spectra can be easily interpreted by the RPM of geminate 1–naphthoxl and hydrogen atom pair. However, at the higher laser power or higher concentration of 1–naphthol, CIDEP pattern of 1–naphthoxyl changed drastically. Figure 6–1–2 shows the laser power dependence of CIDEP spectra of 1–naphthoxyl radical. CIDEP pattern is still E/A multiplet polarization in higher laser power(Fig.6–1–2b) but the additional emissive polarization appears in comparison to that at low laser power. The similar tendency was observed with the concentration change of 1–naphthol (Fig.6–1–3). At the higher concentration of 1–naphthol, additional net emissive polarization was observed on 1–naphthoxyl radical. These results can be explained reasonably by the RTPM. The higher laser power makes the concentration of triplet state of 1–naphthol and generated 1–naphthoxyl much higher and then, contribution of

RTPM is increased to produce net emissive polarization. The higher concentration of 1–naphthol also makes the higher concentration of triplet 1–naphthol and radical and, hence, net emissive polarization appears.

These two systems demonstrate that RTPM is actually operative at higher concentration of parent molecules or higher laser power in the photochemical reaction system. It is, therefore, concluded that RTPM should be consider to analyze CIDEP signals in actual photochemical systems.
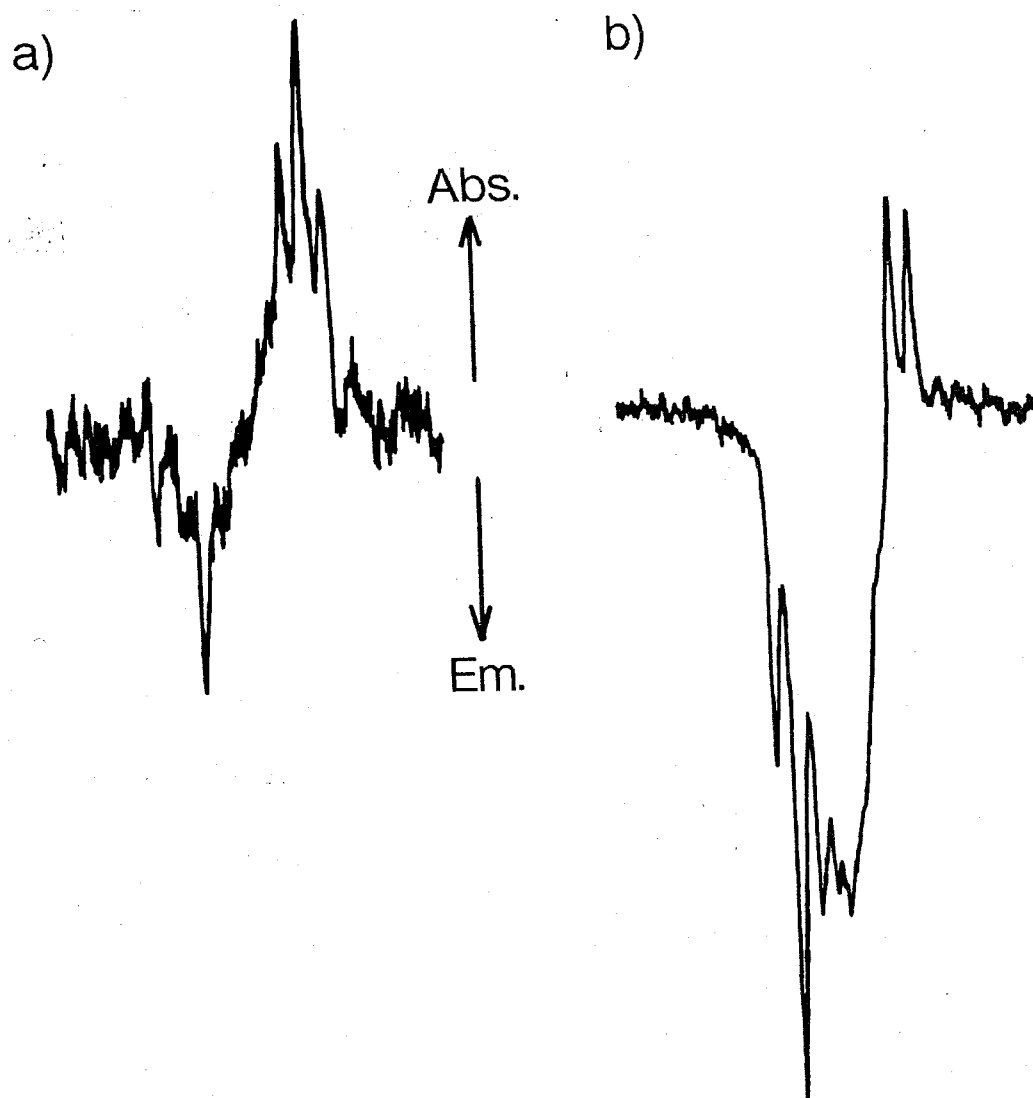
Fig.6-1-1 TR-ESR spectra of benzil (0.05 M) -DTBP (0.05 M) system

a) at low laser power and b) high laser power.

The gate is opened from 1.0 to 2.0 μs after excitation.

Abs.

(a)

Em.

laser intensity
low

(b)

laser intensity
high

10 mT
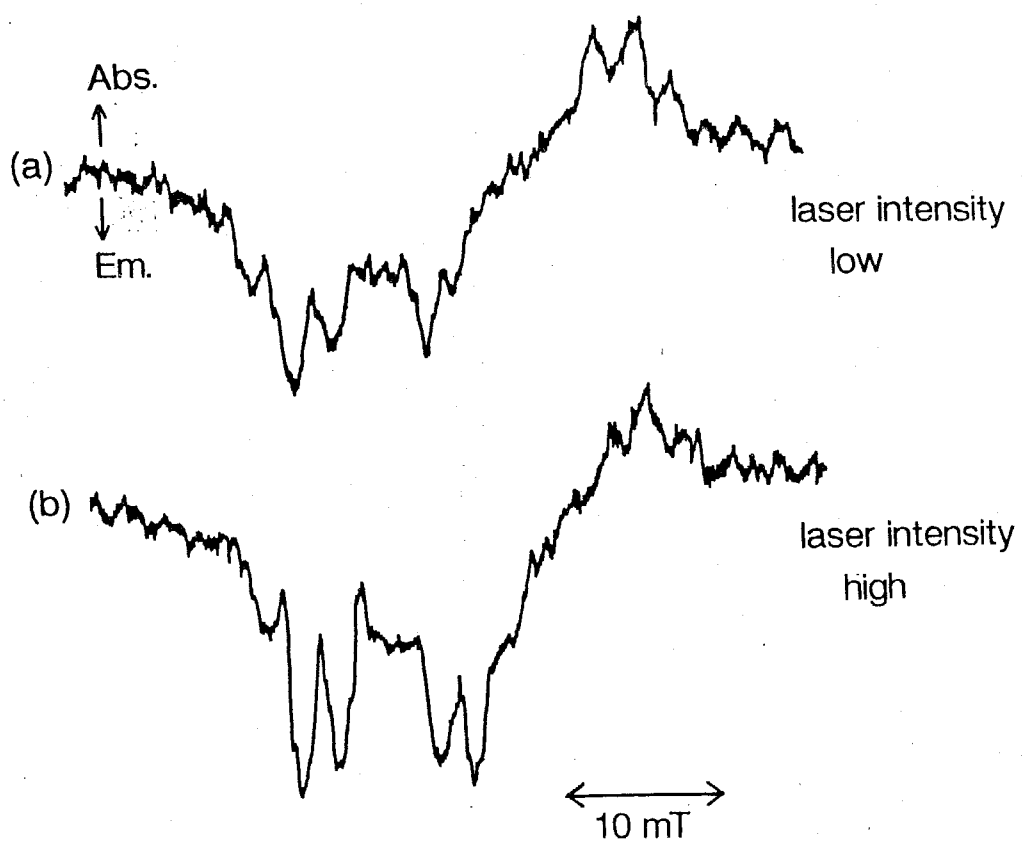
Fig.6-1-2 Laser power dependence of TR–ESR spectra of 1–naphthol (35 mM)

in benzene by 308 nm laser excitation.   The gate is opened from
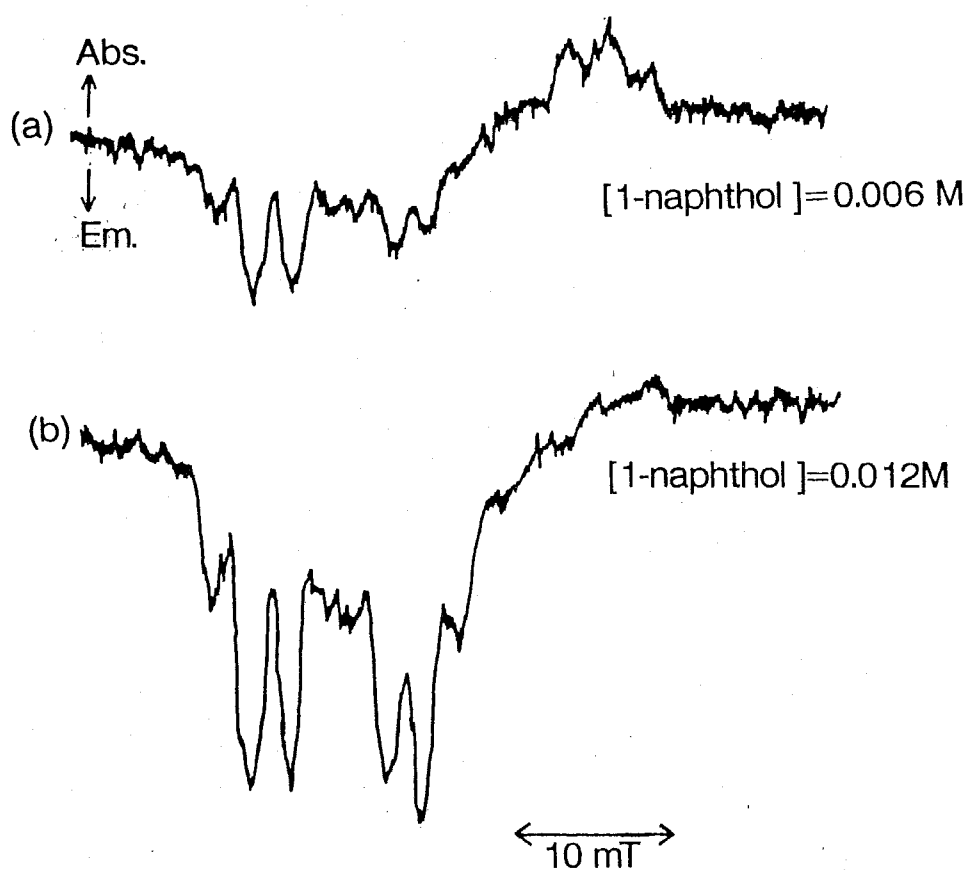
1.0 to 2.0 μs after excitation.

(a)

Abs.

Em.

[1-naphthol]=0.006 M

(b)

[1-naphthol]=0.012M

10 mT

Fig.6-1-3 Concentration dependence of TR-ESR spectra of 1-naphthol in benzene by 308 nm laser excitation. The gate is opened from 1.0 to 2.0 μs after excitation pulse.

a) Introduction.

RTPM makes variety of CIDEP signal patterns on free radicals, which are consistently explained by the difference in quenching processes and interactions between the radical and excited molecule pairs. However, relative intensity of CIDEP among different photochemical systems has not been discussed yet. As the magnitude of the signal in TR-ESR measurements changes with a lot of experimental factors as well as the efficiency of CIDEP generation itself, it is hard to discuss quantitatively the experimental results of CIDEP intensities. However, if the intensity of signal changes drastically, such as 10000 times, it is possible to discuss qualitatively the difference of the mechanism. Such drastic changes in CIDEP intensity are expected to happen in RTPM because the intensity of CIDEP due to RTPM changes depending on wide range of the quenching rates of excited molecules.

In this section, a trial examination of RTPM signals will be carried out to visualize the quenching mechanism of excited states molecule.

b) Quenching Rate Dependence of the Intensity of RTPM Signal.

Figure 6-2-1a shows CIDEP spectrum of TEMPO obtained in the 4-benzoylbiphenyl(4BB)-TEMPO system by 308 nm laser excitation. Net emissive polarization of TEMPO appears with weak E/A multiplet polarization, which is generated by quartet precursor RTPM of 4BB-TEMPO pair. On the other hand, Fig.6-2-1b shows the CIDEP spectrum of TEMPO obtained in the 4BB-TEMPO system in the presence of phenazine. In this case, CIDEP signal of TEMPO is fairly reduced to about one seventh though the experimental conditions are same in both cases except for the addition of phenazine in latter system.

The T_1 energies of 4BB and phenazine[11] are about 22000 and 15500 cm^{-1}, respectively, and D_1 energy of TEMPO is estimated to be about 18000 cm^{-1} from the absorption spectrum. In this case, energy transfers from 4BB to TEMPO and to phenazine are possible whereas that from phenazine to TEMPO is impossible. There are mainly two mechanisms for the quenching of excited molecules with nitroxide radicals.[12] One is the energy transfer from excited molecules to nitroxide radicals, whose rate is determined by the diffusion rate, 10^{10} s^{-1}M^{-1}. The other mechanism is the enhanced ISC, whose quenching rate constant is ca. 10^6 s^{-1}M^{-1}. The enhanced ISC occurs when the triplet energy is lower than the D_1 energy of nitroxide radial. These two mechanisms have apparently different rate constants and are expected to show significant difference in CIDEP intensity on nitroxide radical. In the case of Fig.6-2-1a, interaction between 4BB and TEMPO generated E*/A multiplet polarization on TEMPO, where the rate of the T_1 quenching was estimated to be 6 x 10^6 s^{-1}. On the other hand, the origin of RTPM in Fig.6-2-1b is considered to be phenazine-TEMPO pair because of the efficient T-T energy transfer from 4BB to phenazine in this system. In this case, the quenching rate by TEMPO is estimated to be about 6 x 10^2 s^{-1} assuming the enhanced ISC. Thus, if the magnitude of CIDEP is in proportion to the quenching rate, the difference of CIDEP magnitude between the 4BB-TEMPO and phenazine-TEMPO systems should be in order of 10000. However, the difference of experimental results is only less than 10 times. This inconsistency will be discussed later.

To investigate the quenching rate dependence of RTPM signals, the spin polarization in several triplet-doublet systems was examined where the relative energy between T_1 and D_1 was varied. Triplet molecules used were benzophenone, benzil, phenazine and anthracene and radicals were TEMPO and galvinoxyl. Figure 6-2-2 shows energy diagram of these molecules.[13] The D_1 energy of galvinoxyl is estimated to be higher than 11000 cm^{-1} from its absorption spectra. Galvinoxyl is known as an efficient triplet

quencher. Figure 6–2–3a shows spin polarized galvinoxyl in the benzil–galvinoxyl system. Galvinoxyl has hyperfine structure in a narrow magnetic field region compared to TEMPO and its g value is estimated to be 2.00410 from the center of its hyperfine structure. TR–ESR spectra were measured for various triplet molecules in the presence of TEMPO and galvinoxyl whose concentrations were kept constant in each system. Emissive CIDEP spectra of TEMPO and galvinoxyl were observed in benzophenone and benzil systems(Fig.6–2–4a and 4–b), where energy transfer was possible for both radicals. On the other hand, in the phenazine and anthracene systems(Fig.6–2–4c and 4–d), the relative CIDEP intensity of TEMPO to galvinoxyl became weak in comparison to that in the benzophenone and benzil systems. Since energy transfer is operative only to galvinoxyl but not to TEMPO in these systems, the CIDEP signals of TEMPO should be generated through enhanced intersystem crossing. These results suggest that energy transfer makes a major contribution to CIDEP generation in triplet–doublet systems. However, the difference in CIDEP intensities caused by energy transfer and enhanced ISC is not so large though the quenching rates of energy transfer and enhanced ISC are different in order of ca. 10000. The discrepancy between relative CIDEP intensity observed and that estimated from rate constants would be interpreted by the difference in the enhancement factors for CIDEP in energy transfer and enhanced ISC.

The experimental results obtained here are summarized in Tables 6–I and II. To evaluate the relative CIDEP intensities of TEMPO and galvinoxyl, the CIDEP intensity of galvinoxyl in each system is used as reference because the quenching of triplet molecules by galvinoxyl occurs by energy transfer process in all system studied here. The order of quenching rate is also listed in Tables 6–I and II. The enhancement factor is defined as follows,

$$I_{CIDEP} = f_e \times k_q[TEMPO]$$

where I_{CIDEP} is the relative CIDEP intensity, f_e is the enhancement factor, k_q is the quenching rate constant of triplet state by TEMPO and [TEMPO] is the concentration of TEMPO. According to the Tables 6-I and II, it is concluded that the CIDEP generation in RTPM is much more efficient in enhanced ISC process than in energy transfer process.

c) A Breakdown of the Spin Selective Quenching in Energy Transfer.

According to the above results, the magnitude of CIDEP depends on the nature of triplet quenching process, but before discuss this point, other factors of CIDEP generation will be discussed here.

From the principal of the RTPM, there are three main factors to determine the magnitude of CIDEP on radicals. One is the magnitude of D value of the triplet molecule. Large D value would induce the rapid quartet-doublet mixing that generates the large magnitude of CIDEP on radical. However, the zfs values of the triplet molecules used here are about 0.1 cm^{-1} and it is hard to attribute the large difference of f_e among these systems to the difference of D value. The second factor is the rotational correlation time of the radical and triplet molecule. Effective D value is given as a average by the rotational modulation of the triplet molecule and hence, the rotation correlation time is important in CIDEP generation. However, the triplet molecule used here is almost the same size and it is also difficult to attribute the difference of f_e to the rotational effect. The third factor is the spin selectivity in the quenching process. As there is no report on the spin selectivity of the triplet quenching by free radical, doublet pair states are assumed in the RTPM to act as the only exit channel to the pair states of radical and ground state molecule. If this assumption is correct, f_e is constant for any systems. Actually, there are a lot of perturbations in the triplet quenching and then, many paths exist in the triplet quenching process. It is still unknown how the spin

selection rules act for each path. In what follows, considerable paths will be proposed with spin selection rules and the efficiency of CIDEP is tried to be explained.

Figure 6-2-5 indicates the schematic representations of the potentials in the interactions between radicals and excited or ground state molecules. Figure 6-2-5a shows the case where energy transfer from triplet molecule to radical is impossible, whereas Fig.6-2-5b shows the case where that is possible. In the former case, the quenching path from the $| D_1 >$ states is only to the $| D_0 >$ states and the spin selection rule holds in this system. Hence, this is the ideal case for the explanation of RTPM because of the simplicity in quenching process. However, it is complicated in the case of b), in which several state conversions are possible. The most important path is the conversion from quartet states of radical-triplet pair to that of radical-ground state molecule pair where the radical is correlated to the quartet excited states. There is no information about the energy of the quartet excited state of radical but it is estimated to lie little higher than the lowest doublet excited state. Therefore, it is considerable that the quartet state of radical to lies close to doublet state just as shown in the Fig.6-2-5b. In this case, the spin selection rule is broken down: Both doublet and quartet states of radical-triplet pair convert to the radical-ground state molecule pair. Therefore, the remaining pairs show a little difference between the populations of doublet and quartet states which causes the decrease of the CIDEP magnitude. This is considered to be a reason for the difference in f_e of energy transfer and enhanced ISC processes.

It is a long way to confirm this interpretation and needs a lot of experimental results concerning the evidence of energy transfer process to quartet states. However, the breakdown of the spin selective quenching, will open a new field of investigation in quenching process and in my opinion, this suggestion is one of the results of CIDEP studies based on RTPM.

Table 6-I Enhancement Factor of CIDEP Generation

Excited Molecule	rel. CIDEP Intensity	$T_1 \quad k_f$	Enhancement Factor
4-benzoylbiphenyl	7.5	10^{10}	0.00075
phenazine	1	10^6	1

Table 6-II Enhancement Factor of CIDEP Generation

Excited Molecule	rel. CIDEP Intensity	$T_1 \quad k_q$	Enhancement Factor
benzophenone	5.3	10^{10}	0.00053
benzil	6	10^{10}	0.0006
phenazine	1	10^6	1
anthracene	1	10^6	1
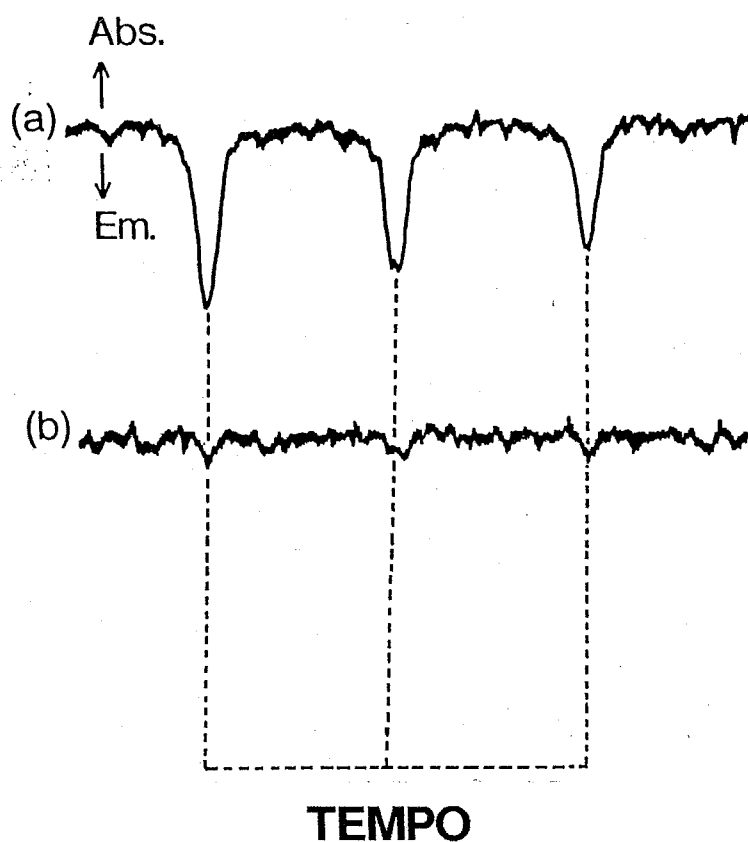
Fig.6–2–1 a) RTPM signal obtained in 4benzoylbiphenyl (9.7 mM) –TEMPO (0.60 mM)

system by 308 nm excitation.

b) RTPM signal obtained by a) + phenazine (92.5 mM).

The gate is opened from 1.0 to 1.5 μs.
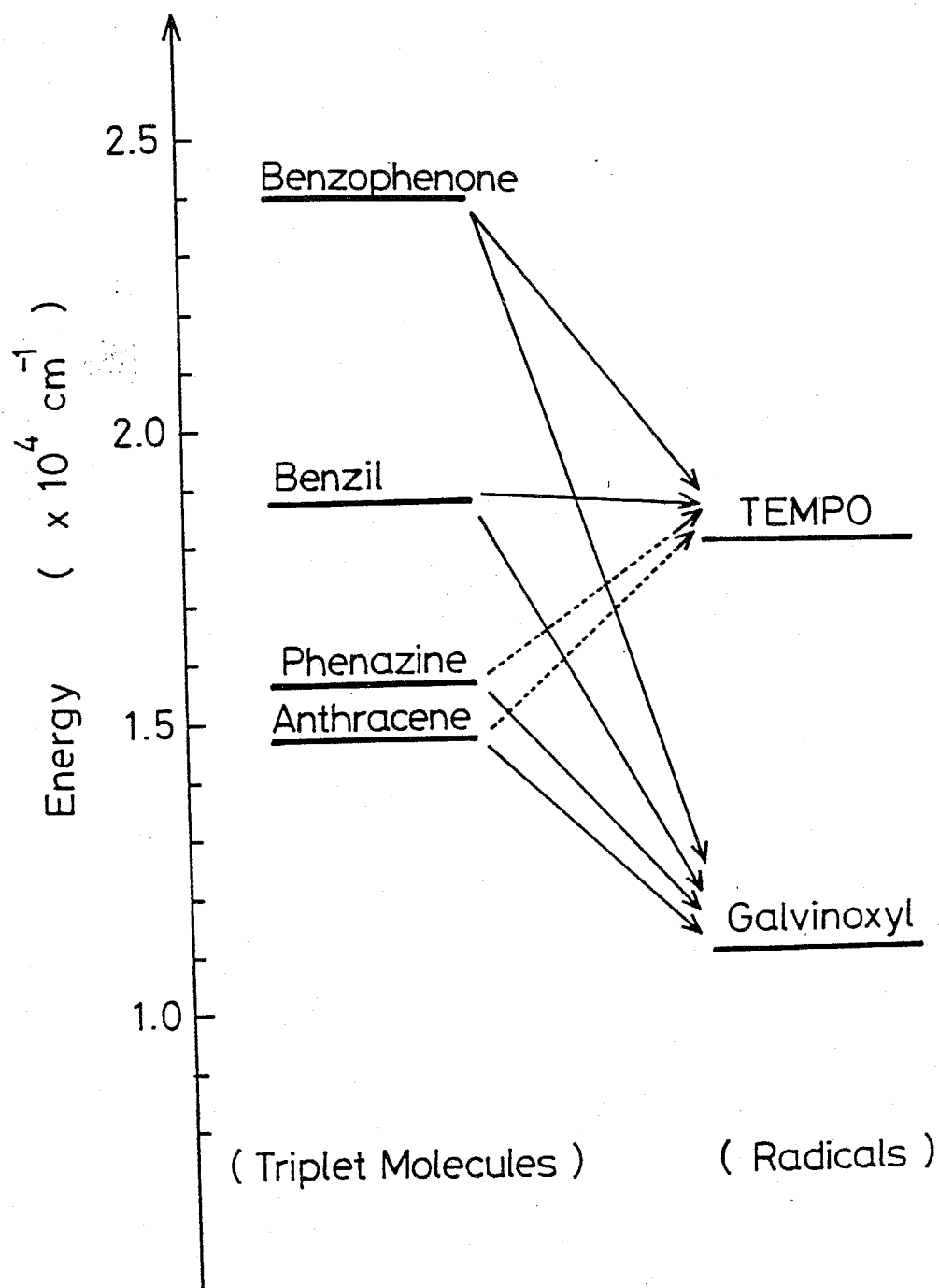
Fig.6-2-2 Energy diagram of T_1 of benzophenone, benzil, phenazine and anthracene and D_1 of TEMPO and galvinoxyl.
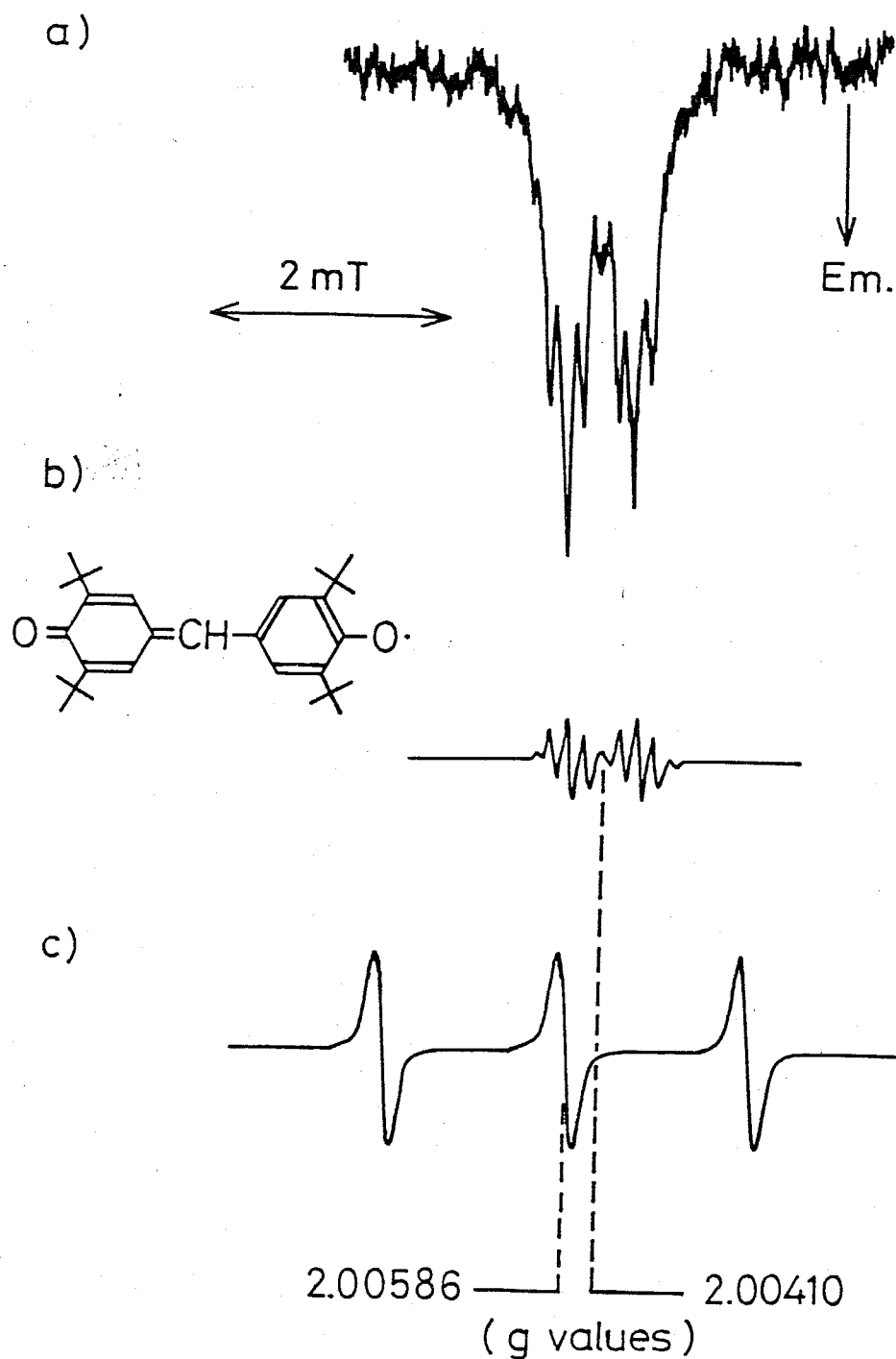
Fig.6-2-3 a) TR–ESR spectrum of galvinoxyl (0.59 mM) in the system of benzil (48 mM)–galvinoxyl in benzene. b)CW–ESR spectrum of galvinoxyl and c)CW–ESR spectrum of TEMPO.
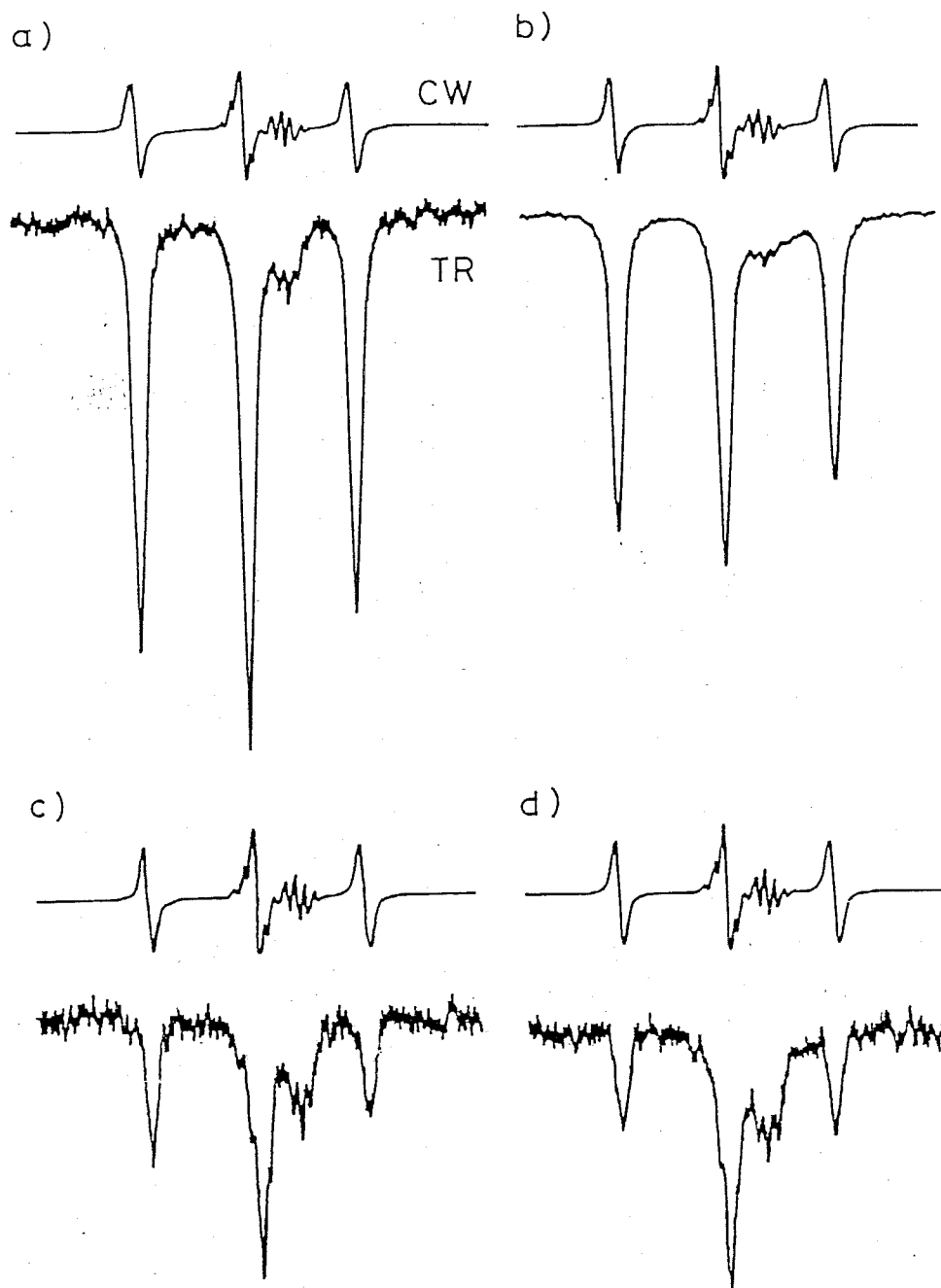
Fig.6-2-4 CW and TR-ESR spectra of TEMPO (0.61 mM) and galvinoxyl(0.23 mM)

mixtures containing a) benzophenone (37 mM), b) benzil (63 mM),

c) phenazine (56 mM) and d) anthracene (56 mM).

a) **Enhanced ISC**

b) **Energy Transfer**

transitions

$|D_1\rangle \to |D_0\rangle$

$|D_2\rangle \to |D_1\rangle$

$|Q_1\rangle \to |Q_0\rangle$
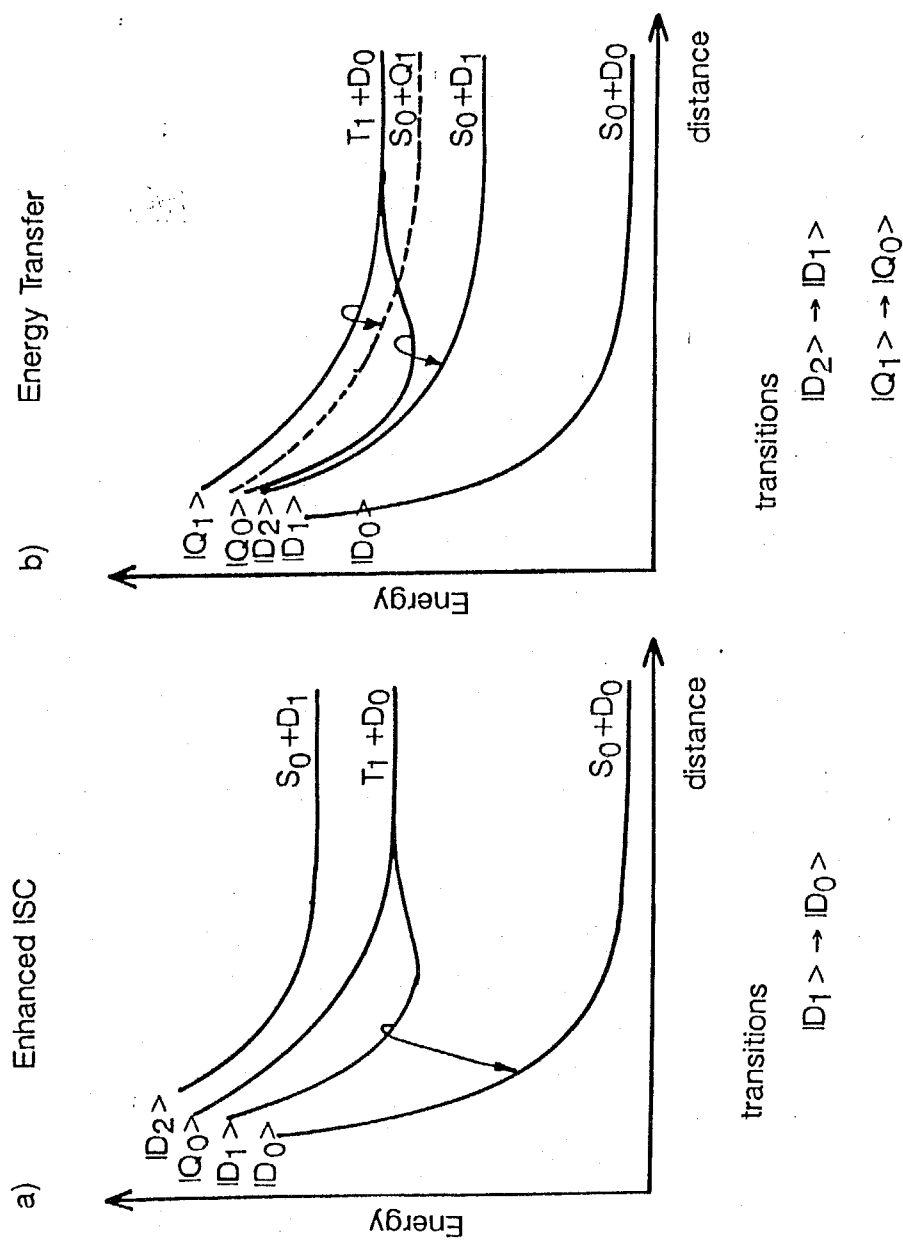
Fig.6-2-5 Potential energy surfaces of radical and excited or ground state molecules, where a) energy transfer from triplet to radical is impossible and a) energy transfer is possible.

References

[1] C. Blattler, F. Jent and H. Paul, *Chem. Phys. Lett.*, **166**, 375, (1990).

[2] A. Kawai, T. Okutsu and K. Obi, *J. Phys. Chem.*, **95**, 9130, (1991).

[3] A. Kawai and K. Obi, *J. Phys. Chem.*, (1992) in press.

[4] L. T. Muus, P. W. Atkins, K. A. McLauchlan and J. B. Pedersen,

    Chemically Induced Magnetic Polarization, Reidel, Dordrecht, (1977).

    ; N. Yu, Molin, (Eds.), *Spin polarization and magnetic effect*

    in radical reactions, Elsevier Amsterdam, (1984).

[5] F. J. Adrian, *Rev. Chem. Intermediates*, **3**, 3, (1979)

[6] S. K. Wong and J. K. S. Wan, *J. Am. Chem. Soc.*, **94**, 7197, (1972).

[7] M. Mukai, S. Yamauchi and N. Hirota, *J. Phys. Chem.*, **93**, 4411, (1989).

    ; T. Okutsu, Yano, A. Kawai and K. Obi, *J. Phys. Chem.*, **95**, 5401, (1991).

[8] J. Pannell, *Chem. Ind. (London)*, 1797, (1962).

[9] T. Takemura, K. Hara and H. baba, *Bull. Chem. Soc. Jpn.*, **44**, 977, (1971).

[10] W. T. Dixon, W. E. J. Foster and D. Murphy, *J. Chem. Soc. Perkin II*, 779, (1978).

[11] V. L. Ermolaev and A. N. Terenin, *J. Chim. Phys.*, **55**, 698, (1958).

[12] V. A. Kuzmin, A. S. Tatikolov, *Chem. Phys. Lett.*, **53**, 606, (1978)

    ; K. Bhattacharyya, P. K. Das, R. W. Fessenden, M. V. George, K. R. Gopidas, K. R.

    G. L. Hug, *J. Phys. Chem.*, **89**, 4164, (1985).

    ; N. N. Quan and A. V. Guzzo, *J. Phys. Chem.*, **85**, 2303, (1981).

    ; K. Razi Naqvi, *J. Phys. Chem.*, **85**, 2303, (1981).

[13] S. L. Murrov, *Handbook of Photochemistry*,

    Marcel Dekker INC., New York, (1973).

ACKNOWLEDGMENTS